



*322 NW 5th Avenue, Suite 234
Portland, OR 97209
Phone 503.226.6810
Fax 503.226.6816
www.pwa-ltd.com*

**Evaluation of Proposed Lake Management
on Hydrodynamics, Water Quality and
Eutrophication in Upper Klamath Lake**

Prepared for

U.S. Bureau of Reclamation, Klamath Falls, Oregon

Prepared by

Philip Williams & Associates, Ltd. (PWA)
Portland, Oregon and
Corte Madera, California

with

Danish Hydraulic Institute–Institute of Water Environment (DHI)
Philadelphia, Pennsylvania and
Horsholm, Denmark

March 28, 2001

Services, opinions, recommendations, plans or specifications and other materials resulting from work performed by PWA and its subconsultant under this contract with the U.S. Bureau of Reclamation, Klamath Falls, Oregon are intended solely for the use and benefit of the U.S. Bureau of Reclamation. Any reuse or modification of the above mentioned materials by the U.S. Bureau of Reclamation or others for purposes outside of this contract shall be at the users sole risk, unless written consent is obtained from Philip Williams & Associates, Ltd., 770 Tamalpais Drive, Suite 401, Corte Madera, California 94925.

TABLE OF CONTENTS

	<u>Page No.</u>
1. INTRODUCTION	1
1.1 Background	1
1.2 Overview and Study Objectives	1
2. FINDINGS	3
3. SITE DESCRIPTION	6
4. PHYSICAL PROCESSES	8
4.1 Circulation	8
4.2 Thermal Stratification	8
5. REVIEW OF DATA SOURCES	9
5.1 Hydrological and hydraulic data	9
5.2 Wind data	9
5.3 Water Quality data	10
5.4 Sediment data	13
5.5 Bathymetry	13
6. MODELS DESCRIPTION	16
6.1 MIKE 11, MIKE 21 and MIKE 3	16
6.1.1 Hydrodynamic Model Description for Mike 11 and Mike 21	17
6.1.2 Basic Equations	17
6.1.3 Solution Techniques	19
6.2 Water Quality Models	19
6.2.1 MIKE11-3 WQ/EU	19
6.2.2 MIKE 11 EU model	19
6.3 Wave/Sediment Transport Model	26
6.3.1 MIKE 21 NSW/MT	26
6.3.2 MIKE 21 Sediment Transport (Multi-layer mud-model)	27
7. MODEL CALIBRATION	33
7.1 MIKE 11 HD	33
7.2 MIKE 21 HD	33
7.3 MIKE 11 EU	35
7.3.1 Eutrophication (EU) Model Setup and Calibration	35
7.3.2 Calibration of the EU model	38

8. MODEL APPLICATIONS AND RESULTS	47
8.1 Description of the scenarios for different lake operations	47
8.2 Hydrodynamic scenarios for circulation model	47
8.2.1 2D Hydrodynamic Model Results	48
8.3 Water Quality	56
8.3.1 Water Quality Model Descriptions	56
8.3.2 Heat Exchange and Water Temperature	57
8.3.3 Dissolved Oxygen	61
8.4 Model results of eutrophication simulations	78
8.4.1 Regulation of water level	78
8.4.2 Chlorophyll and phytoplankton biomass	78
8.4.3 Total Nitrogen	85
8.4.4 Total Phosphorous	85
8.4.5 Net Primary Production, Sediment Oxygen Demand and Oxygen Consumption in the Water	86
8.4.6 Summary	87
8.4.7 EU simulation with reduced load	89
8.5 Wave Modeling – Sediment transport	98
8.5.1 Wave Modeling	98
8.5.2 Sediment Modeling	101
9. RECOMMENDATIONS	107
10. REFERENCES	109
11. LIST OF PREPARERS	116

LIST OF FIGURES AND TABLES

Figure 1-1	Effect on Lake Hydrodynamics and Water Quality	2
Figure 3-1	Upper Klamath and Agency Lakes	6
Figure 3-2	Operational Rules and Average Water Levels for Upper Klamath Lake	7
Table 3-1	Comparison of UKL water quality values to OECD standards	7
Figure 5-1	View on Upper Klamath Lake - Rattlesnake Point	9
Figure 5-2	Upper Klamath Lake Nutrient Inflow Study	10
Table 5-1	WQ Measurements Sites on Tributaries (BIA)	11
Figure 5-3	Upper Klamath Lake - Bathymetry	14
Figure 5-4	UKL retention Storage Curve	15
Figure 6-1	General schematics of 1-D, 2-D and 3-D models applied to Upper Klamath Lake	16
Figure 6-2	Carbon Flow in Pelagic Part of EU Model	21
Figure 6-3	Nitrogen Flow in Pelagic Part of EU Model	22
Figure 6-4	Phosphorus Flow in Pelagic Part of EU Model	22
Figure 6-5	N flow in sediment module to EU model	24
Figure 6-6	P flow in sediment P module to EU model	25
Figure 6-7	MIKE 21 Sediment Transport Model and Physical Processes	29
Figure 7-1	Comparison for Simulated and Observed Water Levels	33
Figure 7-2	Comparison of Daily Measured and Hourly Computed Water Levels	34
Figure 7-3	Comparison of Measured and Computed Daily Average Water Levels	34
Figure 7-4	Water temperature used by EU model	36
Figure 7-5	Seasonal Variation Of Photosynthetic Active Radiation (PAR) Used By The EU Model	36
Table 7-1	Load of Nutrients to Agency and Upper Klamath Lakes	37
Table 7-2	Load of Nutrients to Agency and Upper Klamath Lakes in 1997, Tones	37
Table 7-3	P And N Load Used in Simulation with Reduced Load, Tones Per Year	37
Figure 7-6	Simulated and Measured Values of Total P and SRP	39
Figure 7-7	Simulated and Measured Values of Total N, NH4-N And NO3-N	40
Figure 7-8	Measured and Simulated Secchi Depth, Ph and Chlorophyll	41
Figure 7-9	Simulated and Measured Oxygen Concentrations	41
Figure 7-10	Sediment Parameters	43
Figure 7-11	Measured and Simulated Values of TN, TP, And Chlorophyll at Stations MN and ER in UKL	44
Figure 7-12	Measured and Simulated Values of TN, TP, and Chlorophyll at Stations ML and PM in UKL	46

LIST OF FIGURES AND TABLES (continued)

Figure 8-1	Lake Elevation Changes Simulated in the Water Quality and Eutrophication Model	47
Figure 8-2	Velocity Field for UKL Lake Scenario A	49
Figure 8-3	Velocity Field for UKL Lake Scenario B	50
Figure 8-4	Velocity Field for UKL Lake Scenario C	51
Figure 8-5	Velocity Field for UKL Lake Scenario D	52
Figure 8-6	Velocity Comparison – West of Bare Island [Upper] – East of Bare Island [Lower]	53
Figure 8-7	Particle tracking for Wocus Bay	54
Figure 8-8	Particle tracking for Upper Klamath and Agency Lakes	55
Figure 8-9	Wind direction and speed for August 6-20, 1997	57
Figure 8-10	Daily Average Air Temperature for August 6-20, 1997	58
Figure 8-11	Stations on Upper Klamath Lake	59
Figure 8-12	Average Spatial Variation in Lake Water Surface Temperature (August 6-20, 1997). (Left figure shows 1997 condition and right figure shows 1997 condition with a decrease in water surface by 1 meter).	60
Figure 8-13	Vertical Variation in Lake Water Column Temperature (August 6-20, 1997) for Stations BB, HB, MN and SB (from top left to lower right)	60
Figure 8-14	Lake Elevation Changes Simulated in the Water Quality and Eutrophication Model	61
Table 8-1:	Maximum primary production at noon [gC/m ² /day]	62
Table 8-2:	Algae respiration [gO ₂ /m ² /day]	62
Table 8-3:	Water respiration [gO ₂ /m ² /day]	62
Table 8-4:	Sediment oxygen demand [gO ₂ /m ² /day]	63
Figure 8-15	Location of Comparison Points	64
Figure 8-16	Dissolved Oxygen Concentration in Klamath Lake (Upper/Middle/Lower layers)	66
Figure 8-17	Dissolved Oxygen Concentration in Agency Lake (Upper/Middle/Lower layers)	67
Figure 8-18	Dissolved Oxygen Concentration in Ball Bay (Upper/Middle/Lower layers)	68
Figure 8-19	Dissolved Oxygen Concentration in Shoalwater Bay (Upper/Middle/Lower layers)	69
Figure 8-20	Dissolved Oxygen Concentration in Wocus Bay (Upper/Middle/Lower layers)	70
Figure 8-21	Schema of the Layer Presentation - /Layer 51, Layer 49 and Layer 45 are used/.	71
Figure 8-22	Minimum Dissolved Oxygen Concentration for Upper Layer during August 10-17, 1997 simulating period.	72
Figure 8-23	Minimum Dissolved Oxygen Concentration for Middle Layer during August 10-17, 1997 simulating period	73

LIST OF FIGURES AND TABLES (continued)

Figure 8-24	Minimum Dissolved Oxygen Concentration for Bottom Layer during August 10-17, 1997 simulating period	74
Figure 8-25	Mean Dissolved Oxygen Concentration for Upper Layer during August 10-17, 1997 Simulating Period	75
Figure 8-26	Mean Dissolved Oxygen Concentration for Middle Layer during August 10-17, 1997 Simulating Period	76
Figure 8-27	Mean Dissolved Oxygen Concentration for Bottom layer During August 10-17, 1997 Simulating Period	77
Figure 8-28	Chlorophyll, phytoplankton biomass, TN and TP for the water level scenarios, St. ER and ML in UKL. RED: reduced outflow. INC: increased outflow. REF: reference 1997	79
Figure 8-29	Chlorophyll, phytoplankton biomass, TN and TP for the water level scenarios, St. ER and ML in UKL. RED: reduced outflow. INC: increased outflow. REF: reference 1997.	80
Figure 8-30	Chlorophyll, TN and TP for the Water Level Scenarios, Ball Bay, Shoalwater Bay and Wocus Bay	81
Figure 8-31	Simulated chlorophyll, plankton biomass, DO production and respiration, Agency Lake St. AS	82
Figure 8-32	Simulated plankton biomass, DO production and respiration, UKL and Ball Bay	83
Figure 8-33	Simulated plankton biomass, DO production and respiration, Shoalwater Bay (SH) and Wocus Bay	84
Table 8-5	Change In Chlorophyll, TN, TP, And DO Processes In Simulation With Reduced Outflow In The Growth Season Relative To Reference Simulation	88
Table 8-6	Change in chlorophyll, TN, TP and DO processes in simulation with increased outflow in the growth season relative to reference simulation	88
Figure 8-34	Simulated water quality in Agency Lake (St. AS) with reduced P load (RED) and present load (REF): TN, TP, Chlorophyll, Phytoplankton biomass, Net primary production, Sediment DO consumption and Do consumption in the water.	92
Figure 8-36	Simulated water quality in Ball Bay with reduced P load (RED) and present load (REF): TN, TP, Chlorophyll, Phytoplankton biomass, Net primary production, Sediment DO consumption and Do consumption in the water.	94
Figure 8-37	Simulated water quality in Shoalwater Bay with reduced P load (RED) and present load (REF): TN, TP, Chlorophyll, Phytoplankton biomass, Net primary production, Sediment DO consumption and Do consumption in the water.	95
Figure 8-38	Simulated water quality in Wocus Bay with reduced P load (RED) and present load (REF): TN, TP, Chlorophyll, Phytoplankton biomass, Net primary production, Sediment DO consumption and Do consumption in the water.	96

LIST OF FIGURES AND TABLES (continued)

Table 8-7	Mean concentrations from April to September in reference simulation. AG (Agency), KL (Klamath Lake), Ball (Ball Bay), SH (Shoalwater Bay), WO (Wocus Bay).	97
Table 8-8	Mean concentrations from April to September in simulation with 37% P reduction. AG (Agency), KL (Klamath Lake), Ball (Ball Bay), SH (Shoalwater Bay), WO (Wocus Bay).	97
Table 8-9	Difference in concentrations from April to September between simulation with 37% P reduction and reference simulation. AG (Agency), KL (Klamath Lake), Ball (Ball Bay), SH (Shoalwater Bay), WO (Wocus Bay).	97
Table 8-10	Table 8-6 Difference in % from April to September between simulation with 37% P reduction and reference simulation. AG (Agency), KL (Klamath Lake), Ball (Ball Bay), SH (Shoalwater Bay), WO (Wocus Bay).	97
Figure 8-39	Wind Time Series from The Klamath Falls Airport	98
Figure 8-40	Wind Roses for The Summer Period (5/1/1997 - 10/1/1997) (Right) and Entire Period 1995-2000 (Left)	99
Figure 8-41	Simulated significant wave height and wave period. Lake level 4141 feet, wind speed 10 miles/hour from northwest	100
Figure 8-42	Simulated bottom shear stress. Lake level of 4138 feet, Wind speed of 10 miles/hour from northwest	103
Figure 8-43	Simulated bottom shear stress. Lake level of 4141 feet, Wind speed of 10 miles/hour from northwest	104
Figure 8-44	Simulated bottom shear stress. Lake level of 4142 feet, Wind speed of 10 miles/hour from northwest	104
Figure 8-45	Simulated bottom shear stress. Critical shear stress of 0.05 m ² /sec., Lake level of 4141 feet, Wind speed of 10 miles/hour from northwest	105
Figure 8-46	Simulated bottom shear stress. Critical shear stress of 0.05 m ² /sec. Lake level of 4141 feet, Wind speed of 13.5 miles/hour from northwest	105
Figure 8-47	Simulated bottom shear stress. Critical shear stress of 0.05 m ² /sec. Lake level of 4142 feet, Wind speed of 10 miles/hour from northwest	106
Figure 8-48	Simulated bottom shear stress. Critical shear stress of 0.05 m ² /sec. Lake level of 4142 feet, Wind speed of 13.5 miles/hour from northwest	106

1. INTRODUCTION

1.1 BACKGROUND

The Bureau of Reclamation (BOR) is developing an Environmental Assessment (EA) for the long-term operation of the Klamath Project. The Bureau is required to determine the impacts of altering Upper Klamath Lake (UKL) and Agency Lake (together the UKL system) elevations on the hydrodynamic and water quality conditions. The EA involves a proposed action to develop operations scenarios that establish minimum UKL water elevations and minimum Klamath River flows downstream of Iron Gate Dam. The alternatives will be comprised of a combination of one or more of the operations scenarios.

The Bureau contracted with Philip Williams & Associates, Ltd. (PWA) and PWA's subconsultant, the Institute for Water and Environment (DHI) to develop a set of integrated hydrodynamic and water quality models of the UKL system as part of the analysis of alternative operations scenarios. In order to provide a quantitative evaluation of the impacts of lake level change on water quality in UKL, PWA used models capable of describing lake circulation, eutrophication, sediment re-suspension, and dissolved oxygen.

1.2 OVERVIEW AND STUDY OBJECTIVES

PWA used one-, two- and three-dimensional models to simulate physical and water quality processes of the UKL system and to estimate the effects of alternative operations scenarios on the system. The models provided numeric and graphic output to illustrate affect of seasonal wind patterns and inflow and outflow from the UKL system on hydrodynamic conditions, such as water level and velocity.

The model was also used to simulate resulting changes in concentration of dissolved oxygen (DO), Chlorophyll, nutrients (N and P), and resuspension of cohesive sediment.

The objectives of the project were to: 1) develop an appropriate set of models capable of simulating both lake hydrodynamics and selected water quality parameters; 2) estimate relative changes in the water quality parameters under different operating scenarios (i.e. changes in water level) and summarize key findings; 3) identify data gaps and provide recommendations to resolve such gaps.

It is important to note that, although the models provide quantitative data as output, the models and their output should be considered preliminary at this time. Due to the accelerated schedule of this project and the lack of key data, the emphasis of this work was to construct the models based on readily available data and identify data gaps to resolve, so that the modeling and model results can be refined and improved as time progresses. In this regard, the models are used to estimate the relative change between alternatives, as opposed to determining absolute values of parameters.

Individual alternatives are in detail describe in chapter 8.1. The focus of the modeling effort is to analyze operating scenarios ranging from maximum lake elevation 4143 ft a.s.l. (above the sea level) to a minimum lake elevation 4138 ft a.s.l. **Figure 3-2.**

Changes in reservoir outflow effect lake hydrodynamic and water quality as shows on Figure 1-1. The main objective of this study is to determine the effect of the lake operation on these parameters used a suite of HD and WQ models.

Model simulation will be limited to those which are physically possible at this time. Currently maximum lake level is 4143 ft, and cannot be increased without structural changes to the physical system (e.g. levee height, additional flooding agricultural land and wetlands, road and bridge elevations). Modeled scenarios will facilitate comparison of various operating rules which effect outflows during summer months.

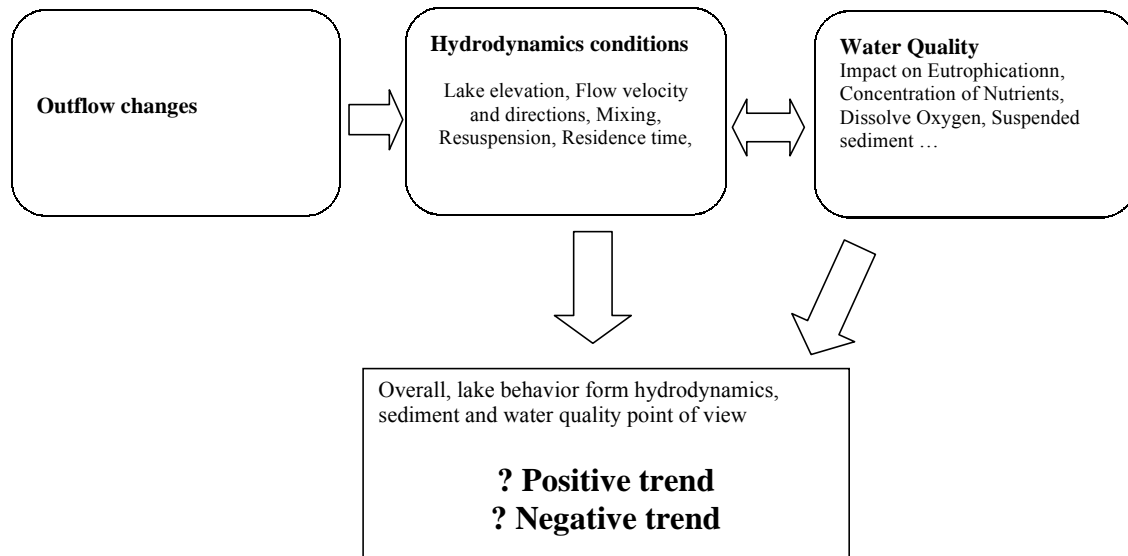


Figure 1-1 Effect on Lake Hydrodynamics and Water Quality

2. FINDINGS

This chapter summarizes findings related to the effect of lake level rise or lowering on key water quality parameters.

Lake level and dissolved oxygen.

For the reduced outflow scenario (increased lake elevation in late summer months) the results show improvement in DO (dissolved oxygen) condition in 57% of control stations; no change in 39% control stations a worse condition is in less than 4% percent of the control stations.

Results indicate that higher lake levels keep DO values greater near the water surface, but not at the bottom of the water column. There appears to be less fluctuation in DO within in the water column with increased lake depth. DO values increase with increased lake depth.

Lake level and eutrophication.

The reduced outflow scenarios show that an increase in nutrient or chlorophyll concentration in 67% of the control stations; a decrease in concentrations in 17% of the control stations, and no change in 16% of observed stations.

The findings in terms of increase or decrease in concentrations or primary production and respiration are summarized in Chapter 8 - Model applications and Results.

Lake level and sediment re-suspension.

The dominant seasonal wind direction is from the northwest, generally in line with the primary axis of Upper Klamath Lake. During summer months, northwest winds are on order of 10 miles per hour more than 25% of the summer season. Results show that when the lake level is greater than or equal than 4138 feet, these winds generate shear stresses on the bed on order of 7 dyn/cm². The critical bed erosion shear stress, estimated at 0.5 dyn/cm², is exceeded in the shallow areas along the eastern shore of the lake. Increasing the water level to 4142 feet results in an almost 10 times lower mean shear stress in the same areas. Moreover, the critical shear stress of 0.5 dyn/cm² is only exceeded very locally. Thus, an increase of the low lake water level from 4138 to 4142 feet is assumed to significantly reduce the re-suspension of sediment, for the wind conditions evaluated.

Lake level and re-suspension of phosphorous.

Previous studies indicate that phosphorous is typically available for re-suspension and release, provided the pH value is sufficiently high during the period of May through August. However, the increase in lake water level from the reduced outflow from the lake during this period is only in the order of 1 foot (from 4141 to 4142 feet). Thus, this rise in lake water level only slightly reduces the phosphorous load from sediment re-suspension. As described above, the lowest lake level will provide the greatest potential for re-suspension of the lake sediments;

however, the modeling indicated peak occurrences of total phosphorous (TP), phosphate (IP), dissolved oxygen (DO) and chlorophyll (ChL) occur before the low lake level.

Wind speed and wave motion.

Dominant seasonal wind direction is from the northwest, Wind speeds from this direction are more pronounced during the summer period when typical wind speeds are in the order of 10 miles /hour for more than 25% of the time. For this predominant wind speed, model simulated maximum significant wave height is on the order of 0.6 feet, and corresponding simulated wave period is in the order of 2 seconds.

Data Gaps.

Flow, water level, and water quality (i.e. temperature, DO, pH, ChL) are available for a continuous period from 1991 through 2000. However, additional data would be valuable in order to refine and improve the modeling effort established with this project. Some known data gaps known include:

1. **Sediment data.** Sediment erosion characteristics and phosphorous content are crucial parameters required for detailed assessment of the release of phosphorous during re-suspension. Field measurements of iron in lake sediments in February or March would be valuable in order to refine model estimates.
2. **Wind data.** An array of wind speed sensors positioned along the length of the lake system would help describe orographic wind distribution, improving hydrodynamic modeling of lake circulation patterns.
3. **Water Velocity Data Measurements.** Water velocities are required for calibration and validation of the hydrodynamics model. These measurements are particularly critical during summer months. Water velocity is a significant factor in water quality conditions and the primary time of concern is during the summer. PWA made some velocity measurements during the course of this project; however, summer measurements would help to calibrate the modeling and increase the predictive capability of the models for water quality conditions during this crucial time period.
4. **Lack of measured lake circulation data.** Using available data, the hydrodynamic model has been used to estimate water circulation and particle tracking paths on the lake. Comparison of these modeled conditions with field data obtained from tracer investigations or floating GPS markers would be valuable to validate the model results;
5. **Water Quality Parameter for small tributaries, drains and pumps.** BOR, BIA and another organization involved in data monitoring should also focus on measurement flow and concentration entering lake from small tributaries, ditches and pumps to more accurately specify incoming flux of the nutrients to the lake.

In general, data for the UKL system appears to be dispersed among different agencies and researchers and some have uncertain quality. A centralized data repository and rigorous data QA/QC policy would significantly reduce the time required for data acquisition and improve the quality of model output. It is important to emphasize that although not all model results can be currently be verified because of the lack of data described above, the established models are based on sound mathematical descriptions of the relevant physical processes and are extremely useful to evaluate the relative impact of different lake management scenarios concerning lake level change and changing water quality loading to the system.

3. SITE DESCRIPTION

Upper Klamath Lake and Agency Lake Lakes (Figure 3-1) are located in south-central Oregon. Average rainfall for Klamath Falls is 13.3 inches and the mean annual temperature is 8.97 °C. References (29). Total drainage area is approximately 3810 square miles. The major tributary, Williamson River, has a drainage area approximately 3000 square miles and supplies Upper Klamath Lake with approximately 51% of the inflow to the lake system. The second major inflow comes from the Wood River, which contributes approximately 16% of the inflow. The smallest inflow is from Seven Mile Channel, which supplies approximately 6%. Precipitation supplies approximately 7%, based on an annual flow analysis for years 1992-1998. The rest of the inflows come from agricultural pumps (3%), and springs (16%).



Figure 3-1 Upper Klamath and Agency Lakes

Upper Klamath Lake has been regulated since 1921-23 to maintain higher lake elevations during the spring. The regulation also allows lake elevations to be drawn down lower than historic conditions during the late summer months. Historic max/min elevations vary from 4142/4140 to 4143/4137 feet (Figure 3-2).

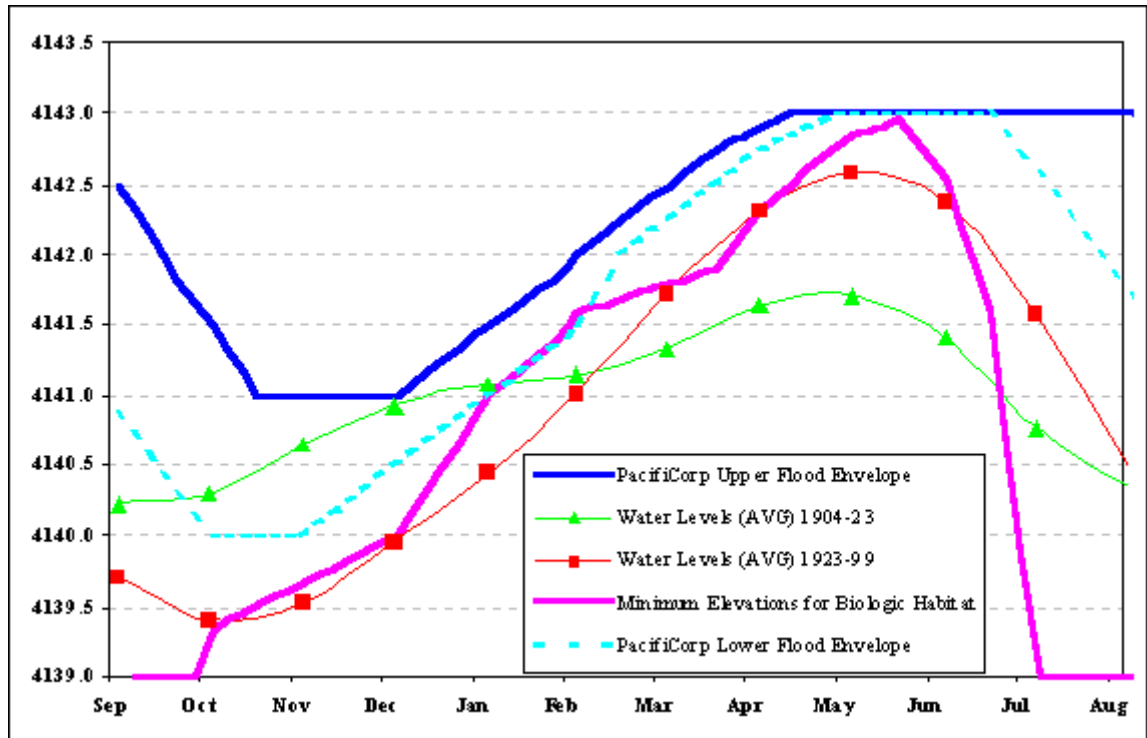


Figure 3-2 Operational Rules and Average Water Levels for Upper Klamath Lake

Historically, UKL was eutrophic. However, in recent years, the Organization for Economic Cooperation and Development (OECD) has classified the lake as a hypertrophic the highest level of eutrophication in the scale from ultraoligotrophy-oligotrophy-mesotrophy-eutrophy to hypertrophy (Table 3-1).

Table 3-1 Comparison of UKL water quality values to OECD standards

Parameter	OECD standard for hypertrophic lake	UKL values
mean TP	≥ 100 µg/l	150-200 µg/l
mean Chl _a	≥ 25 µg/l	50-100 µg/l
peak Chl _a	≥ 75 µg/l	300 µg/l
mean SD	≤ 1.5 m	1.0-0.5 m
peak SD	≤ 0.7 m	0.2 m

4. PHYSICAL PROCESSES

4.1 CIRCULATION

Upper Klamath and Agency Lakes (the ULK lake system) are connected to the four major bays (Pelican, Ball, Shoalwater and Wocus Bays) on the west side of Upper Klamath Lake (Figure 3-1). Agency Lake represents an almost independent part of the lake to the north. The hydrodynamic behavior of the lake system depends largely on seasonal wind speed and direction. Lake water levels can differ by more than one foot between Pelican Bay and the outlet to the lake at the dam. Flow between Upper Klamath and Agency Lake depends on water level changes and provides a reversible exchange of water volumes. The west part of the lake is the deepest and has the greatest flow velocities. Flow circulation (clock wise or anti-clock wise) between the north and middle parts of the lake is dependent on wind direction. During northern winds, the circulation is clock wise around Bare Island and anti-clock wise during southern winds.

4.2 THERMAL STRATIFICATION

Because lake system is shallow, and high winds lead to strong vertical mixing, thermal stratification is not observed in the lake.

In most cases, an increase in nutrients (i.e. nitrogen and phosphorous) is responsible for acceleration of the rate of lake enrichment (and diminished water quality). Both water quality and eutrophication depend on physical, chemical, and biological processes in the lake and its tributaries. The process depends on many variables and their interaction, competition, and weather conditions, as well as nutrient loading. At present, the high concentration of blue green algae is one of the most visible indications of poor water quality in the UKL system.

5. REVIEW OF DATA SOURCES

5.1 HYDROLOGICAL AND HYDRAULIC DATA

Upper Klamath and Agency Lakes have been studied in detail since the late 1960's; hydrologic data (i.e. discharge, water level, precipitation.) is readily available, whereas meteorological are limited. However, limited meteorological data proved reasonable for extended modeling applications. Because of the necessarily short time period for this project (three months), only readily available (i.e. existing) data from various sources were used. PWA conducted a one-day field reconnaissance to obtain lake water velocity measurement for calibrating the two-dimensional hydrodynamic model. The water balance, flows, water levels, wind data, and water quality were obtained from USGS, Bureau and Bureau of Indian Affairs (BIA) (29) as well as through personal communications with Jake Kann (Aquatic Ecosystem Sciences, LLC) and Bureau employees.

5.2 WIND DATA

The wind data were obtained from BOR and from BIA. Only one reliable station (Rattlesnake Point) with long term records currently exists in the close proximity of the UKL. Unfortunately, this station is effected by its geographical position at East part of the UKL. Figure 3-1 and Figure 5-1 The additional data were obtained for wind station at Klamath Falls airport. This station is approximately 20 miles southeast from the lake.



Figure 5-1 View on Upper Klamath Lake - Rattlesnake Point

5.3 WATER QUALITY DATA

PWA did not collect any additional data from Agency Lake, Upper Klamath Lake or tributaries. All Water Quality data were obtained from BOR and BIA stations and measurement sites. Figure 5-2 and Table 5-1.

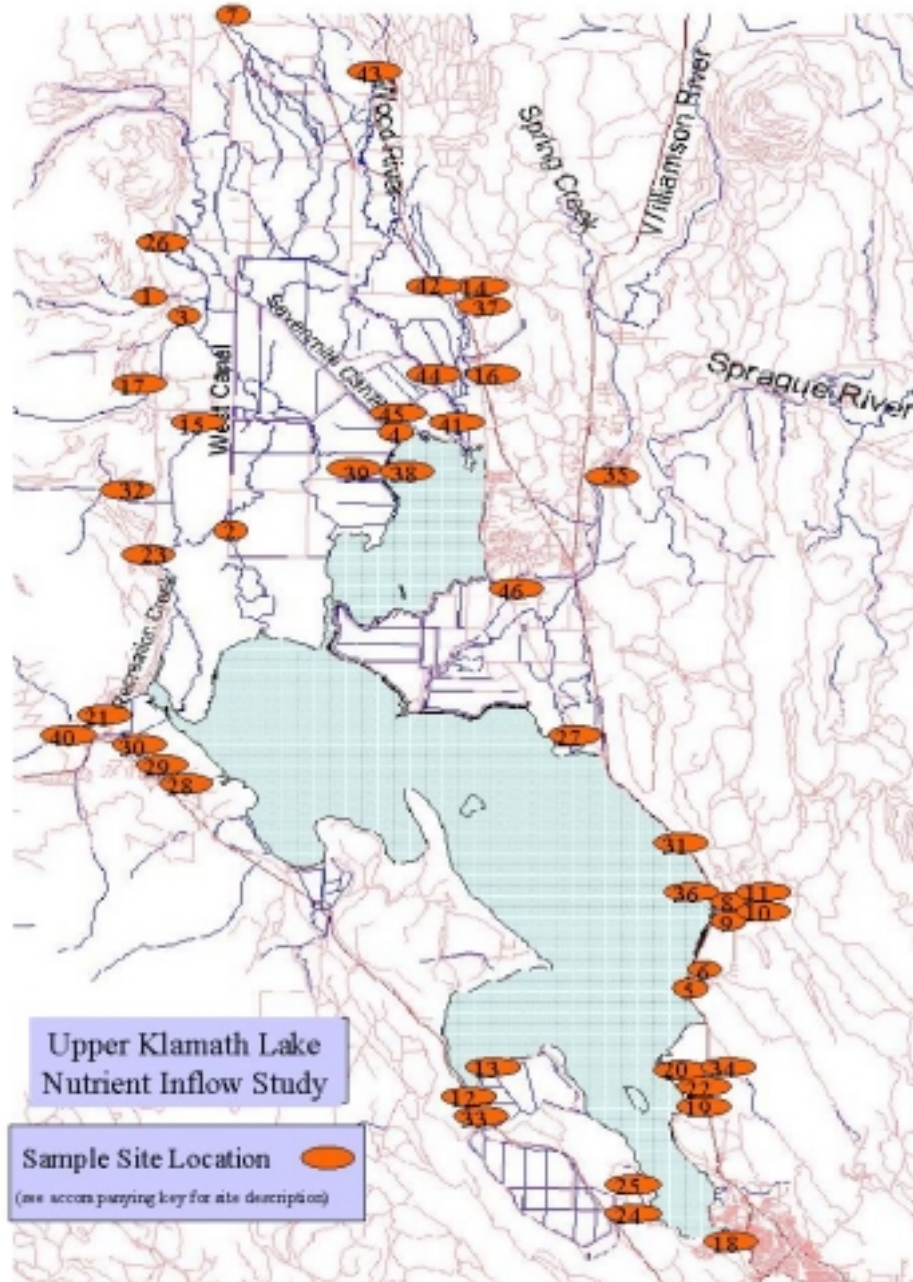


Figure 5-2 Upper Klamath Lake Nutrient Inflow Study

Table 5-1 WQ Measurements Sites on Tributaries (BIA)

Site #	Site Code	Description
1	3MCR	Three Mile Creek
2	4MCA	Four Mile Canal
3	4MSP	Four Mile Spring
4	7MCA	Seven Mile Canal
5	ALGOMA BRIDG	Hwy 97 where Alogoma drains to UKL
6	ALGPU	Rattlesnake Point Pump (ALGOMA PUMP)
7	ANCR	Annie Creek at USFS Bridge near Snow park
8	BSCA	Barkely Canal
9	BSFD	Barkley Field
10	BSPU	Barkley Pump
11	BSSP	Barkley Springs @ Hagelstein Park
12	CACA	Caledonia Canal (Lakeside of Hwy 140)
13	CAPU	Caledonia Pump - Draining Caledonia marsh
14	CC62	Crooked Creek AT HWY 62 BRIDGE
15	CCLO	Crystal Creek LODGE CHANNEL
16	CCPA	Crooked Creek AT PAIGE'S
17	CHCR	Cherry Creek.
18	FRBR	Freemont Bridge at Outlet of Klamath Lake
19	HAFD	Hanks Field
20	HAMA	Hanks Marsh (in marsh east of 97)
21	HASP	Harriman Spring
22	HMPU	Hanks Marsh Pump (draining ag area below marsh)
23	MASP	Malone Spring
24	MCPS	McCornack Pump South
25	MCPU	McCornack Pump
26	MESP	Mares Egg Spring
27	MOCA	Modoc Canal
28	ODCR	Odessa Creek
29	ODESSA CANAL	Odessa Canal draining to pump
30	ODPU	Odessa Pump
31	OXSP	Ouxy Springs
32	ROCR	Rock Creek (Draining to Crystal Creek)
33	RYPU	Wocus, Caledonia Canal South Pmp (RUNNING Y PUMP SOUTH)
34	SPPU	Shady Pine Pump (discharging into the marsh)
35	SRKB	Sprague @ Kirchers
36	SUSP	Sucker Springs
37	TESP	Tecumseh SPRINGS
38	TULANA PUMP	TULANA PUMP (LAKESIDE)

Site #	Site Code	Description
39	TUPU	Tulana Ranch Pump (into Agency Lake south of sevenmile)
40	VACR	Varney Creek
41	WODR	Wood River @ AGENCY LAKE (Dike Rd.)
42	WOWR	Wood River (WEED ROAD)
43	WODX	Wood River Dixon Road
44	WRRPE	Wood River Ranch PUMP EAST (INTO WOOD RIVER)
45	WRRPW	Wood River Ranch PUMP WEST (INTO 7-MILE CANAL)
46	WRST	Williamson River @ Store (Bridge Crossing on Modoc Pt. Rd.)

5.4 SEDIMENT DATA

Model parameters are necessary for describing sediment behavior (e.g. critical shear stress for sediment resuspension, suspended sediment concentration, sediment composition, fall velocity). Unfortunately, these types of data are not currently available in the necessary form. Although no data are available with respect to sediment characteristics, critical shear stress for erosion (resuspension) is typically on the order of 0.02 to 0.1 N/m² for fine lake bottom sediments (clays, silt). Previous studies (in similar type of lakes) assumed a shear stress of 0.05 N/m² (0.5 dynes/cm²).

5.5 BATHYMETRY

Figure 5-3 shows bathymetric map of the lake. Mean bed elevation is approximately 4134.5 ft. Consider maximum lake water level at 4143 and minimum water level 4139 ft lake is shallow and some part of the lake bed became dry during summer months. Exception is deep ridge in west part of the lake with depth up to 25-30 ft. The maximum water volume in the lake is 0.47 mil ac-ft. Figure 5-4

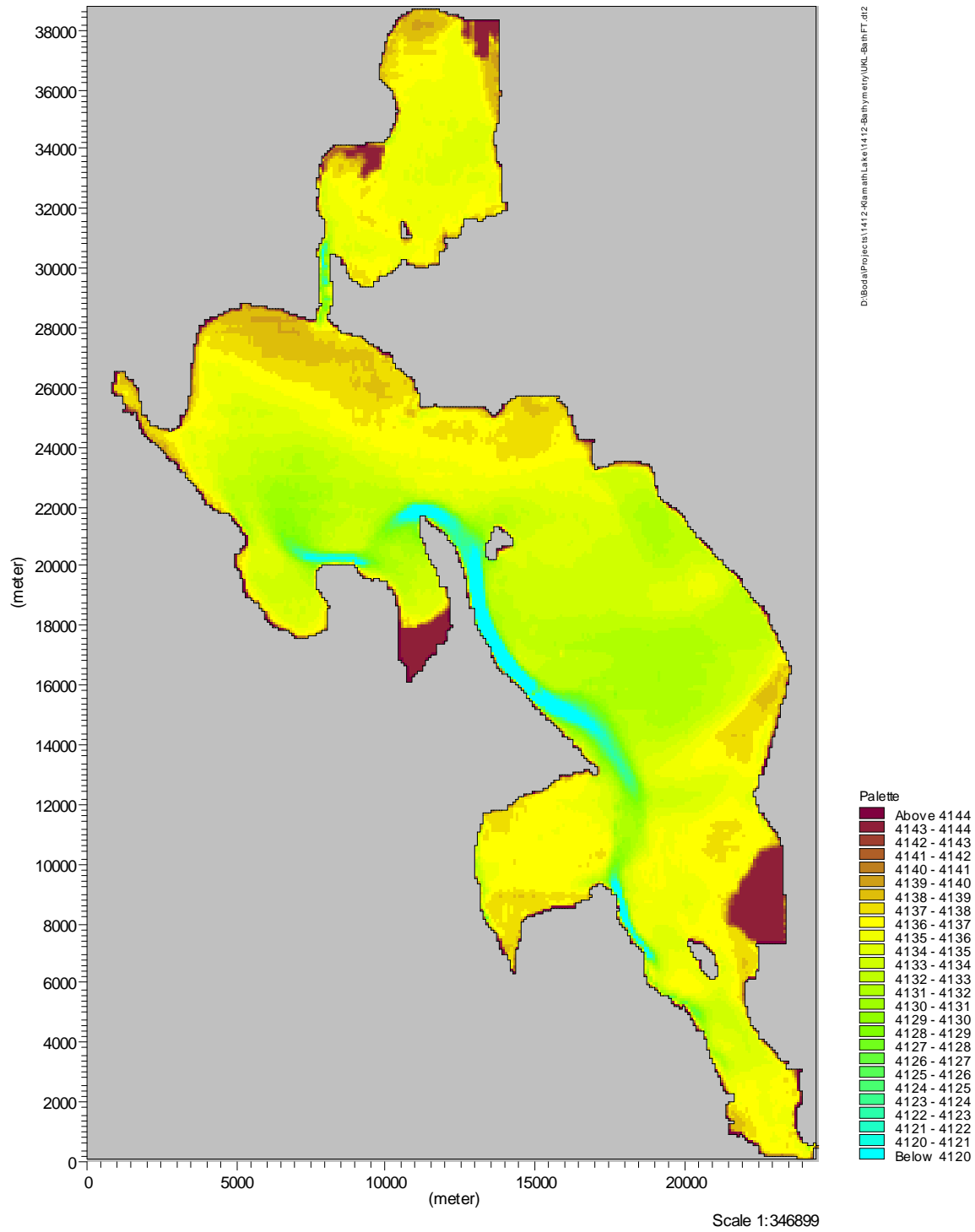


Figure 5-3 Upper Klamath Lake - Bathymetry

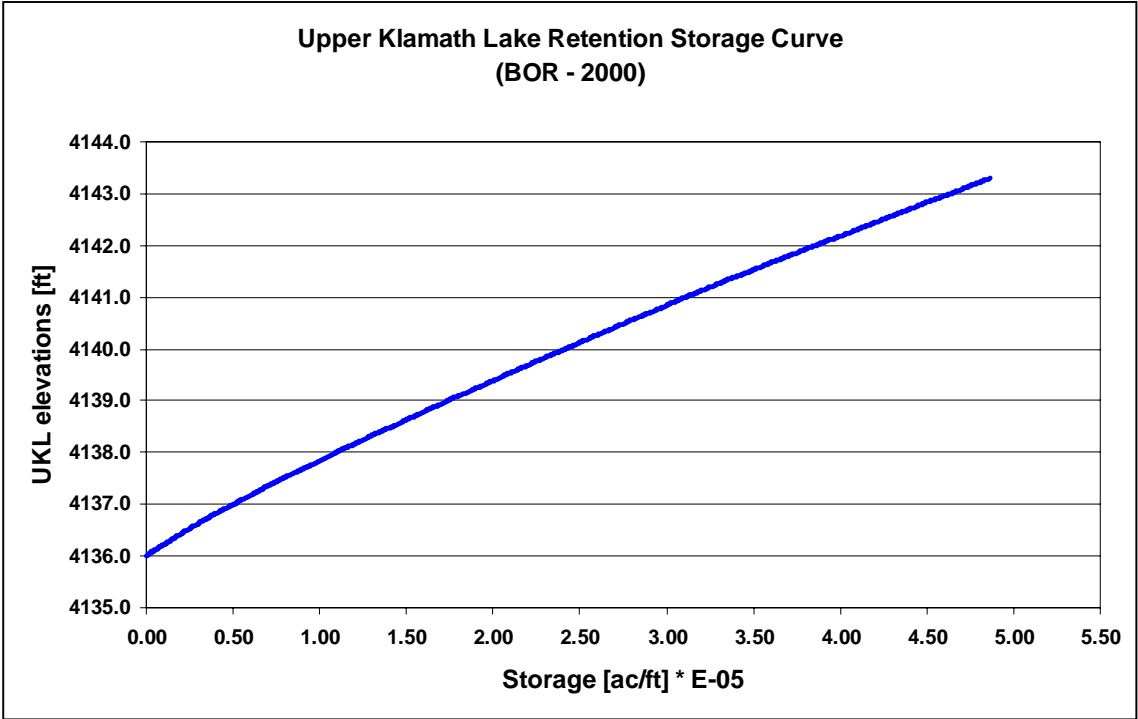


Figure 5-4 UKL retention Storage Curve

6. MODELS DESCRIPTION

6.1 MIKE 11, MIKE 21 AND MIKE 3

The MIKE suite of models can be used to simulate flow, water quality and sediment transport in rivers, channels, estuaries, lakes, seas, and coastal waters. The model suite is built in a modular manner, thus allowing for individual configurations as determined by project needs. The number specified in the model name describes the dimension of the model. For example, MIKE 11 is a one-dimensional, one layer model, MIKE 21 is two-dimensional and one layer model, and MIKE 3 is a fully three-dimensional model (Figure 6-1). The models are fully dynamic, employing a finite difference solution scheme. PWA and DHI used all three models, MIKE 11, MIKE 21, and MIKE 3 for this project. MIKE 11 was used to simulate long-term hydrodynamic (HD) and eutrophication (EU); MIKE 21 was used to simulate short-term hydrodynamic and sediment transport (MT); and MIKE 3 was used to simulate short-term hydrodynamic and water quality/dissolved oxygen simulations (WQ/DO).

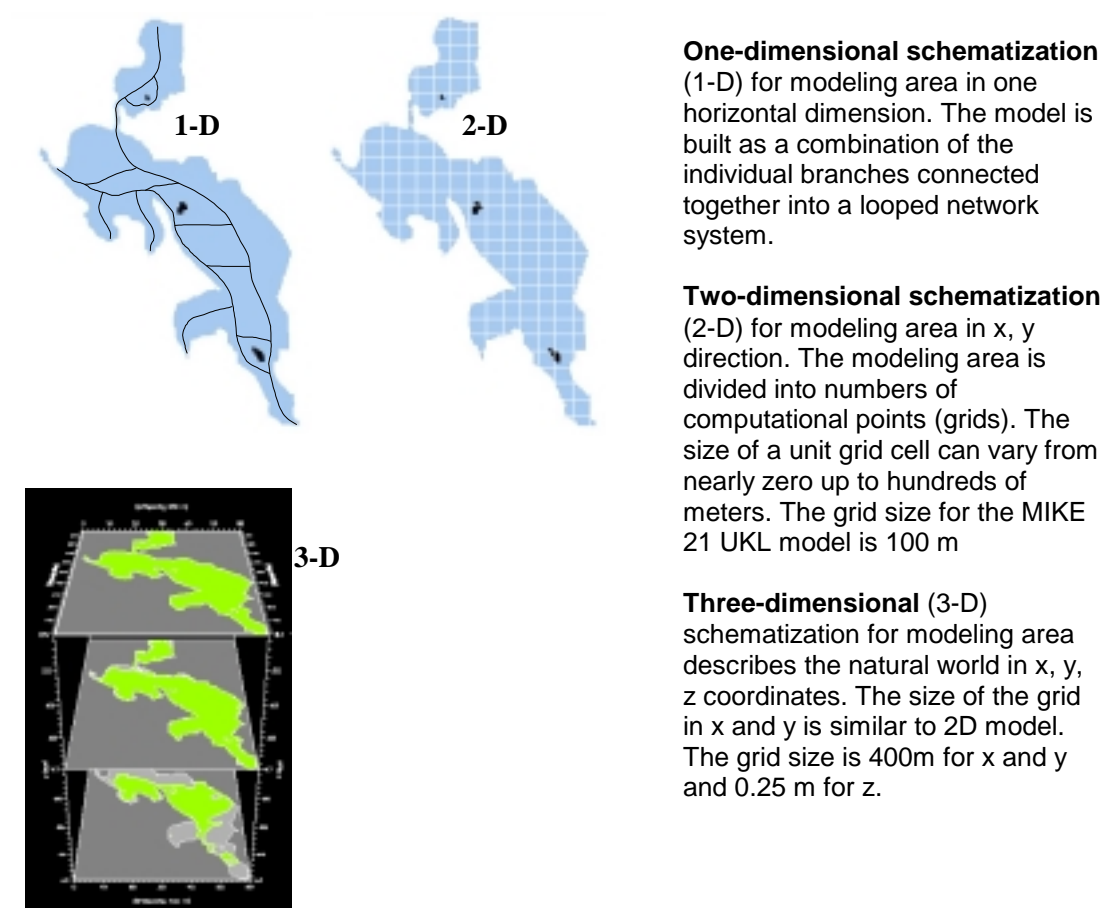


Figure 6-1 General schematics of 1-D, 2-D and 3-D models applied to Upper Klamath Lake

6.1.1 Hydrodynamic Model Description for Mike 11 and Mike 21

The hydrodynamic description for MIKE 11 HD is based upon the equations of conservation of mass and momentum (the Saint-Venant equations), including hydraulic resistance (e.g. Chezy coefficient) and lateral inflow. The system solves the time dependent equation in one (x) dimension.

MIKE 21 HD simulates variation in water level and flow in response to a variety of forcing functions in lakes, estuaries, bays, and coastal areas. Water level and flow are resolved on a rectangular grid covering the area of interest.

MIKE 21 HD includes formulations for the effects of:

- convective and cross momentum
- bottom shear stress
- wind shear stress at the surface
- barometric pressure gradients
- Coriolis forces
- momentum dispersion (through the Smagorinsky formulation)
- wave-induced currents
- sources and sinks (mass and momentum)
- evaporation
- flooding and drying

Hydrographic boundary conditions can be specified as a constant or variable (in time and space) level or flux at each open model boundary, as a constant or variable source or sink anywhere within the model, and as an initial free surface level map applied over the entire model.

6.1.2 Basic Equations

MIKE 21 is a general numerical modeling system for the simulation of water levels and flows in estuaries, bays, and coastal areas. It simulates unsteady 2D flows in one layer (vertically homogeneous) fluids.

The following equations for the conservation of mass and momentum are integrated over the vertical to describe the flow and water level variations:

CONTINUITY

$$\frac{\partial \zeta}{\partial t} + \frac{\partial p}{\partial x} + \frac{\partial q}{\partial y} = 0$$

x-MOMENTUM

$$\begin{aligned} \frac{\partial p}{\partial t} + \frac{\partial}{\partial x} \left(\frac{p^2}{h} \right) + \frac{\partial}{\partial y} \left(\frac{pq}{h} \right) + gh \frac{\partial \zeta}{\partial x} + \frac{gp\sqrt{p^2 + q^2}}{C^2 h^2} \\ - \frac{1}{\rho_w} \left[\frac{\partial}{\partial x} (h\tau_{xx}) + \frac{\partial}{\partial y} (h\tau_{xy}) \right] - \Omega q - fVV_x + \frac{h}{\rho_w} \frac{\partial p_a}{\partial x} = 0 \end{aligned}$$

y-MOMENTUM

$$\begin{aligned} \frac{\partial q}{\partial t} + \frac{\partial}{\partial y} \left(\frac{q^2}{h} \right) + \frac{\partial}{\partial x} \left(\frac{pq}{h} \right) + gh \frac{\partial \zeta}{\partial y} + \frac{gq\sqrt{p^2 + q^2}}{C^2 h^2} \\ - \frac{1}{\rho_w} \left[\frac{\partial}{\partial y} (h\tau_{yy}) + \frac{\partial}{\partial x} (h\tau_{xy}) \right] + \Omega p - fVV_y + \frac{h}{\rho_w} \frac{\partial p_a}{\partial y} = 0 \end{aligned}$$

x, y	space coordinates (m)
T	time (s)
$h(x, y, t)$	water depth (m)
$\zeta(x, y, t)$	surface elevation (m)
$u(x, t)$	velocity in x-direction (m s^{-1})
$v(y, t)$	velocity in y-direction (m s^{-1})
$p(x, t)$	flux density in x- direction ($\text{m}^3 \text{s}^{-1} \text{m}^{-1}$)
$q(y, t)$	flux density in y-direction ($\text{m}^3 \text{s}^{-1} \text{m}^{-1}$)
$C(x, t)$	Chezy resistance ($\text{m}^{1/2} \text{s}^{-1}$)
g	acceleration due to gravity (m s^{-2})
$f(V)$	wind friction factor
$V, V_x, V_y(x, y, t)$	wind speed and components in x- and y-direction (m s^{-1})
$\Sigma(x, y)$	Coriolis parameter, latitude dependent (s^{-1})
$p_a(x, y, t)$	atmospheric pressure ($\text{kg s}^{-2} \text{m}^{-1}$)
ρ_w	density of water (kg m^{-3})
ϑ	components of effective shear stress

6.1.3 Solution Techniques

The equations are solved by implicit finite difference techniques with the variables defined on a space staggered rectangular grid. A “fractioned-step” technique combined with an Alternating Direction Implicit (ADI) algorithm is used in the solution to avoid the necessity for iteration. Second order accuracy is ensured through the centering in time and space of all derivatives and coefficients. The ADI algorithm implies that at each time step a solution is first made in the x-momentum equations followed by a similar solution in the y-direction.

Application of the implicit finite difference scheme results in a tri-diagonal system of equations for each grid line in the model. The solution is obtained by inverting the tri-diagonal matrix using the Double Sweep algorithm, a very fast and accurate form of Gauss elimination.

The implicit scheme is used in MIKE 21 in such a way that stability problems do not occur, provided, of course, that the input data is physically reasonable, so that the time step used in the computations is limited only by accuracy requirements.

6.2 WATER QUALITY MODELS

6.2.1 MIKE11-3 WQ/EU

The Eutrophication (EU) model is normally used to predict water quality in terms of concentrations of nutrients (N and P), chlorophyll and oxygen concentration for different scenarios of external nutrients loads. The EU can be extended with a sediment-N and P description, which improve the description of the internal load of N and P. Agency and Upper Klamath Lakes are dominated by internal loads of P, therefore sediment N & P description is included in model formulations. The EU model, including sediment N and P, exists in a module which can communicate with a 3-D hydrodynamic model (MIKE 3) or a 1-D hydrodynamic model (MIKE 11). In the case of Upper Klamath Lake, it was decided to use the EU module with the simplest hydraulic model, MIKE 11, as this combination allows the opportunity to make long term simulations up to a decade, while minimizing computation time that typically extended over a night.

6.2.2 MIKE 11 EU Model

The eutrophication module used for the Upper Klamath Lake is a special version of the standard EU model with sediment N and P description, ref. (11). In the pelagic, the EU model has been extended with an additional algae group (blue greens) able to make nitrogen fixation. An empirical description of pH has been added which is valid for Upper Klamath Lake and Agency Lake, ref. (30), (28). The sediment P description has been changed so the sediment P sorption capacity is dependent on the pH above 8.5 in the water. Details on the simulation techniques for this model are described in the remainder of this section.

State variables. Simulated state variables in the EU model for UKL are listed below. State variables indicated with bold have been specially implemented for the UKL set up:

Pelagic:

PC1	Phytoplankton other than blue greens, carbon, g C/m ³	
PN1	Phytoplankton other than blue greens, nitrogen, g N/m ³	
PP1	Phytoplankton other than blue greens, phosphorus, g P/m ³	
PC2	Phytoplankton blue greens, carbon, g C/m³	Additional Algae Group
PN2	Phytoplankton blue greens, nitrogen, g N/m³	Additional Algae Group
PP2	Phytoplankton blue greens, phosphorus, g P/m³	Additional Algae Group
Chl	Chlorophyll-a mg/m ³	
ZC	Zooplankton carbon, g C/m ³	
DC	Detritus carbon, g C/m ³	
DN	Detritus nitrogen, g N/m ³	
DP	Detritus phosphorus g P/m ³	
NO3	Nitrate nitrogen, g N/m ³	
NH4	Total ammonium, g N/m ³	
IP	Phosphate-P, g P/m ³	
DO	Dissolved oxygen, g O ₂ /m ³	

Sediment N

SON	Exchangeable organic N in sediment, g N/ m ²
SN3	NO ₃ -N in pore water, g N/ m ³
SNH	NH ₄ -N in pore water, g N/ m ³

Sediment P

SOP	Exchangeable organic P in sediment, g P/ m ²
SIP	PO ₄ -P in pore water, g P/ m ³
FESP	Sorbed P to oxidised metals (Fe, Mn), g P/ m ²
SPAD	Sorbed P to reduced, g P/ m ²

The processes involved in the flow of carbon, nitrogen, and phosphorus in the pelagic are illustrated (Figure 6-2, Figure 6-3, and Figure 6-4).

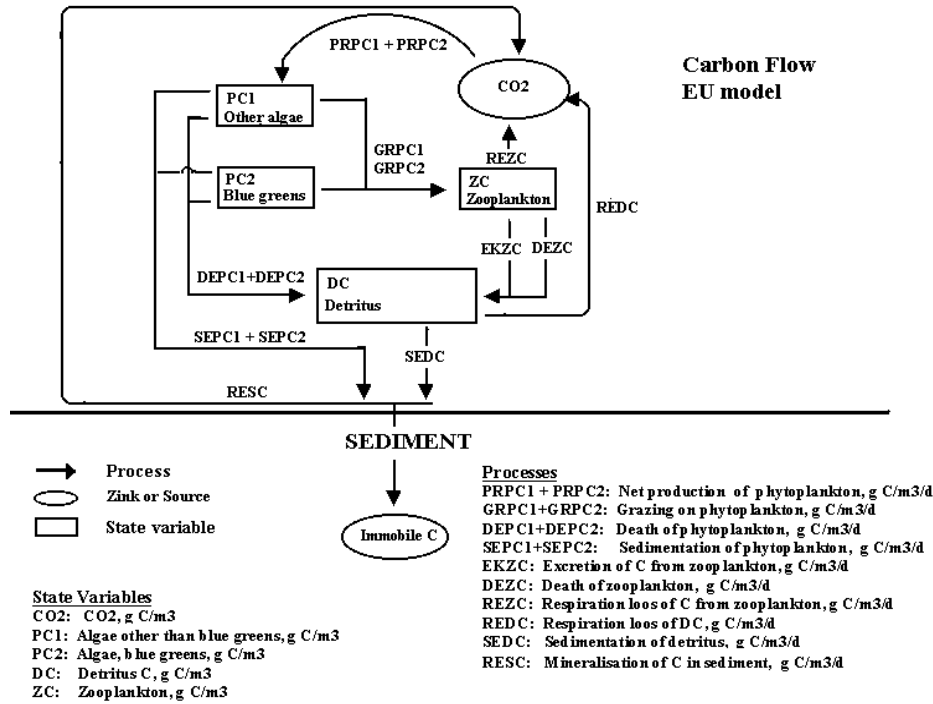


Figure 6-2 Carbon Flow in Pelagic Part of EU Model

Introduction of blue green algae in the model gives three new state variables C, N and P in the algae (PC2, PN2 and PP2). The N-fixation is assumed to take place according to N/P ratio below 14 by weight. The N fixation is described according to Monod kinetics with N/P ratio as an independent variable.

Nitrogen Fixation. Nitrogen fixation by blue greens in the EU model is described using the following equation:

$$NFIX = PC2 * KNFIX1 * \frac{(14 - N/P)}{(14 - N/P) + KQOPPN2}$$

where:

- PC2: Biomass of blue greens, g C/ m³
 KNFIX1: Max specific N fixation, g N/g C
 KQOPPN2: Half saturation constant.

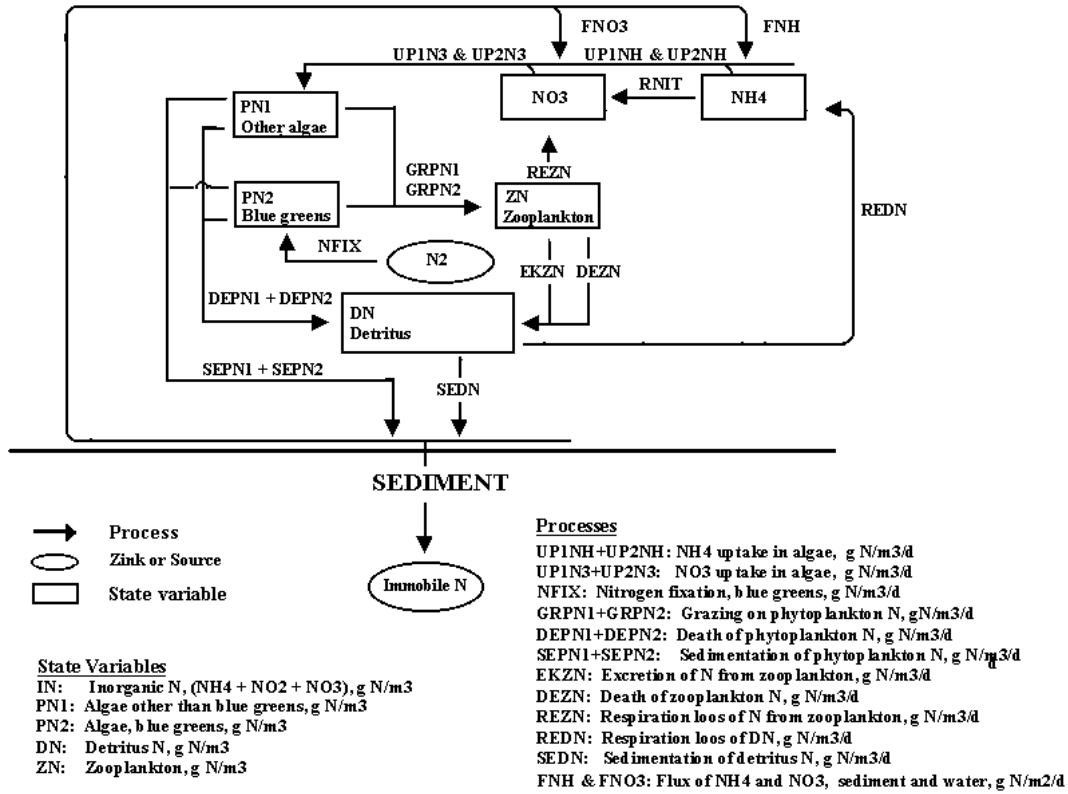


Figure 6-3 Nitrogen Flow in Pelagic Part of EU Model

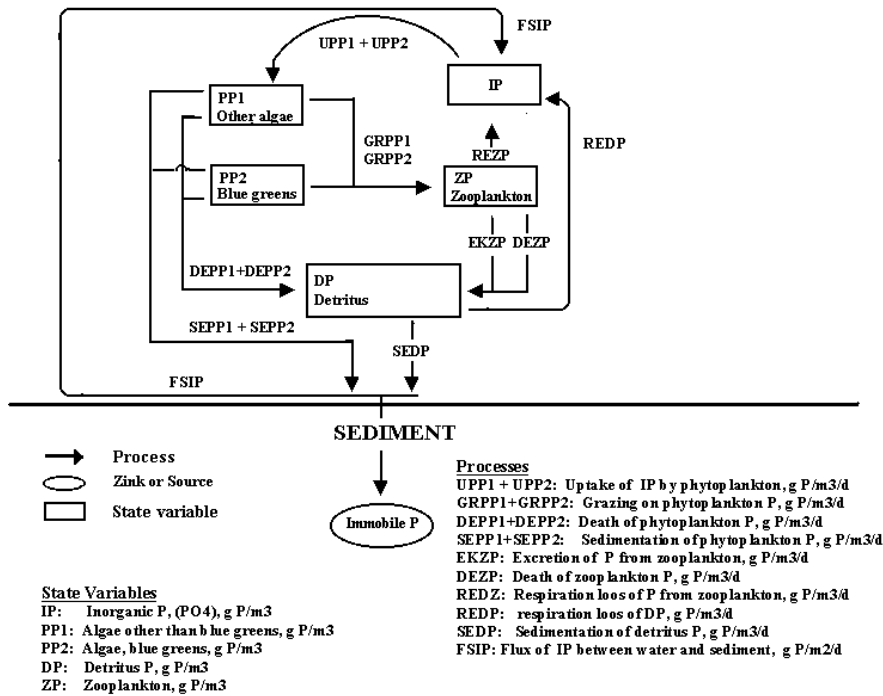


Figure 6-4 Phosphorus Flow in Pelagic Part of EU Model

Nitrogen fixation is well documented in Agency Lake and Upper Klamath Lake through mass balance calculations and by observations of heterocyst formation by the N-fixation blue green algae *Aph. flos-aquae*. ref. (29), (30), (46).

The competition between the two algae groups in the model is the result of the N- fixation blue greens having a lower maximum specific growth rate, a lower affinity to pick up inorganic nutrient from the water, a lower sinking rate, and lower affinity to be grazed by zooplankton. This combination will give the blue greens an advantage in shallow systems with ambient access to phosphate and low access to inorganic N.

pH and P Sorption Capacity. pH in the water is described according to the below relation with chlorophyll as the driving variable, ref. (30), (28).

$$pH = 0.161 * \ln(Chla) , \text{ valid from June to October}$$

The relation is valid only for Agency and Upper Klamath Lakes.

pH is used to simulate the P sorption capacity of oxidized Fe in the sediment. Besides iron, aluminum oxides are able to adsorb PO₄-P. The adsorption capacity of P for these metals is changed with pH, with the highest sorption capacity at low pH and lowest sorption capacity at high pH. Besides pH, the redox potential in the sediment changes the sorption capacity of Fe, as reduced Fe has a much lower P sorption capacity. P sorbed by Al-oxides does not occur in the same way as P sorbed by Fe which is effected by the redox potential in the sediment.

Sediment P Module. These mechanisms for P sorption to Fe are included in the sediment P module, (Figure 6-6). The pool of P sorbed to oxidized Fe (SPFE) is dependent on the oxidized layer of the sediment. This layer is defined as the penetration depth of O₂ or NO₃-N into the sediment. Normally O₂ only will penetrate a few millimeters whereas NO₃-N can be present a few centimeters into the sediment. The penetration of NO₃-N into the sediment is simulated in the sediment N module (Figure 6-5). In spring, the temperature will raise and the biological activity will increase, whereby the oxidized layer will decrease. P sorbed to Fe⁺⁺⁺ will be liberated into the pore water and be transported into the water by different mechanisms.

Parallel to this mechanism, pH in the water raises due to photosynthesis. Experiments have shown that increased pH in the water increases the flux of P from the sediment into the water because pH increases in the surface sediment. This results in P being adsorbed to oxidized iron and aluminum liberated into the pore water, ref. (1) and (24).

The pH effect is included in the sediment P module by reducing both the P sorption capacity of oxidized sediment (Fe⁺⁺⁺) and reduced sediment (Al) with pH above 8.5 in the water. Data from Lake Kvind and Lake Esrum ref. (1), (22), has been used to estimate the model parameters for the pH dependent P release. If the surface sediment is resuspended into water with high pH, P sorbed to Fe and Al will be released immediately, this process is however not included in the

model. The processes for releasing sorbed P is closely coupled as indicated below, and it can be difficult find the domination or triggering process for P release resulting in an algae bloom.

Increased temperature => decreased oxidized layer => increased P flux from sediment.

Increased pH in water => decreased P sorption by Fe, Al => increased P flux from surface sediment.

Resuspension of surface sediment into water with high pH => release of PO₄-P.

Increased P flux from sediment or release of PO₄-P from resuspended sediment => Increased photosynthesis => increased pH.

The flux of PO₄ between pore water and water is described as the product of the concentration difference and a diffusion constant. At an early stage of this project, it became clear that this diffusion constant had to vary over the season with a maximum at the end of July to get the simulated and the measured total P concentration in the water to fit. The reason for this variation could be increased resuspension, bioturbation by the large benthic fauna in the lake or simply a loosening of the surface sediment through gas formation.

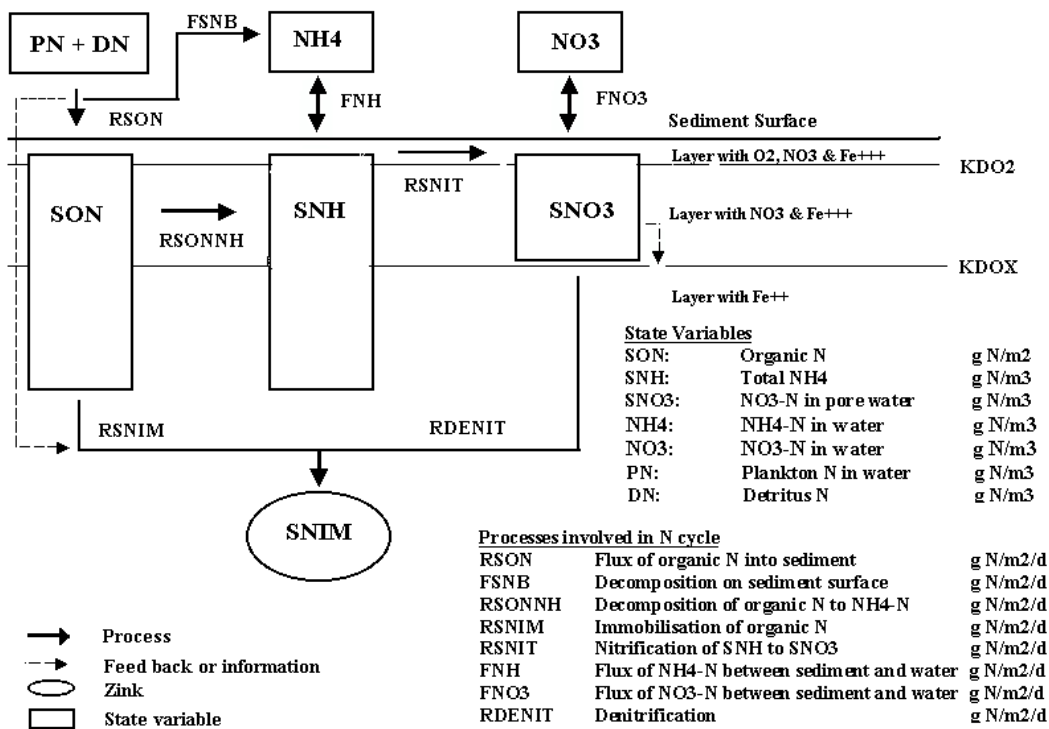


Figure 6-5 N flow in sediment module to EU model

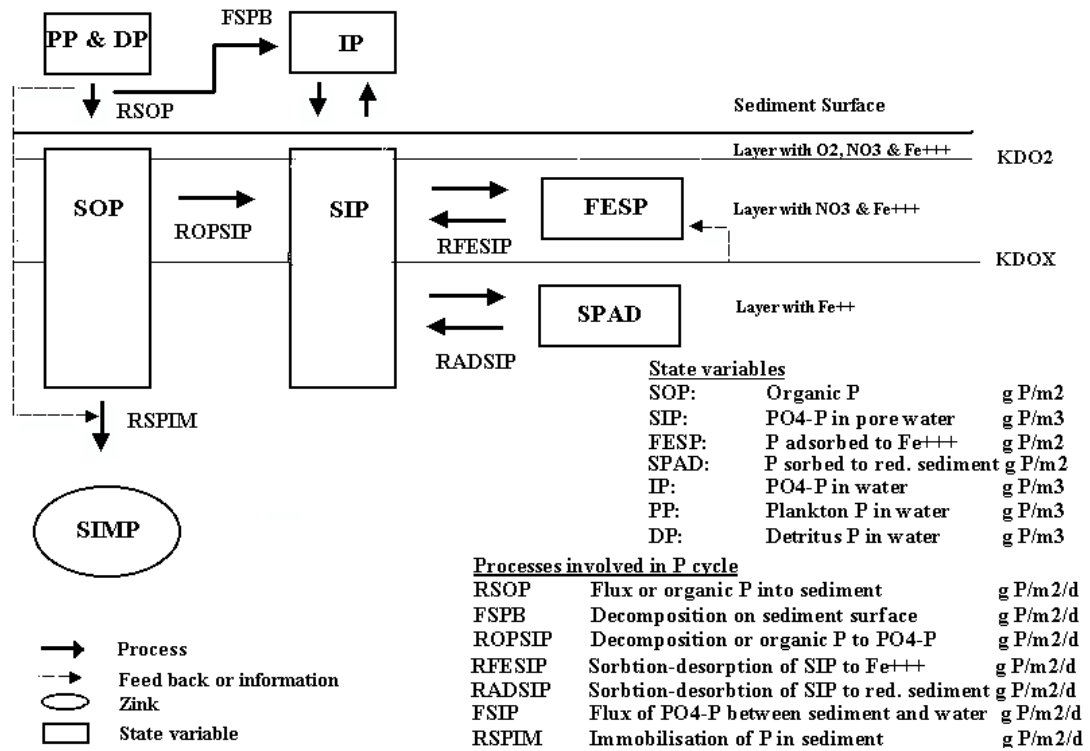


Figure 6-6 P flow in sediment P module to EU model

In the sediment P module, the variation of the diffusion is expressed by the below equation:

$$P - \text{diffusion} = KFIP * \text{EXP}\left(\frac{\text{abs}(\text{day} - 230)}{180}\right), \text{ m2/d}$$

where:

$KFIP$ = Diffusion constant, m2/d

day = Julian day.

The EU module calculates all processes on a daily basis, although some of the processes have a diurnal variation such as the production of oxygen through photosynthesis. This has the implication that the EU module is unable to simulate diurnal variation in the oxygen concentration in the water column.

Measurements from Klamath Lake show that these variations are quite significant, with over saturation at noon, and severe under saturation at dawn. The 1-D MIKE 11 model results show a daily average for oxygen concentration averaged over depth and cross-section. MIKE 11's interpretation of simulated oxygen concentration should be taken into account.

However, the sediment respiration, respiration in the water, and production of oxygen simulated by the EU can be extracted and put into the Water Quality model as a forcing function for

simulating daily variations in oxygen concentration over short periods. Model results from EU module will be used as input to the WQ module using a 3-D hydrodynamic model.

6.3 WAVE/SEDIMENT TRANSPORT MODEL

6.3.1 MIKE 21 NSW/MT

The MIKE 21 nearshore spectral wind-wave module (NSW) is a stationary, directionally decoupled, parametric, spectral wind wave model that describes the propagation, growth, and decay of short period waves in near shore areas. The model takes into account the effect of refraction and shoaling due to varying depth, wind generation, energy dissipation due to bottom friction, and wave breaking. The effects of currents on these phenomena are included. To include the effects of currents, the basic equations in the model are derived from the conservation equation for the spectral wave action density. MIKE 21 MT describes the processes of resuspension, erosion, transport, and deposition of silt, mud and clay particles under the action of waves and currents.

Basic Equations. The basic equations in MIKE 21 NSW are derived from the conservation equation for the spectral wave action density based on the approach proposed by Holthuijsen et al. (1989). A parameterization of this equation in the frequency domain is performed introducing the zeroth and first moment of the action spectrum as dependent variables. This leads to the following two coupled partial differential equations:

$$\frac{\partial(c_{gx}m_0)}{\partial x} + \frac{\partial(c_{gy}m_0)}{\partial y} + \frac{\partial(c_\theta m_0)}{\partial \theta} = S_0$$

$$\frac{\partial(c_{gx}m_1)}{\partial x} + \frac{\partial(c_{gy}m_1)}{\partial y} + \frac{\partial(c_\theta m_1)}{\partial \theta} = S_1$$

The spectral moments $m_n(\theta)$ are defined by:

$$m_n(\theta) = \int_0^\infty \omega^n A(\omega, \theta) d\omega$$

Where ω is the absolute frequency and A is the spectral wave action density. The propagation speed c_θ and group velocities c_{gx} and c_{gy} are obtained using linear wave theory. The left-hand side of the basic equations accounts for the effect of refraction and shoaling. The source terms S_0 and S_1 account for the effect of energy input from the wind, bottom dissipation and wave breaking. The effects of current on these phenomena are included.

In MIKE 21 NSW, the source terms for the local wind generation are derived directly from the Shore Protection Manual (1984) formulation for fetch-limited wave growth in deep water. The

description of the bottom dissipation is based on the quadratic friction law to represent bottom shear stress (Svendsen and Jonsson, 1980) and the description of the wave breaking is based on the expressions given by Battjes and Janssen (1978). The effects of the bottom dissipation and wave breaking on the mean frequency are also included.

From $m_0(\theta)$ and $m_1(\theta)$, two wave parameters can be calculated; the directional wave action spectrum $A_0(\theta) = m_0(\theta)$ and the mean frequency per direction $\omega_1(\theta) = m_1(\theta)/m_0(\theta)$.

Symbol	Units
$m_0(x, y, \theta)$	zeroth moment of the action spectrum (m^2)
$m_1(x, y, \theta)$	first moment of the action spectrum (m^2/s)
c_{gx}, c_{gy}	components in the x- and y-direction, respectively, of the group velocity c_g (m/s)
c_θ	propagation speed representing the change of action in the θ -direction (m/s)
x and y	Cartesian coordinates (m)
θ	direction of wave propagation (deg.)
S_0, S_1	source terms (m^2 and m^2/s)

Solution Technique. The spatial discretization of the basic partial differential equations is performed using an Eulerian finite difference technique. The zero and first moment of the action spectrum are calculated on a rectangular grid for a number of discrete directions. In the x-direction, linear forward differencing are applied, while in both the y- and θ -directions it is possible to choose between linear upwind differencing, central differencing and quadratic upwind differencing. The best results are usually obtained using linear upwind differencing both in the y- and θ -directions.

The source terms due to the local wind generation are introduced explicitly, while the source terms due to bottom dissipation and wave breaking are introduced implicitly. Hence, a non-linear iteration is performed at each grid point. The non-linear algebraic equation system resulting from the spatial discretization is solved using a once-through marching procedure in the x-direction (the predominant direction of wave propagation) restricting the angle between the direction of wave propagation and the x-axis to be less than 90 degrees. In practice, this angle must be less than about 60 degrees due to numerical stability considerations. MIKE 21 NSW can be applied for waves with wave periods between 0.21 seconds and 21 seconds.

6.3.2 MIKE 21 Sediment Transport (Multi-layer Mud Model)

The mud transport module of MIKE 21 (multi-layer mode) describes the erosion, transport, and deposition of silt, mud, and clay particles under action of currents and waves. For a correct solution of erosion, the consolidation of sediment layers deposited on the bed is also included. The model is essentially based on the principles in Mehta et al. (1989) with the innovation of including the bed shear stresses due to waves.

Mud mainly consists of cohesive sediments, which are so called because of the electrical Van der Waal binding forces between particles causing them to coagulate into 'flocs' in suspension and form a 'sticky mass' on the bed. A deterministic physically based description of the behavior of cohesive sediments has not yet been developed. Consequently, the mathematical descriptions of erosion and deposition are essentially empirical, although they are based on sound physical principles.

The lack of a universally applicable, physically-based formulation for cohesive sediment behavior means that any model of this phenomenon is heavily dependent on field data. Data over the entire area to be modeled is recommended, its "erodibility", settling velocities, insitu flocculation characteristics, vertical velocity and suspended sediment concentration profiles, compaction of layers under the sea bed surface, effect of wave action, and critical shear stresses for deposition and erosion. Naturally, the dynamic variation of water depth and flow velocities must also be known along with boundary values of suspended sediment concentration. The MIKE 21 mud module (multi-layer mode) consists of a 'water-column' and an 'in-the-bed' module. The link between these two modules is source/sink terms in an advection-dispersion model.

Settling velocities of fine, cohesive material is very low. Hence, the concentration of suspended material does not adjust immediately to changes in the hydraulic conditions. In other words, the sediment concentration at a given time and location is dependent on the conditions upstream of this location at an earlier time. In order to describe this process, the sediment computation has been built into the advection-dispersion module, MIKE 21AD. The two-dimensional differential transport equation is solved using a finite difference technique. The source and sink term S in the equation depends on whether the local hydrodynamic conditions cause the bed to become eroded or allow deposition to occur. Empirical relations are used, and one possible formulation for evaluating S is given below.

The mobile suspended sediment is transported by long-period waves only, which are tidal currents, whereas the wind-waves are considered as "shakers". Combined they are able to re-entrain or re-suspend the deposited or consolidated sediment.

The processes in the bed are described in a multi-layer bed (max 12 layers), each described by a critical shear stress, erosion coefficient, power of erosion, density of dry sediment and erosion function. The bed layers can be dense and consolidated or soft and partly consolidated. Liquefaction by waves is taken into account as a weakening of the bed due to breakdown of bed structure. Consolidation is included between the layers as a transition rate of sediment between

the layers. In areas with deep channels or large variations in water depths it is possible to include a sliding process, which allows sediment to slide down to deeper areas due to gravity and current motion. This is described by a dispersion equation.

Model Description. The physical processes are modeled by a 'multi bed layer approach'. An example with 3 bed layers is shown in Figure 6-7.

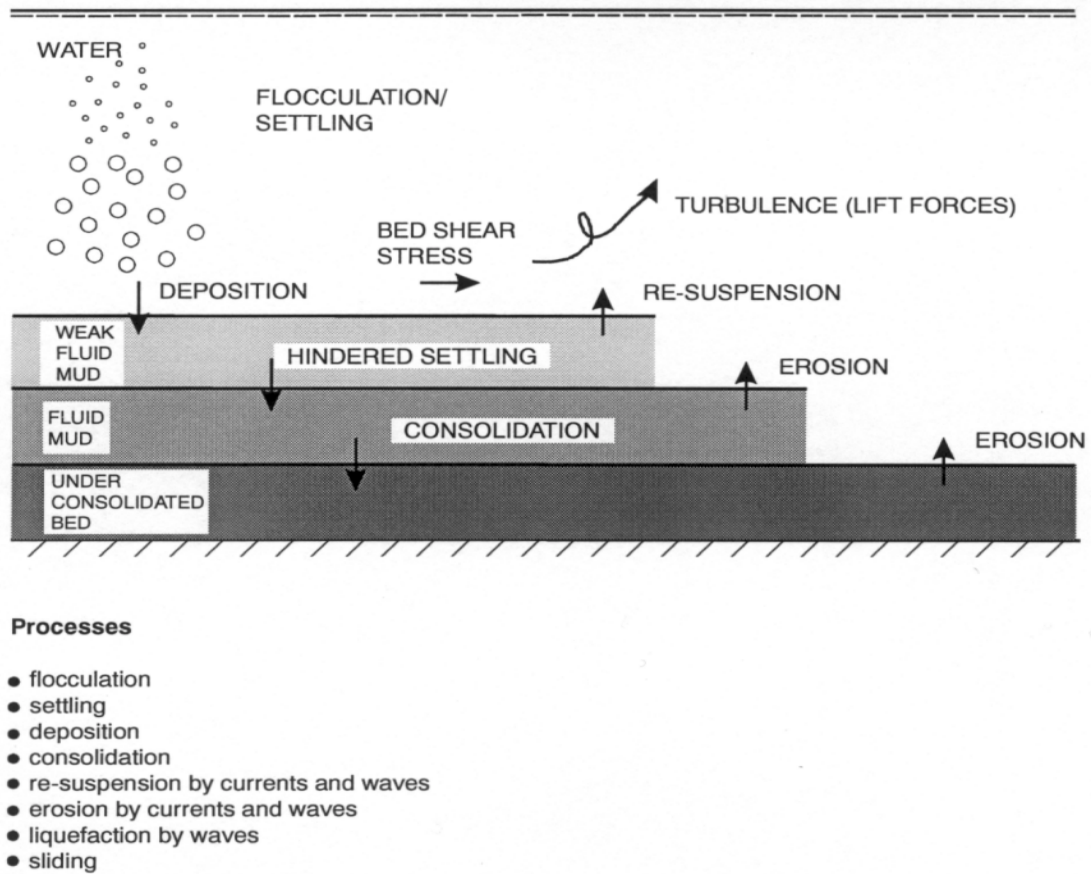


Figure 6-7 MIKE 21 Sediment Transport Model and Physical Processes

Advection-Dispersion. The advection/dispersion equation in two horizontal dimensions reads:

$$\frac{\partial \bar{c}}{\partial t} + V_x \frac{\partial \bar{c}}{\partial x} + V_y \frac{\partial \bar{c}}{\partial y} = \frac{1}{h} \frac{\partial}{\partial x} \left(h D_x \frac{\partial \bar{c}}{\partial x} \right) + \frac{1}{h} \frac{\partial}{\partial y} \left(h D_y \frac{\partial \bar{c}}{\partial y} \right) + \sum_{i=1}^n \frac{S_i}{h}$$

where:
 \bar{c} = depth averaged concentration (g/m³)

V_x, V_y	=	depth averaged flow velocities (m/s)
D_x, D_y	=	dispersion coefficients (m ² /s)
h	=	water depth (m)
S_i	=	source/sink term no. i (g/m ² /s)

Information on V_x , V_y and h at each time step is provided by the hydrodynamic module, MIKE 21 HD. For cohesive sediment a stochastic model for flow and sediment interaction is applied. This approach was first developed by Krone (1962).

Deposition. Krone suggests that the deposition rate can be expressed by:

$$\text{Deposition: } S_D = w_s c_b p_d$$

where:

w_s	=	settling velocity (m/s)
c_b	=	near bed concentration (g/m ³)
p_d	=	probability of deposition = $1 - \frac{\tau_b}{\tau_{cd}}$, $\tau_b \leq \tau_{cd}$
τ_b	=	the bed shear stress (N/m ²)
τ_{cd}	=	critical bed shear stress for deposition (N/m ²)

The settling velocity of cohesive sediment depends on the floc size, temperature, and concentration of particles and content of organic material. Several well established relations have been included in the model.

Erosion. Erosion can be described in two ways depending upon whether the bed is dense and consolidated or soft and partly consolidated, Mehta et al. (1989).

Dense, consolidated bed:

$$\text{Erosion: } S_E = E (1 - \tau_b / \tau_{ce})^n , \quad \tau_b > \tau_{ce}$$

where

E	=	erodibility of bed (g/m ² /s)
τ_{ce}	=	critical bed shear stress for erosion (N/m ²)
n	=	power of erosion

Soft, partly consolidated bed:

$$\text{Erosion: } S_E = E \exp[\alpha (\tau_b - \tau_{ce})^{1/2}], \quad \tau_b > \tau_{ce}$$

where

α	=	coefficient (m/N ^{1/2})
----------	---	-----------------------------------

Bed Description. The bed is described by multiple layers, where depositing material enters the first layer. Each layer is described by the critical shear stress for erosion, $\tau_{ce,i}$, power of erosion,

n_i , density of dry bed material, ρ_i , erosion coefficient, E_i , and α_i -coefficient. The layers represent weak fluid mud, fluid mud, and under-consolidated bed, Mehta et al. (1989) and are associated with different time scales. Initial thickness of the layers is required. The consolidation process is described as the transition of sediment between the layers, Teisson (1992).

Liquefaction by waves is taken into account as a weakening of the bed due to breakdown of bed structure. This may cause increased surface erosion, because of the reduced strength of the bed top layer, Delo and Ockenden (1992).

In areas with deep channels or large variations in water depth, the inclusion of sediment sliding from shallow to deeper parts is possible. This is described by a dispersion equation, Teisson (1992), Grishanin (1987). The dispersion equation is solved using an explicit finite difference scheme.

Bed Shear Stress. The bed shear stress can be calculated for a pure current or a combined wave-current motion, Fredsøe (1981). In the case of a pure current motion, the flow resistance is caused by the roughness of the bed. The bed shear stress under a current is calculated using the standard logarithmic resistance law:

$$\tau_c = \frac{1}{2} \rho f_c V^2$$

where

- τ_c = bed shear stress (N/m²)
- ρ = density of fluid (kg/m³)
- f_c = current friction factor

$$f_c = 2 \left(2.5 \left(\ln \left(\frac{30h}{k} \right) - 1 \right) \right)^2$$

- V = mean current velocity (m/s)
- h = water depth (m)
- k = bed roughness (m)

In the case of pure wave motion, the mean bed shear stress reads:

$$\tau_w = \frac{1}{2} \rho f_w U_b^2$$

where

$$\begin{aligned}
 f_w &= \text{wave friction factor} \\
 U_b &= \text{horizontal mean wave orbital velocity at the bed (m/s)} \\
 &= \frac{2H_s}{T_z} \frac{1}{\sinh\left(\frac{2\pi h}{L}\right)} \\
 H_s &= \text{significant wave height (m)} \\
 T_z &= \text{zero-crossing wave period (s)}.
 \end{aligned}$$

An explicit approximation given by Swart (1974) for the wave friction factor is used:

$$\begin{aligned}
 f_w &= 0.47, \quad \frac{a}{k} \leq 1 \\
 f_w &= \exp\left(5.213\left(\frac{a}{k}\right)^{-0.194} - 5.977\right), \quad 1 < \frac{a}{k} \leq 3000
 \end{aligned}$$

where

$$\begin{aligned}
 a &= \text{horizontal mean wave orbital motion at bed (m)} \\
 &= \frac{H_s}{\pi} \frac{1}{\sinh\left(\frac{2\pi h}{L}\right)}
 \end{aligned}$$

An explicit expression of the wave length is given by Fenton and McKee (1990).

$$L = \frac{gT_z^2}{2\pi} \left(\tanh\left[\frac{2\pi}{T_z} \sqrt{\frac{h}{g}}\right]^{3/2} \right)^{2/3}$$

Solution Technique. The advection-dispersion equation is solved using an explicit, third-order finite difference scheme, known as the ULTIMATE scheme, Leonard (1991). This scheme is based on the well-known QUICKEST scheme, Leonard (1979), Ekebjærg et al. (1991).

7. MODEL CALIBRATION

7.1 MIKE 11 HD

The hydrodynamic component of the model was calibrated for a 10-year period to analyze the overall balance and accuracy of the description for retention storage in the lake. Measured and simulated water levels show a reasonably good comparison for the 10-year period (Figure 7-1).

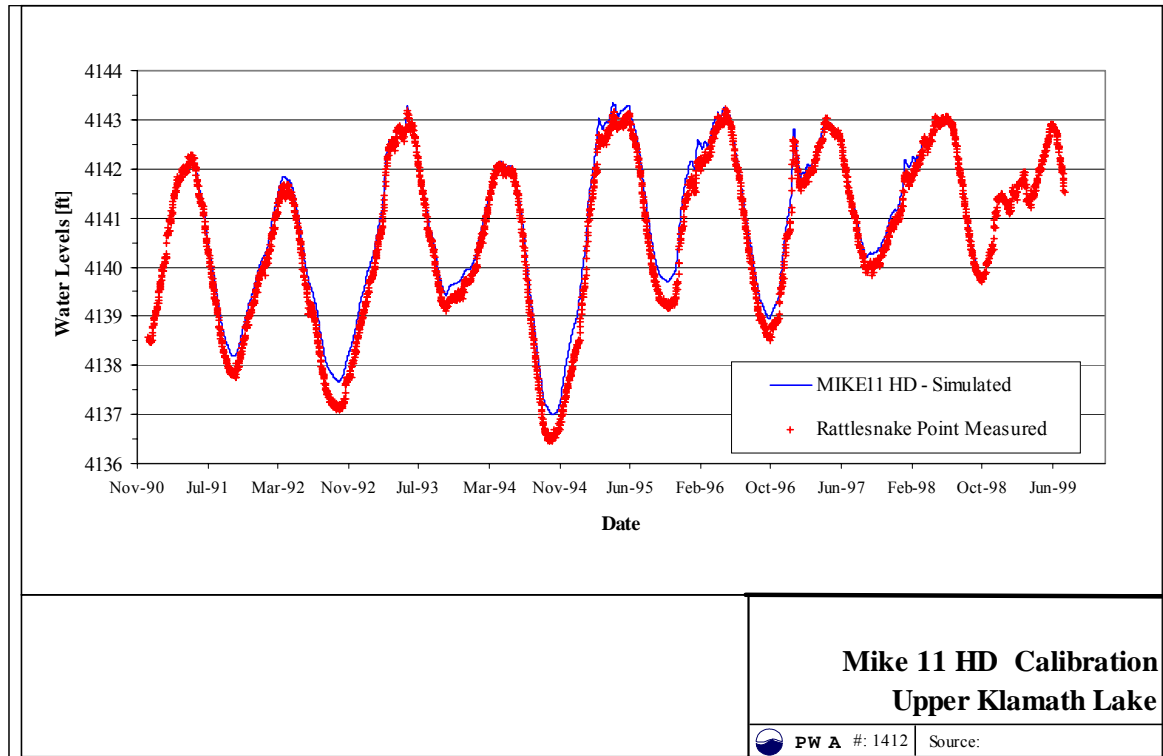


Figure 7-1 Comparison for Simulated and Observed Water Levels

7.2 MIKE 21 HD

The 2-D model was calibrated for a two-week period in the summer of 1997. There are no continuous velocity measurements in the lake for any recent period. In order to check the typical velocity and direction ranges in the lake, PWA conducted velocity measurement transects on 2/9/2000 at multiple locations in Upper Klamath Lake. The velocities measured were similar in both magnitude and direction to those computed for the February 2000 period. Since we had access to continuous water level data for three points around the lake, the model was calibrated in a dynamic way to match water level variation (Figure 7-1 and Figure 7-2).

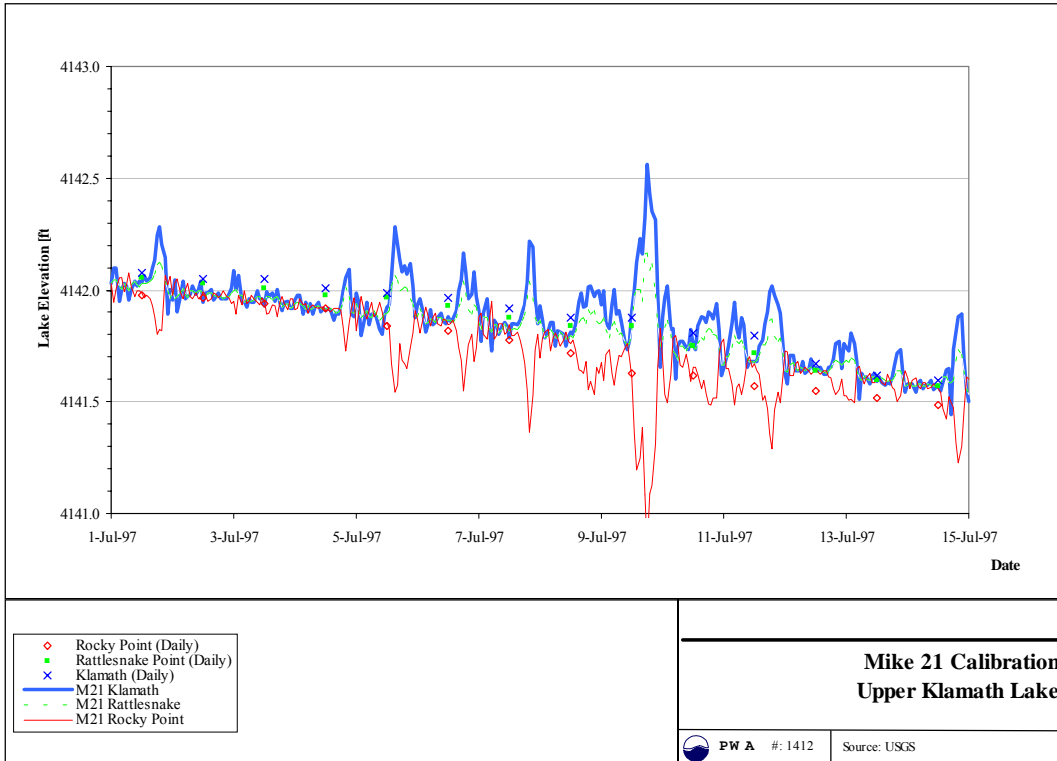


Figure 7-2 Comparison of Daily Measured and Hourly Computed Water Levels

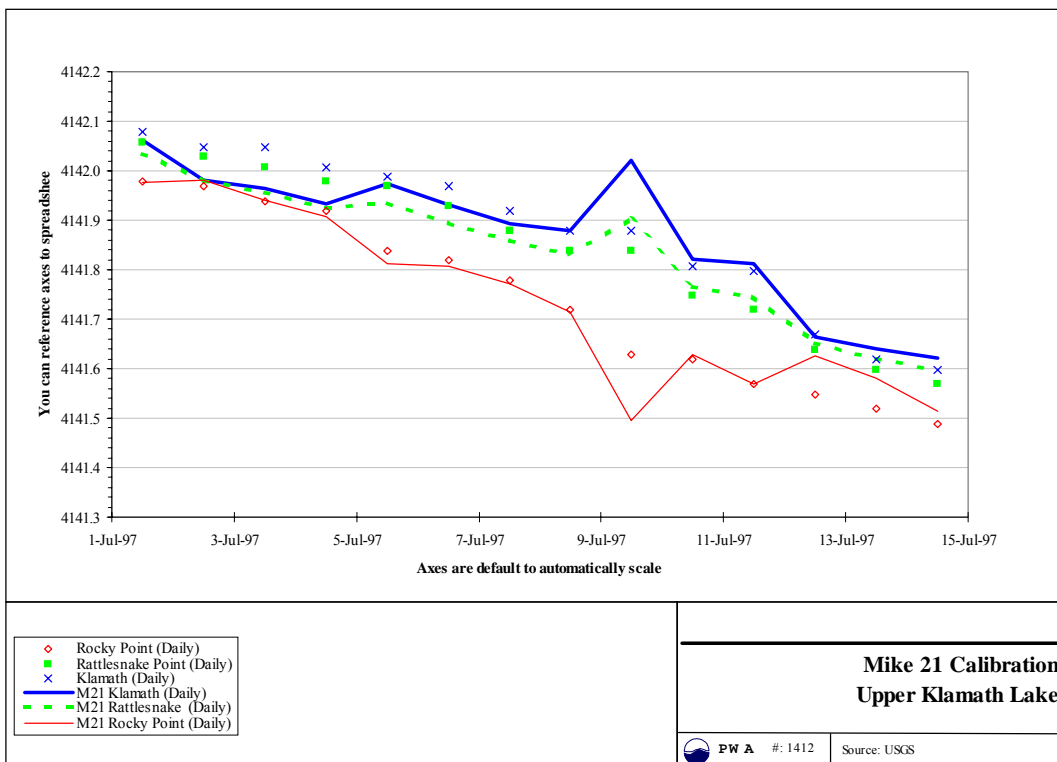


Figure 7-3 Comparison of Measured and Computed Daily Average Water Levels

The results for average daily water levels (Figure 7-3) present reasonable correspondences for overall water level movements. Computed water levels for calm days (July 3 and July 13) show much smaller lake gradients (i.e. spatial difference between water level within the lake) than those observed. This disproportion can be explained in several ways: 1) spatially variable resistance, 2) spatially variable wind speed and direction, and 3) accuracy of data sources.

Future water level and velocity measurements can improve the number of calibration points and, in combination with additional wind measurements, can better match the calibration parameters. However, this does not mean that the modeling results are invalid. The primary objective of the modeling task was to compare relative results for different lake management and/or operation plans. Wind is an important factor in lake circulation; however, only one wind data station exists at Rattlesnake Point. The need for additional wind data collection in order to improve accuracy of the model is discussed in the Chapter 2 - Findings.

7.3 MIKE 11 EU

7.3.1 Eutrophication (EU) Model Setup and Calibration

A MIKE 11 model was set up for Agency Lake and Upper Klamath Lake and used in connection with the eutrophication module to simulate the changes in nutrient, chlorophyll, and oxygen processes caused by change in water level and nutrient load. Details of the MIKE 11 hydrodynamic set up are described below:

Forcing Functions. The EU model utilizes user-defined tables to describe water temperature, photosynthetic active radiation (PAR), nutrient loads from rivers, agricultural pumping, inflows from springs, and precipitation. These user-defined tables are called ‘forcing functions’ because they drive the EU model. The seasonal variation of water temperature and PAR has to be defined for one year and is used repeatedly in long-term simulations. In contrast, the nutrient load is defined for the whole simulation period. Figure 7-4 illustrates the seasonal variation of water temperature used in the EU modeling. The curve is generated as a mean of temperature data from the central stations in Upper Klamath Lake.

No measurements of PAR or solar radiation are available in the form and type as needed for EU model. Therefore, a PAR curve has been calculated based on the latitude and assuming a loss in the atmosphere of 30% (Figure 7-5).

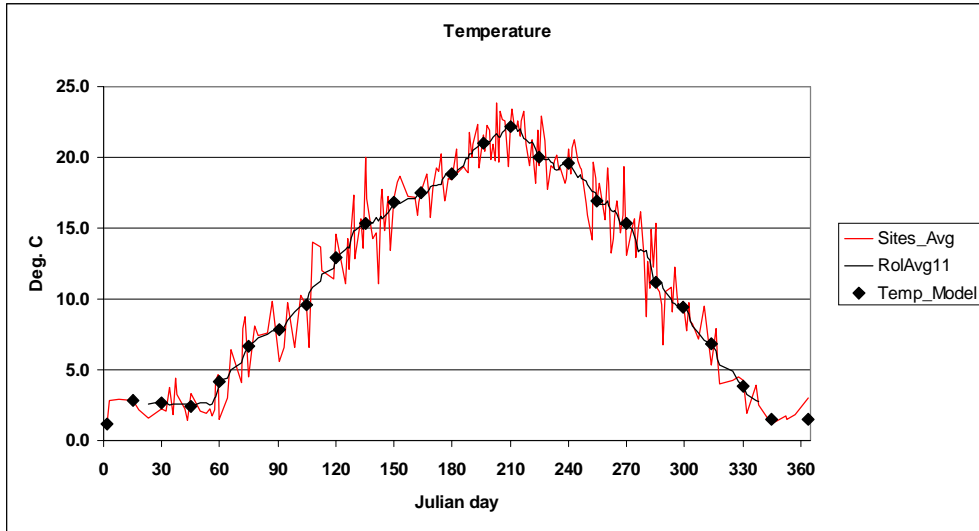


Figure 7-4 Water temperature used by EU model

[Sites_Avg: temperature average from stations AC, AS, ER, GH, ML, MN, NB, SP and UML 1991-98. RoIAvg11: 11 days rolling average of Site avg. Temp_mod: Temperature used in EU model]

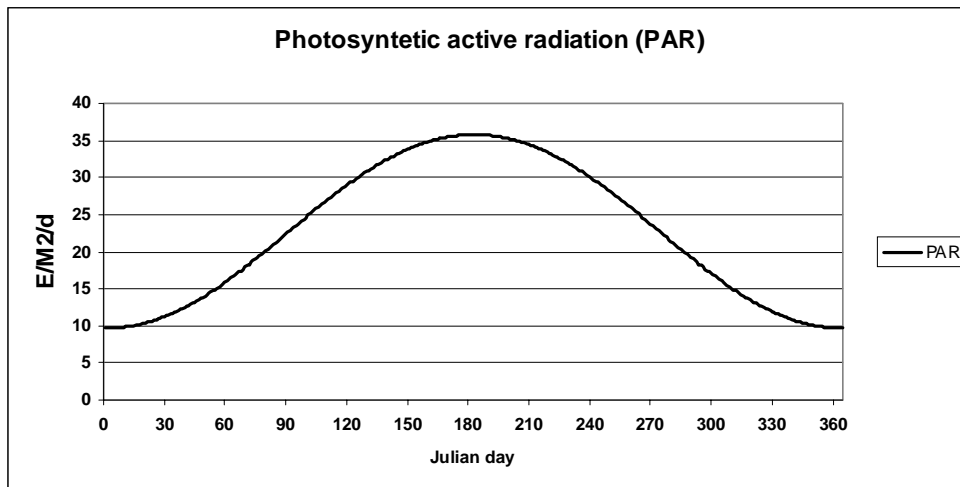


Figure 7-5 Seasonal Variation Of Photosynthetic Active Radiation (PAR) Used By The EU Model

Nutrient Loadings. The nutrient load has been defined based on nutrient loading specified in ref. (29). (Table 7-1 and Table 7-2). The total Phosphorous (TP) load vary between 106 to 250 tones per year and the total Nitrogen (TN) varies between 575 and 1200 tones per year. About 40% of the TN and about 75% of the TP is in its inorganic form giving a N:P ratio of 2.7 on the inorganic nutrients, which is well below the Redfield ratio for N:P in algae of 7.2.

Table 7-1 Load of Nutrients to Agency and Upper Klamath Lakes

Year	TP Tonnes	TN Tonnes
1992	115.0	586
1993	207.2	1047
1994	106.5	575
1995	190.5	990
1996	249.1	1200
1997	204.1	1056

Table 7-2 Load of Nutrients to Agency and Upper Klamath Lakes in 1997, Tones

Component	7-Mile Canal	Wood R. below Weed Rd.	Williamson River	Springs	Ag Pump	Tributary Inflow	Precipitation	Total Inflow
TP	18.5	40.3	101.0	17.3	22.2	199.3	4.9	204.1
SRP	15.0	35.2	71.7	14.7	12.7	149.2	4.9	154.1
TN	73	49	475	33	134	764	292	1056
IN	12	12	56	16	25	120	292	412

The contribution of load from the agriculture pumps is distributed according to drained area and proportional to pumping activity. The precipitation and dry deposition of nutrient is assumed to be constant over time.

Table 7-3 shows scenario for a reduced load. The contribution from agriculture pumps is assumed to stop and the P load from the rivers is reduced by 44%. According to ref (46), 44% of the P load in Wood River is believed to be of anthropogenic origin. If the same is true for the other rivers, and assuming the P load in the springs are the same, the over all reduction in P load to the lakes will be 37%. The N load without anthropogenic input is difficult to assess. However, any reduction will probably be compensated by N fixation by the blue green algae as long as the N:P ratio is below 7. Therefore, in the present simulation the N load is only reduced by the contribution from the agricultural pumps.

Table 7-3 P And N Load Used in Simulation with Reduced Load, Tones Per Year

Component	7-Mile Canal	Wood R. below Weed Rd.	Williamson River	Springs	Ag Pump	Tributary Inflow	Precipitation	Total Inflow
TP	12.2	26.6	66.7	17.3	0.0	123	4.9	128
SRP	9.9	23.2	47.3	14.7	0.0	95	4.9	100
TN	73	49	475	33	0	630	292	922
IN	12	12	56	16	0	95	292	387

7.3.2 Calibration of the EU model

In order to reduce the response time, a “fast track” set-up consisting only of Agency Lake was used to test the changes made in the model code and for a first calibration of the EU model. With the Agency Lake setup, it was possible to make a long-term simulation with computation time only extending overnight. Calibration using long-term simulations ensured that the model was able to mimic the most important changes due to example variations in nutrient load. Figure 7-6 through Figure 7-9 show simulated and measures values of nutrients, chlorophyll, secchi depth, pH and DO for Station AS in Agency Lake. Figure 7-10 illustrates important state variables simulated by the sediment N and P modules.

The model is able to simulate the measured maximum total P in 1993, 1994, 1995 and partly in 1992 and 1996. In 1997-98, the model slightly over estimated TP concentration, and in 1991, the model underestimated the TP concentration. In general, the winter TP concentration is simulated too high resulting in a too high concentration at the onset of the new growth season. The TP concentration follows the general year-to-year trend of the measured concentrations.

The simulated PO₄-P (IP) is not in perfect agreement with the measured values for all times. Except for 1995, the simulated IP concentrations during summer are generally too low and the model is not able to mimic the sharp increases in July and August. Crash of the algae community in late summer is a reasonable explanation. During and after the crash nutrients including IP is released from the decaying plankton.

When looking at the simulated and measured values for TN and NH₄-N, a similar pattern is seen (Figure 7-7). When looking at the measured oxygen concentration, low concentrations are recorded in summer 1991, 1993, 1996 and 1997 (Figure 7-9). This pattern supports the idea of algae crashes reducing the DO concentration and releasing PO₄-P, NH₄-N into the water from decaying algae.

The simulated total nitrogen matches the summer peaks in 1991, 1994 and partly in 1992, and 1996. However, in the other years, the simulated summer values are too high (Figure 3-1Figure 7-7). The parameters used for N-fixation may generate too high a N-fixation in Agency Lake. However, changing these parameters will destroy the good match between measured and simulated TN in UKL (Figure 7-11 and Figure 7-12). Therefore, the parameters were not changed. Relatively high NO₃-N concentrations during winter and low concentrations during the growth season dominate the simulated NO₃-N concentrations. As no measurements are available for the winter it is not possible to verify the simulated high winter concentrations.

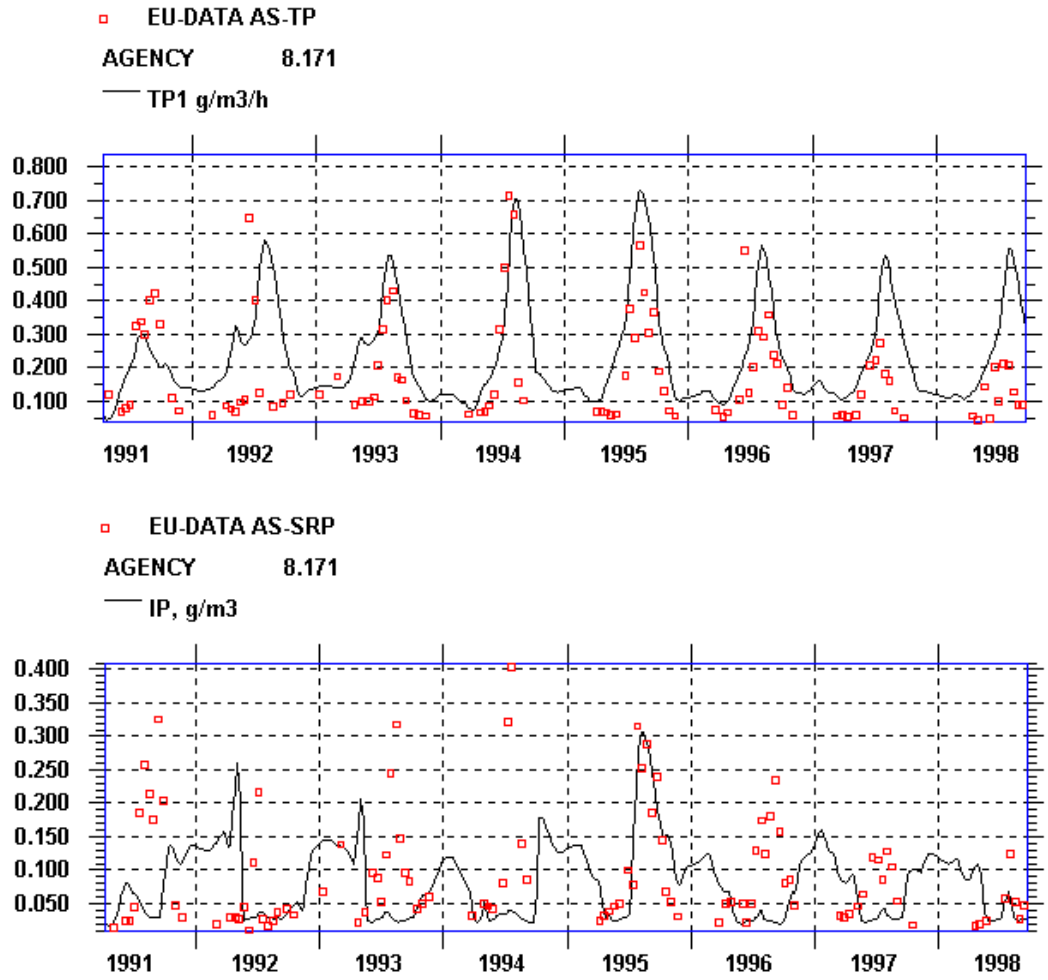


Figure 7-6 Simulated and Measured Values of Total P and SRP

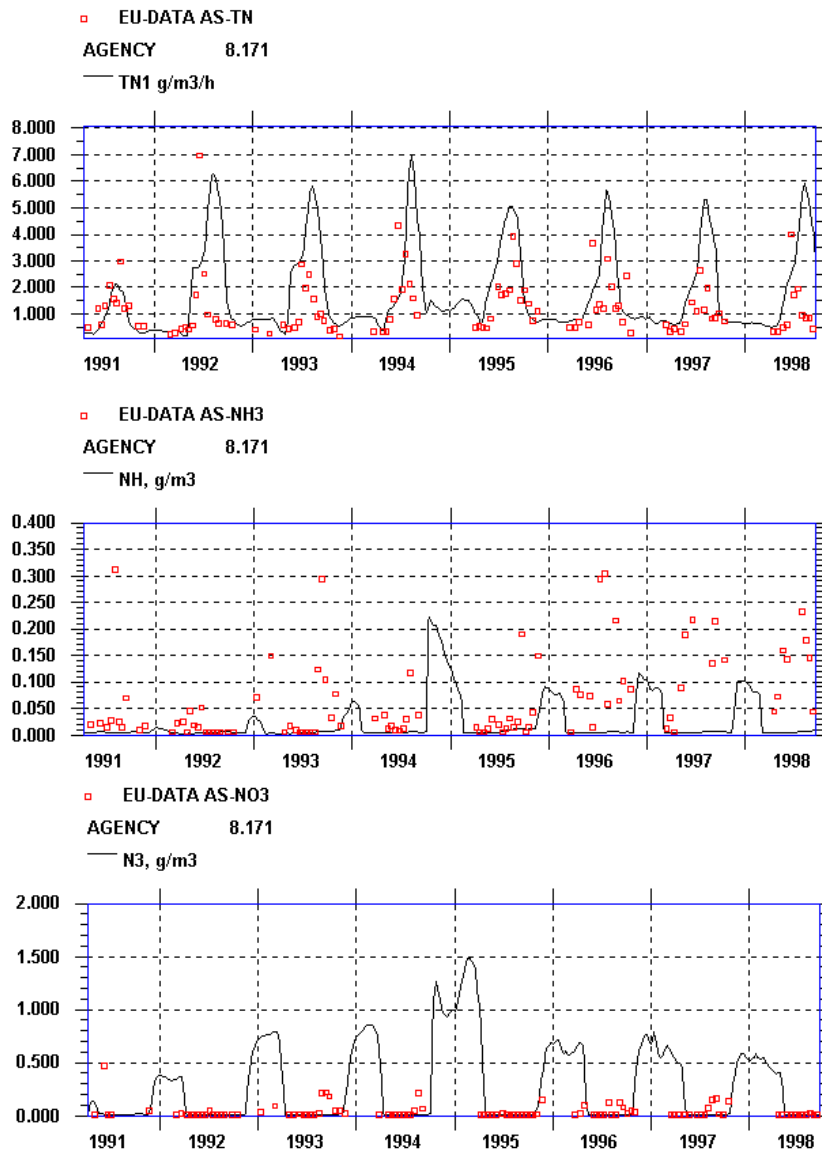


Figure 7-7 Simulated and Measured Values of Total N, NH4-N And NO3-N

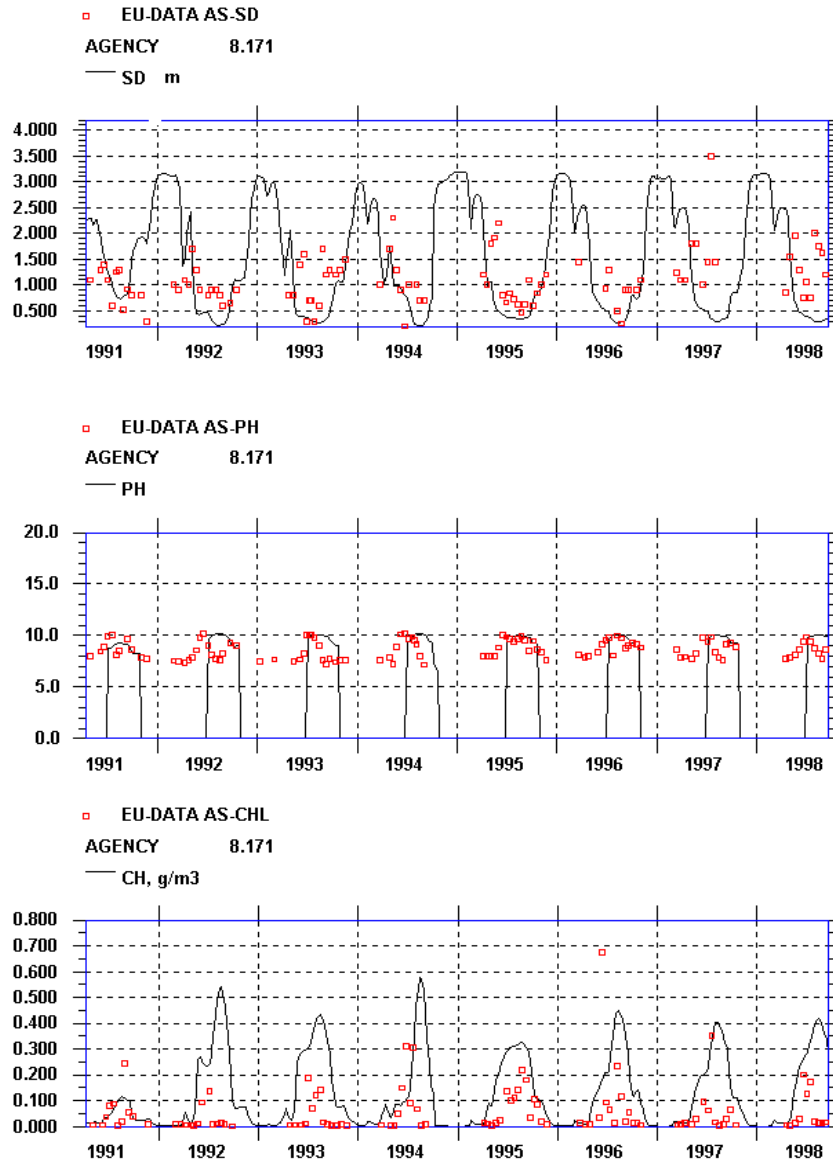


Figure 7-8 Measured and Simulated Secchi Depth, Ph and Chlorophyll

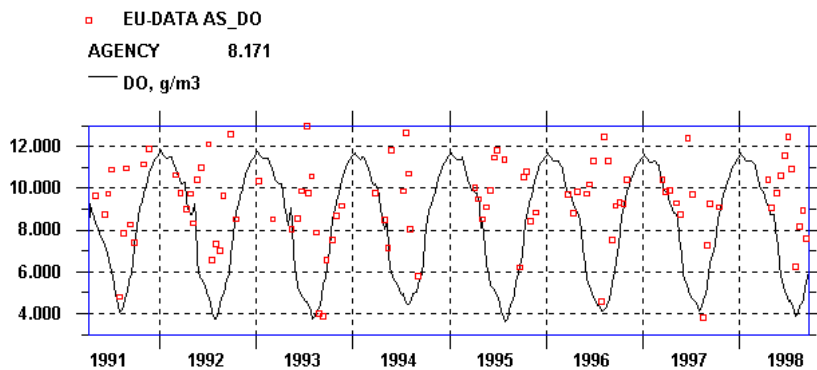


Figure 7-9 Simulated and Measured Oxygen Concentrations

In Figure 7-8 the simulated secchi depth (SD) is presented together with measured values. For the years 1992, 1994, 1995, 1996 the simulated and the measured values agree. However, in 1993, 1997 and 1998 the model predicts lower SD values than recorded during summer. The model has the correct seasonal variation.

The simulated pH values in the model are set to be valid from June to September (Figure 7-8). Simulated pH exceeds 9.5 in June and has a decline in September. Compared with the measured values in 1992, 1993, 1994, and 1997 decline faster. In some years (1992, 1994, 1995, 1997), measured pH reach 9.5 before June. To get a correct start to the simulation, pH could be set to be valid from May, one month earlier than specified for the empirical relation between chlorophyll and pH, ref. (28).

Figure 7-8 illustrates the simulated chlorophyll. For Agency Lake the simulated summer chlorophyll values are overestimated for all years except 1991, 1996, and 1997. However, when comparing the simulated and measured summer concentrations in UKL, these seem to fit in magnitude (Figure 7-10 and Figure 7-11). Therefore, no attempts have been made to change the parameters related to chlorophyll or primary production.

Figure 7-9 illustrates the simulated daily average oxygen concentrations together with average DO concentrations from profile measurements. The profile measurements were done during daytime, thus the measured values show supersaturation during daytime and do not reflect the daily average DO concentration. However, supersaturated day DO concentrations often indicate low DO concentration at dawn. In late summer, the oxygen production decreases and the respiration increased due to high temperatures and high algae biomasses. At a point the algae community may crash and the low day DO concentrations can be recorded. Such records are seen in 1991, 1993, 1996 and 1997.

Selections of important sediment state variables are presented in Figure 7-10. P sorbed to oxidized Fe (SPFE) is presented in the upper right part of the figure.

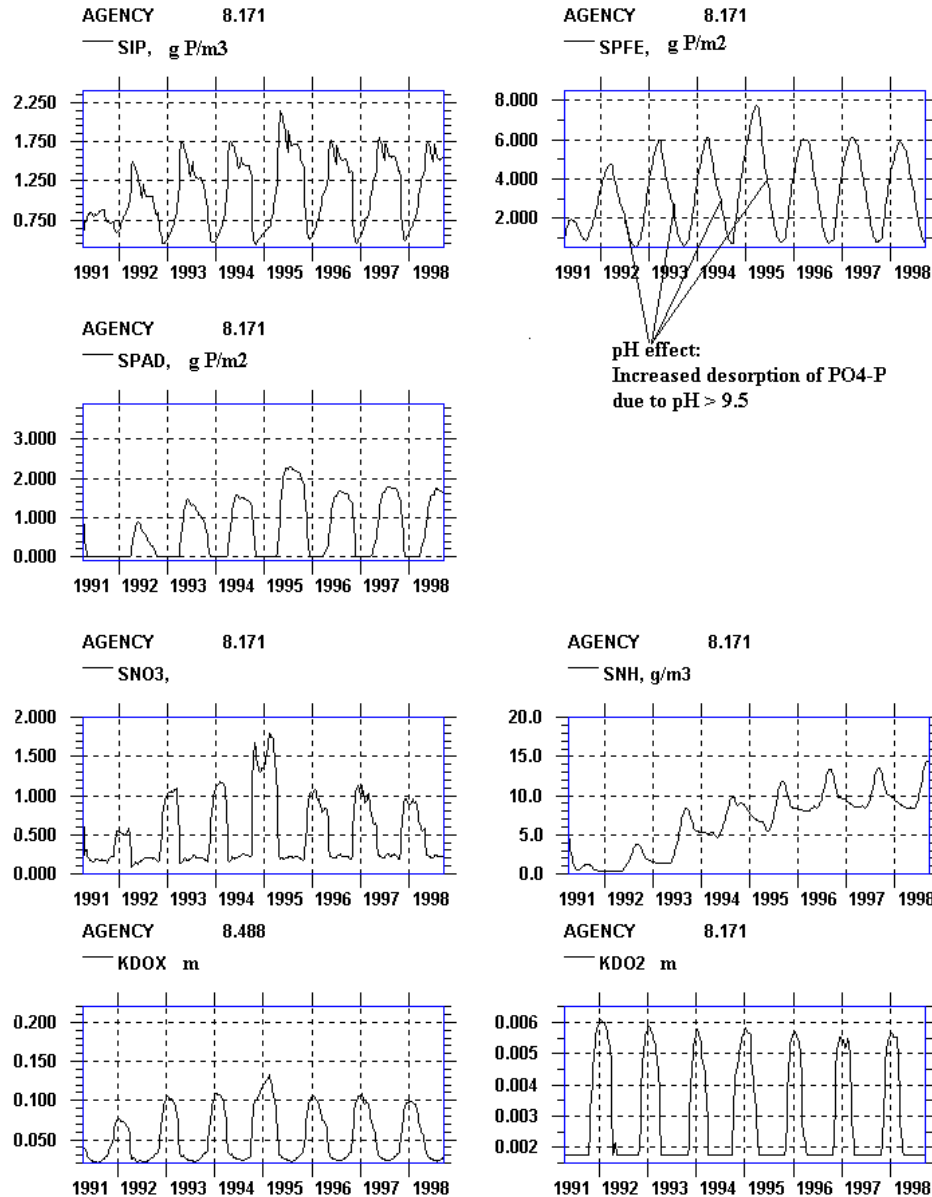


Figure 7-10 Sediment Parameters

SIP: PO₄-P in pore water, SPFE: P sorbed to Fe⁺⁺⁺, SPAD: P sorbed to reduced sediment, SNO₃: max concentration of NO₃-N in pore water, SNH: NH₄-N concentration in pore water, KDOX: penetration of NO₃-N in sediment, KDO₂: Penetration of O₂ in sediment.

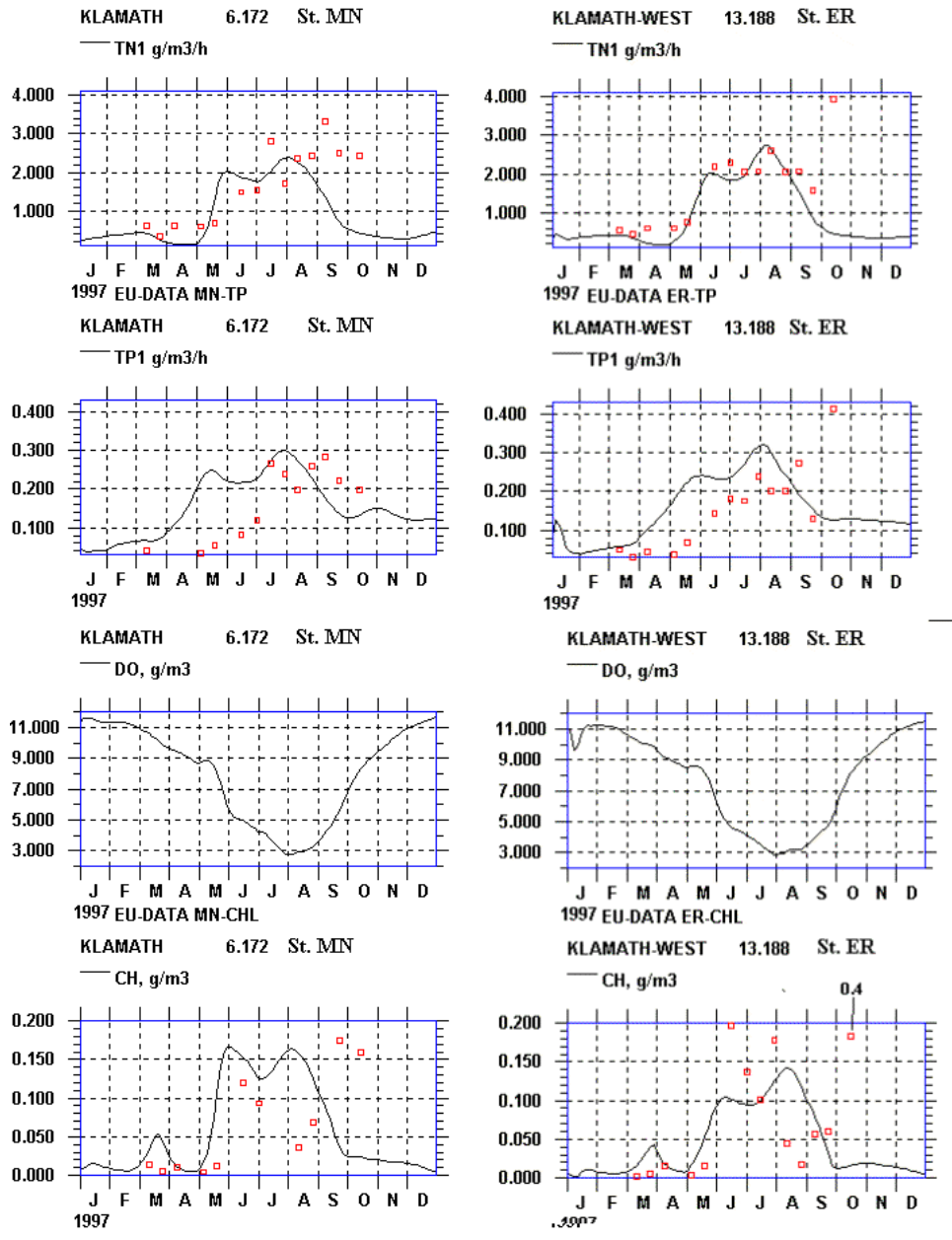


Figure 7-11 Measured and Simulated Values of TN, TP, And Chlorophyll at Stations MN and ER in UKL

SPFE, as g P/m², reached a maximum in March and declined during spring and summer until September-October after which it increased again. The driving force for this variation is the thickness of the oxidized layer (KDOX), which is presented in the lower left part of the figure. During summer this layer decreases because the NO₃-N concentration decreases in the surface sediment. In autumn when the NO₃-N concentration increases, the oxidized layer increases and the pool P sorbed to oxidized Fe (SPFE) increases as well. The pool of SPFE is dependent on the concentration of Fe in the surface sediment, according to ref. (25) the max SPFE (P Sorption

Capacity) can be expressed as $PSC = -4 + 2.19 \cdot \ln(Fe)$. Using this relation and assuming the Fe concentration in UKL sediment to be 10 mg/g DW, ref. (9), the SPC should be about 14 g P/m² per 10 cm oxidized sediment layer. The simulated variation 1-8 g P/m² is below this value as could be expected. The P sorption capacity is influenced by high pH. This process can be seen as an increase in the decline in the SPFE pool. With the decline of SPFE, the concentration of PO₄-P in the pore water (SIP) increases (top left plot in Figure 7-10). At the same time, P sorbed to reduce sediment (SPAD) increases (mid left plot in Figure 7-10). When the SIP concentration increases the flux of PO₄-P from the sediment to the water will increase.

Figure 7-11 and Figure 7-12 diagram the measured and simulated concentrations of TN, TP, DO and chlorophyll for four central stations in UKL. The simulated TN seems to agree with measured values. For TP, the summer concentrations match the measured values, but there is a phase lag between the curves so that the simulated curves increase about one month earlier than the measured values. The best explanation is too early of an onset of the simulated internal P load. For TP, the simulated chlorophyll concentrations reach the measured summer level, but a half to one month too early.

The MIKE 11 EU model has been calibrated against measured data and can make simulations with reduced nutrient loads as well as simulations of the dilution effect of changed water levels. However, the 1-D model is not calibrated to reproduce variations of the onset of blue green blooms of blue green algae. The use of actual measured water temperatures and solar radiation for each individual year may improve the model simulation. The period of pH should be extended to May as well. However, if in the future the objective is to simulate algae community crashes, the driving forces regulating these events must be identified and formulated mathematically before they are implemented into the model for testing. The MIKE 11 model shows that calm weather in late summer in combination with high water temperatures, high algal biomass and declining solar radiation mediates the crashes.

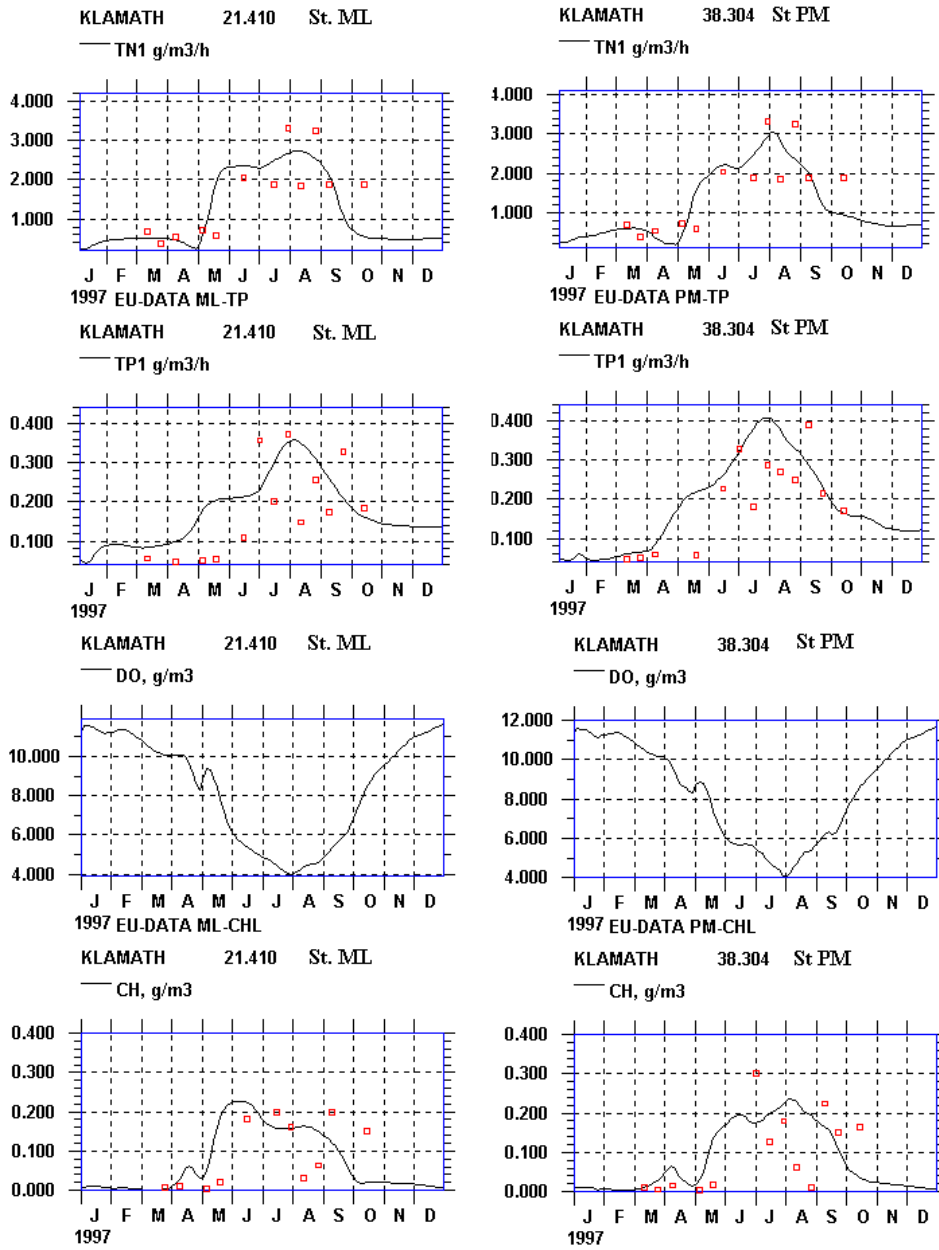


Figure 7-12 Measured and Simulated Values of TN, TP, and Chlorophyll at Stations ML and PM in UKL

8. MODEL APPLICATIONS AND RESULTS

8.1 DESCRIPTION OF THE SCENARIOS FOR DIFFERENT LAKE OPERATIONS

The models were used to simulate different hydrodynamic scenarios for 1997. The base scenario utilizes historic conditions for 1997, which were then compared to the alternatives for different lake elevations. Figure 8-1 shows the lake elevation changes simulated in the eutrophication model. The outflows from the lake were altered to raise or lower water levels respectively.

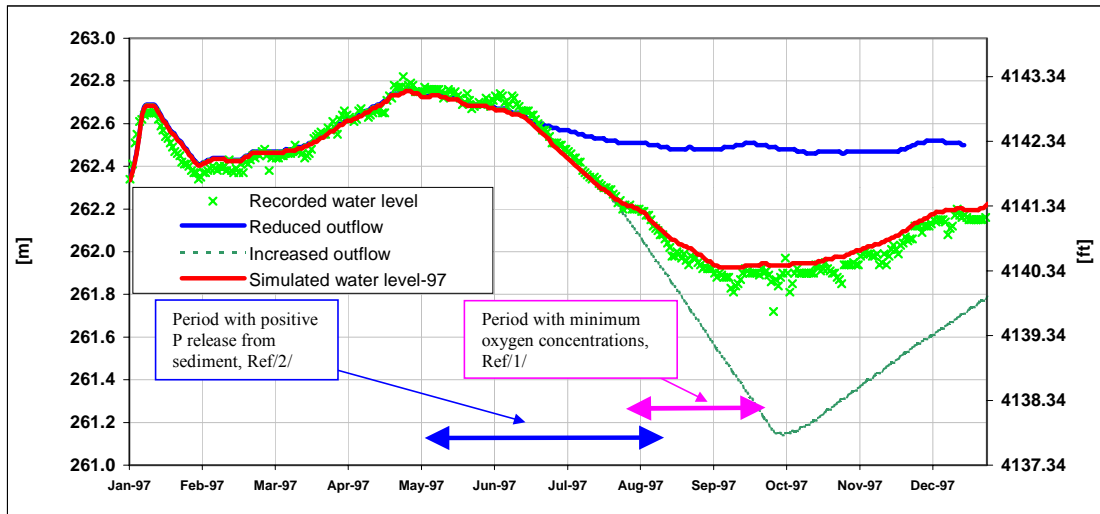


Figure 8-1 Lake Elevation Changes Simulated in the Water Quality and Eutrophication Model

8.2 HYDRODYNAMIC SCENARIOS FOR CIRCULATION MODEL

For the 2-D hydrodynamic model, only the initial conditions water level was altered to simulate circulation patterns for a two week period. The model was run with the same boundary conditions and wind stresses to demonstrate the influence of different lake elevations on circulation.

The hydrodynamic scenarios were as follows:

- A – higher lake elevation (ending water level elevation - 4142 ft)
- B – base conditions for 1997 (ending water level elevation - 4140.30 ft)
- C – lower lake elevation (ending water level elevation - 4139 ft)
- D – minimum lake elevation (ending water level elevation - 4138.25 ft)

8.2.1 2D Hydrodynamic Model Results

Results from the MIKE 21 HD model are presented in three ways:

1. The first is a vector plot of velocity magnitudes and directions for the four scenarios (Figure 8-2 through Figure 8-5). Different flow patterns can be seen in the connection between Agency and Upper Klamath Lakes and in the mid-north and middle part of the Upper Klamath Lake. The lower part of the lake is influenced by outflow through the dam.
2. The second compares the velocity speed and cumulative speed for two points in the lake West and East of Bare Island. The points represent two opposite conditions for lake behavior. The narrow deep channel in the west part of Upper Klamath Lake near Bare Island, transfers water from the lower part to the upper part of the lake depending on the wind directions. During a predominantly NW wind, the flow is north (upward) and during southern winds, the flow is south (downward). The speed in this narrow, deep area definitely depends on the wind conditions but also on the total volume in the lake. As volume increases the speed for the same conditions will increase. The width of the straight is much smaller and deeper than the east part of the lake between Bare Island and Modoc Point, which is 4 to 5 times wider and shallower (Figure 3-1).
3. The third method for presenting results is particle tracking. This method uses the hydrodynamic results (of a two week duration) to track potential particle movements based on a pure advection Lagrangian transport approach. Two sets of particles were used. The first set of four particles was put into Wocus Bay (Figure 8-7). The second set represents two particles in Agency Lake and four just northwest of Bare Island (Figure 8-8). Higher lake elevations will most likely decrease mixing (interchanges) between the water volumes in the Wocus Bay and rest of the lake. In the case that water quality in the Wocus Bay is much worse than in another part of the lake, the lowering interchanges can temporarily improve the water quality condition locally for some time—but it will not solve it. Wocus Bay is an integral part of the lake and mixing cannot be completely avoided.

All of the preceding statements depend on the weather conditions. During the modeling runs, the same weather (wind) conditions as summer 1997 were used. If the weather patterns are not similar or the operation of the lake is not the same, different results might be obtained.

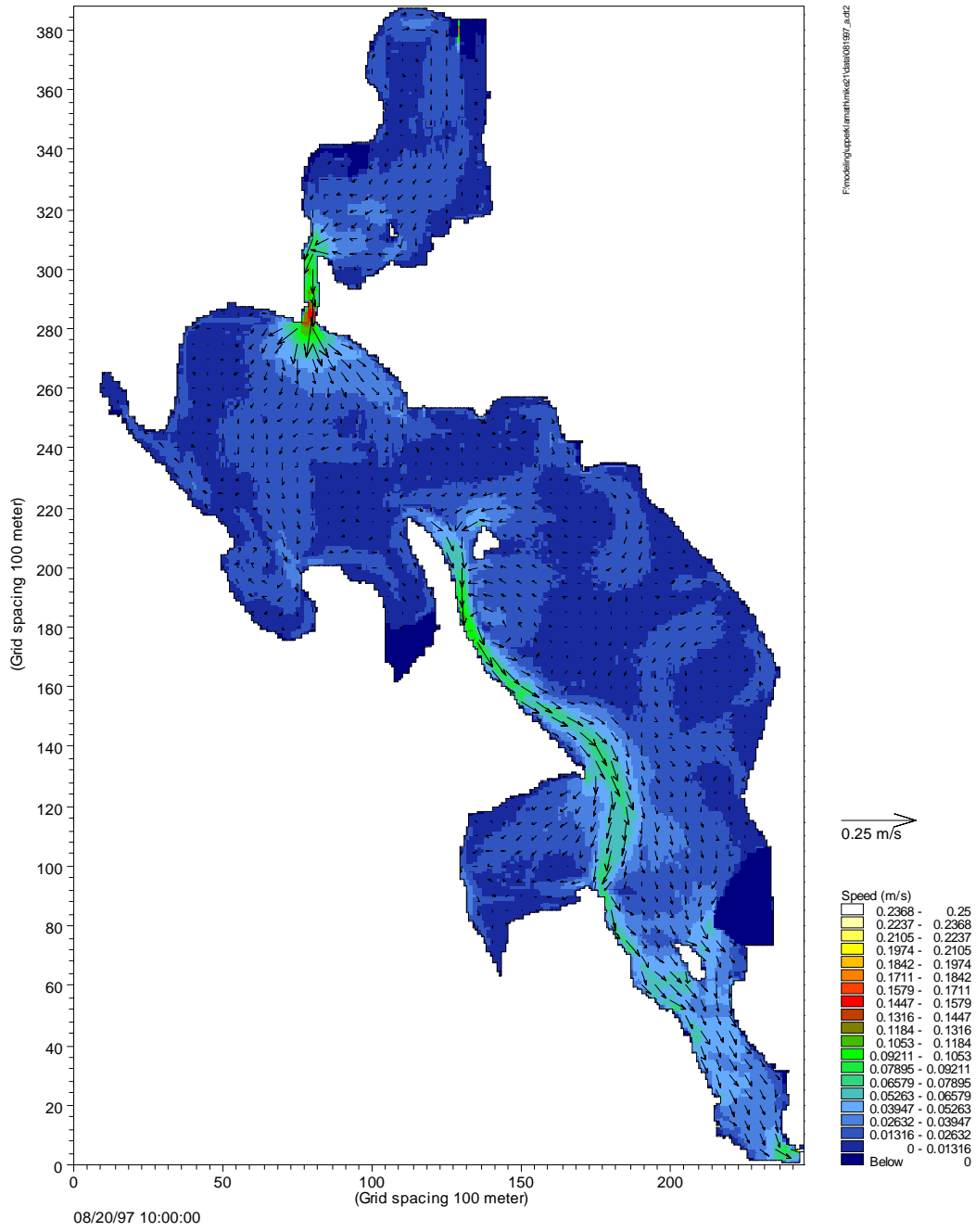


Figure 8-2 Velocity Field for UKL Lake Scenario A

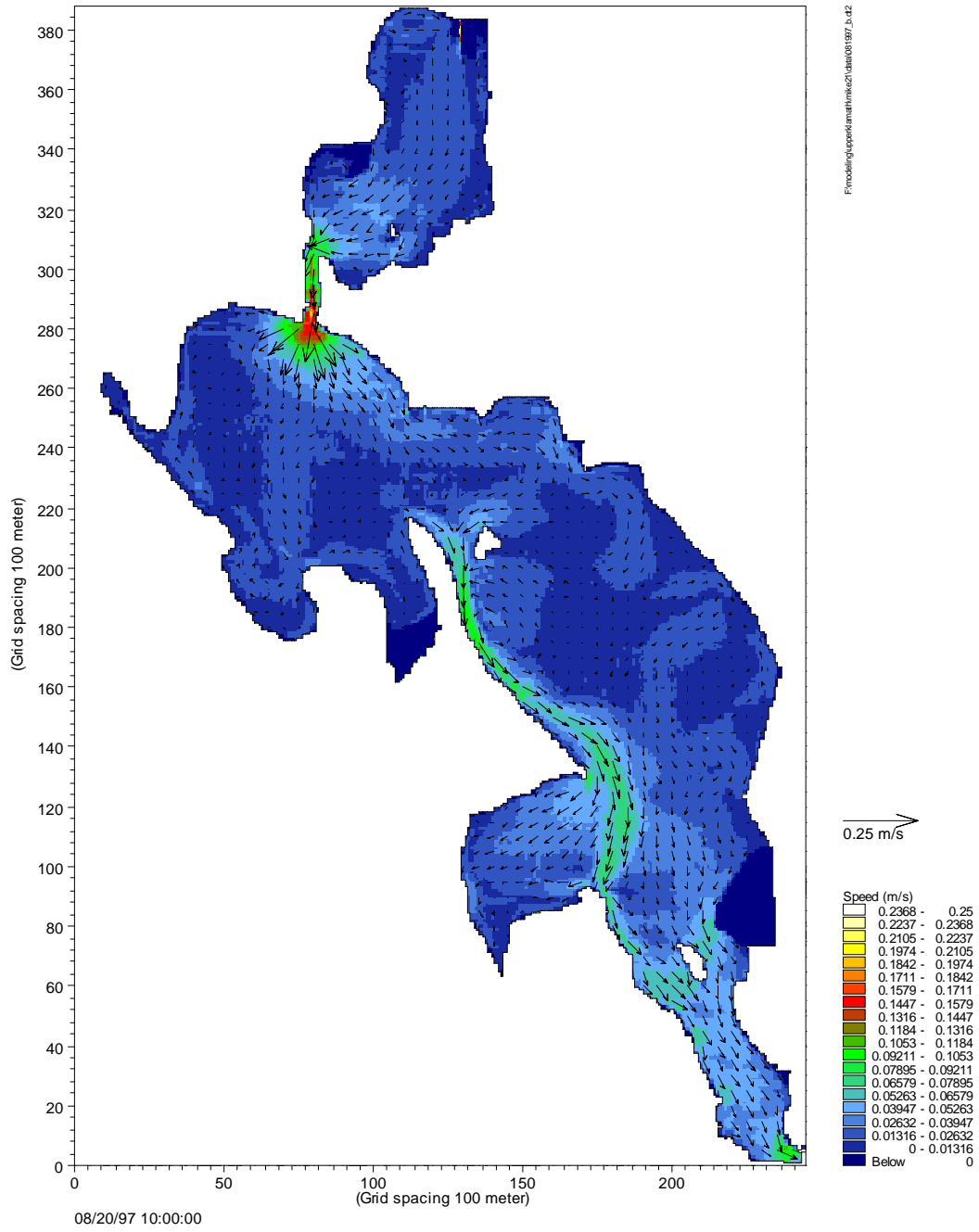


Figure 8-3 Velocity Field for UKL Lake Scenario B

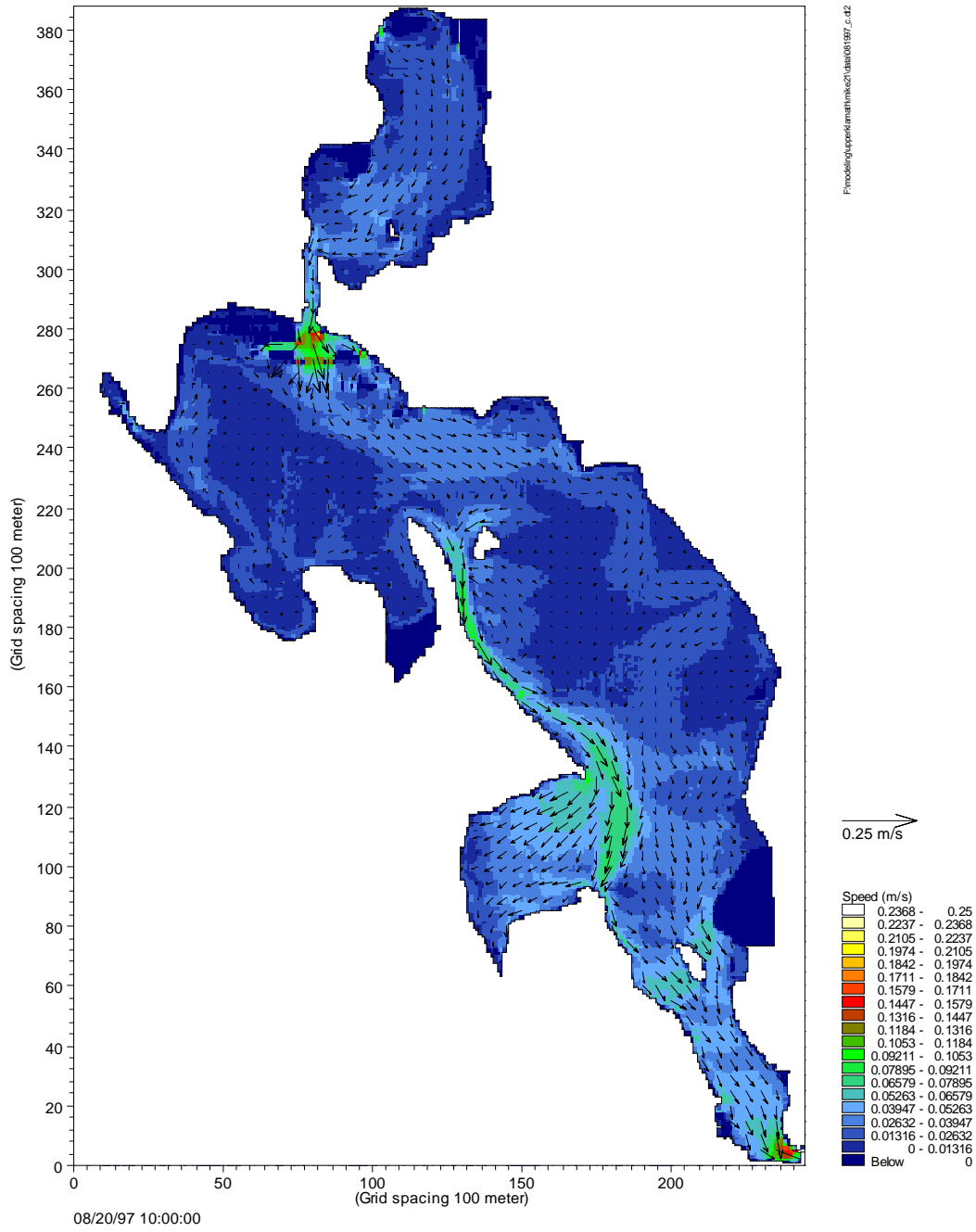


Figure 8-4 Velocity Field for UKL Lake Scenario C

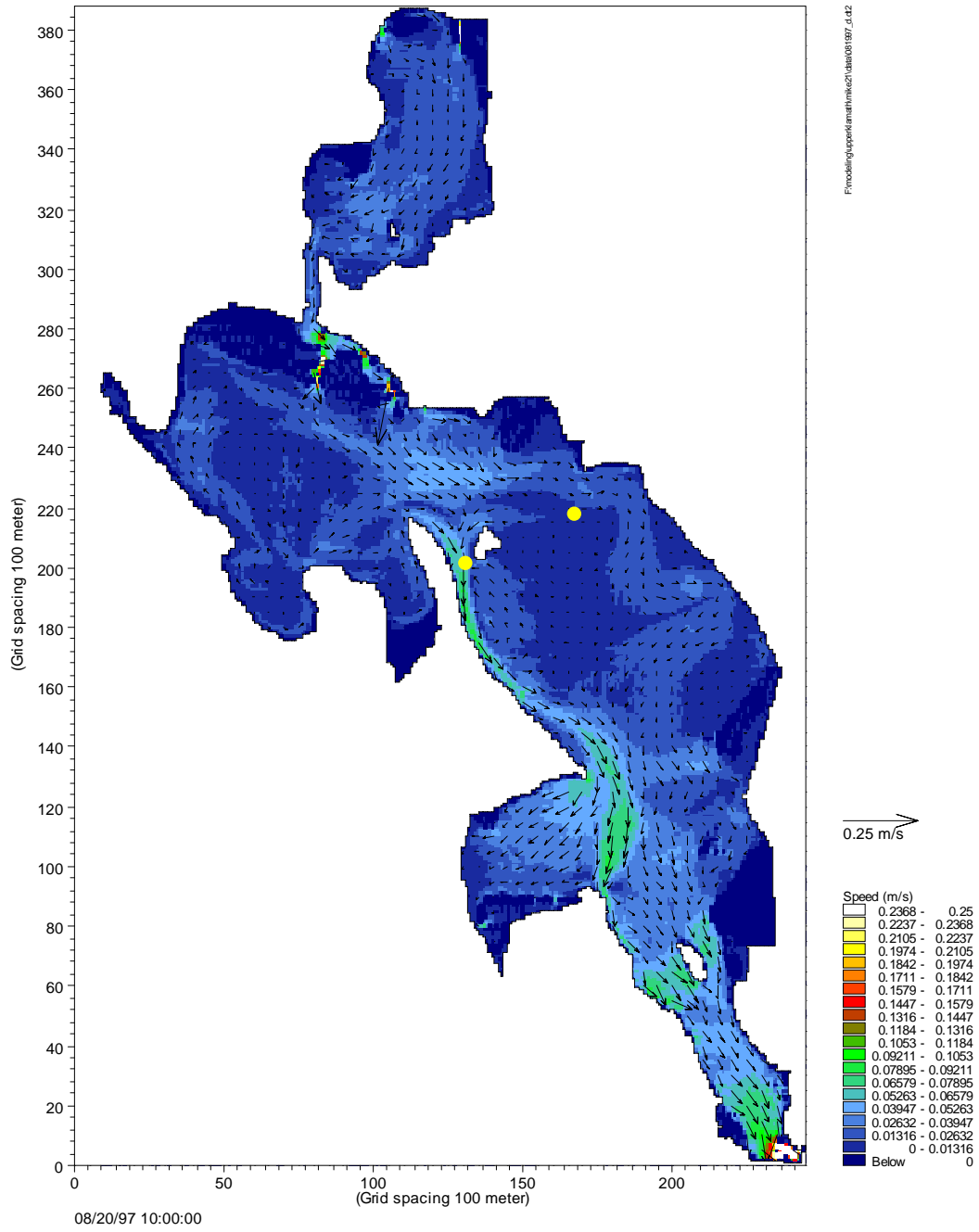


Figure 8-5 Velocity Field for UKL Lake Scenario D

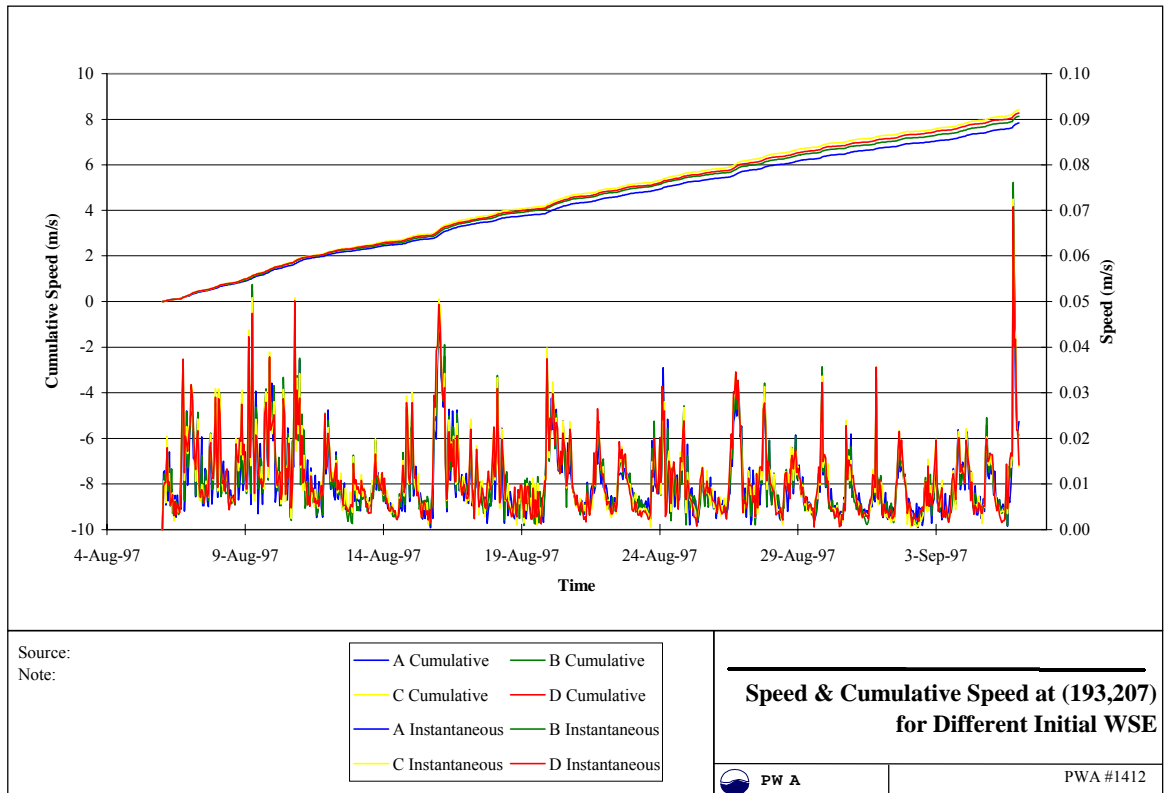
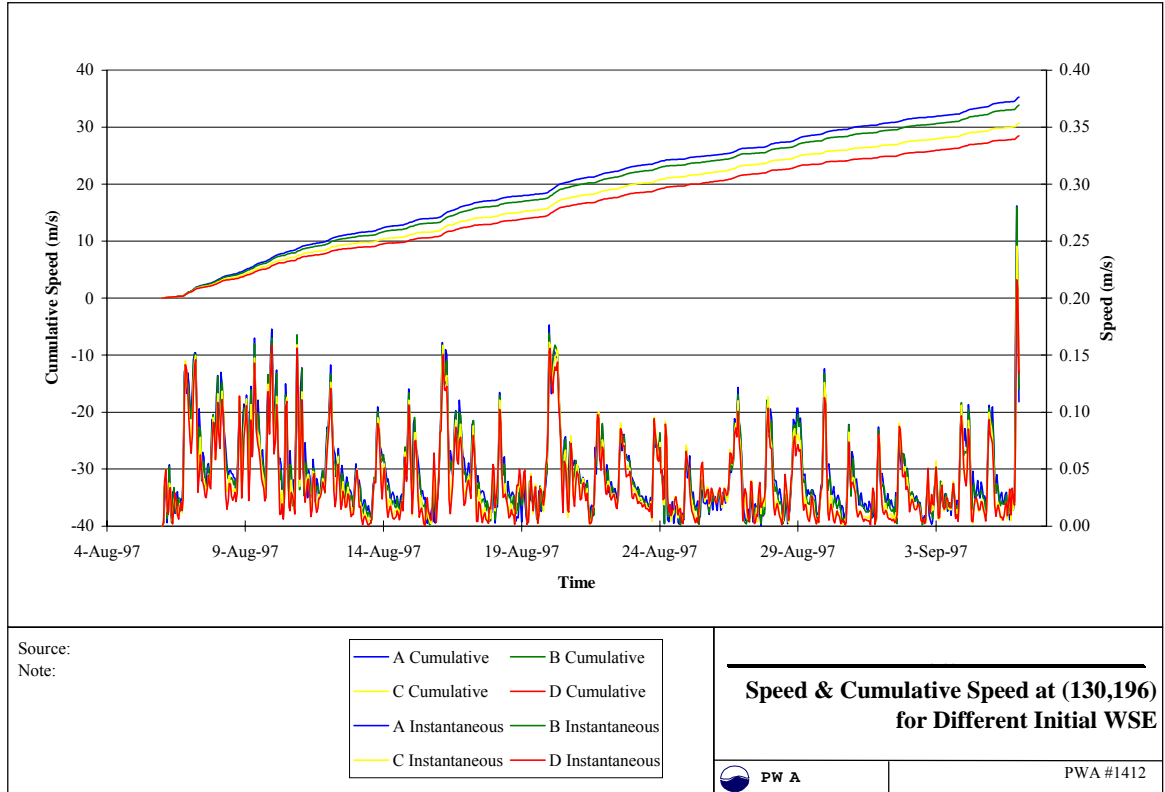


Figure 8-6 Velocity Comparison – West of Bare Island [Upper] – East of Bare Island [Lower]

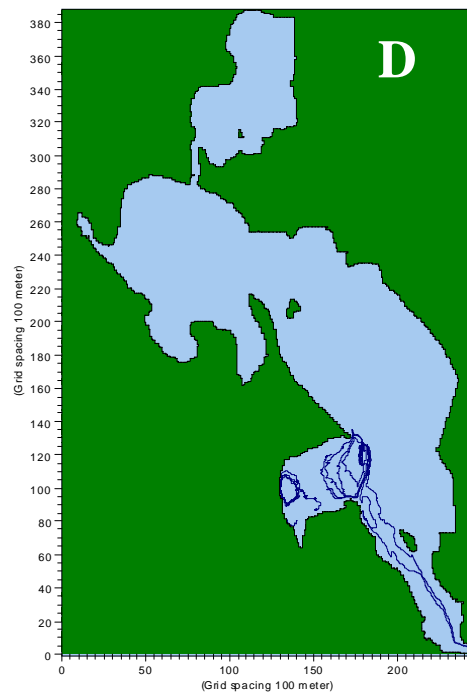
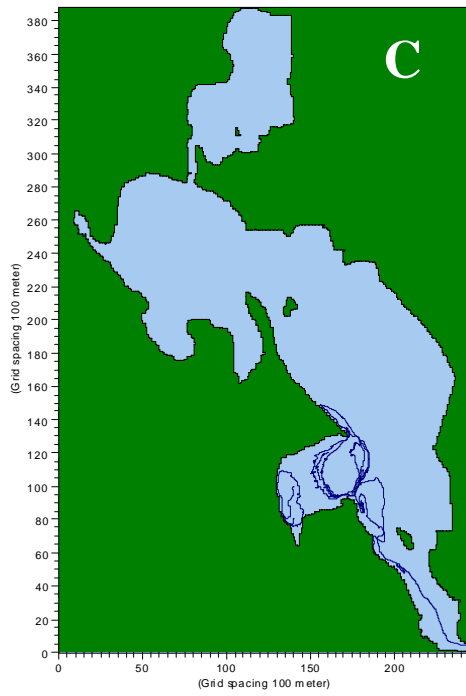
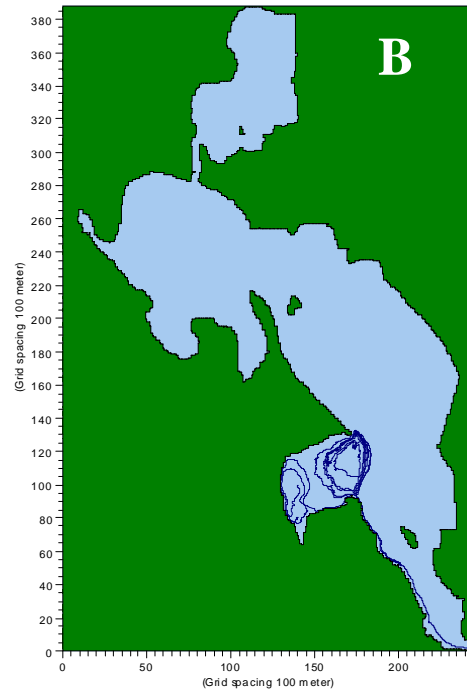
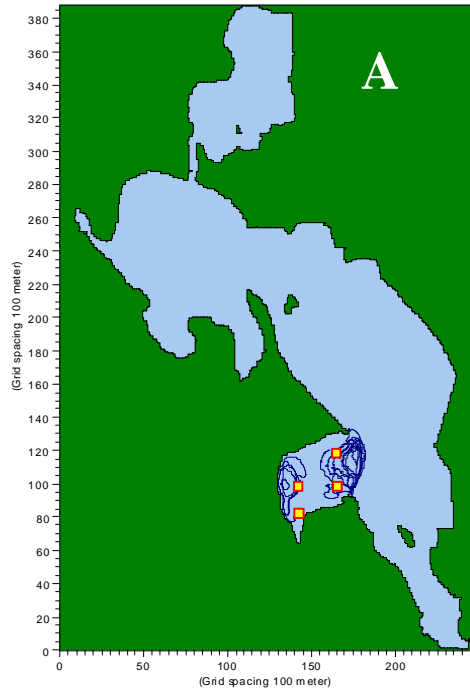


Figure 8-7 Particle tracking for Wocus Bay

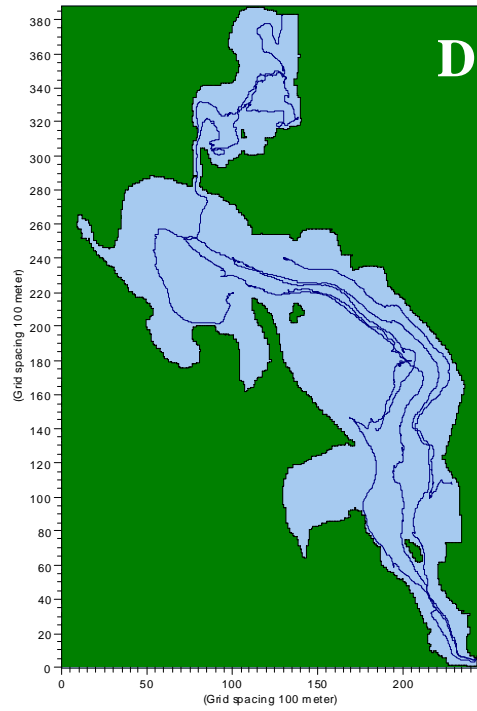
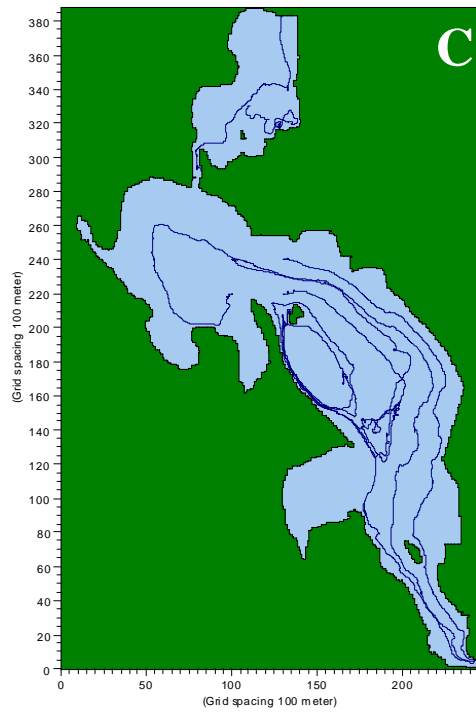
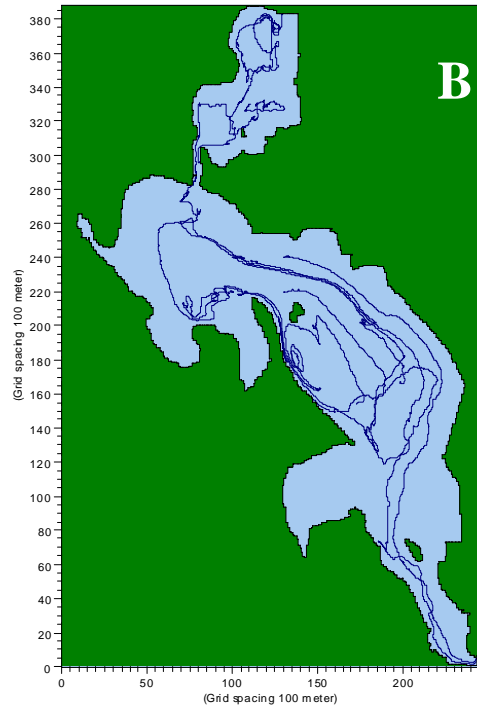
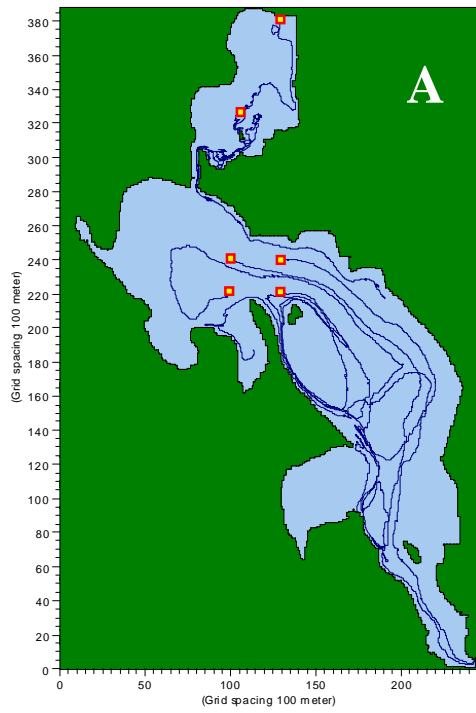


Figure 8-8 Particle tracking for Upper Klamath and Agency Lakes

8.3 WATER QUALITY

8.3.1 Water Quality Model Descriptions

The 1-D model used to simulate eutrophication processes has the drawback of not being able to resolve vertical profiles of oxygen (and water temperature) in the water column. Furthermore, the eutrophication model does not resolve diurnal variations in dissolved oxygen. In order to fully characterize variations in the horizontal, lateral and vertical directions, a 3-D model is required. However, long-term simulations are not practically feasible because of computation time constraints; therefore, simulations focus only on short-term critical periods when minimum oxygen concentrations have been observed (on the order of one to two weeks).

The hydrodynamic model provides the platform for the succeeding water quality calculations. The 3-D model is constructed from the bathymetry as used in the MIKE 21 simulations and comprise a total of 618×10^6 computational points with a horizontal resolution of 400 meters and a vertical resolution of 0.25 meter (up to 51 layers depending on the actual water depth). Figure 8-11 shows the model area and the existing monitoring stations. Forcing functions for the hydrodynamic model includes wind speed, reservoir outflow, precipitation, and heating at the air-water interface. A detailed calibration of the 3-D model is beyond the present scope of work. Such calibration would require extensive measurements of vertical temperature profiles, which are not available. Only single measurements, assumed surface temperatures, have been measured continuously in conjunction with the measurements of dissolved oxygen.

The MIKE 3 hydrodynamics model has been used in combination with the MIKE 3 water quality module that includes sediment respiration, particulate BOD at the sediment surface, and oxygen production through photosynthesis, providing a physical description of spatial and temporal oxygen variation in Klamath Lake. In preliminary BOD-DO simulations, rates of algal production, respiration, and sediment oxygen demand have been estimated from actual physical measurements in the lake. Results from BOD-DO model were compared with physical measurements of oxygen at a number of stations in the lake. Agreement between simulated and observed DO were satisfactory.

Results of the EU-simulations include average daily production which are then converted into maximum daily productions at noon, and then entered into the BOD-DO model. Respiration rates and sediment oxygen demand are extracted from the MIKE 11 EU simulations in a similar manner.

8.3.2 Heat Exchange and Water Temperature

A heat exchange module is included in MIKE 3. This module computes internal water temperature both for simulation of water quality constituents as well as for computation of hydrodynamic mixing processes within the lake itself. In order to compute heat flux at the air-water interface, the model requires input of wind speed, wind friction, relative humidity, cloudiness, a light extinction coefficient, and the latitude of the site. Data for the period August 6-20 1997 has been included in model simulations. The measured wind speed and direction (Figure 8-9) and air temperature (Figure 8-10) for this period, in conjunction with the below rough estimates, were applied: (horizontal dispersion, Smagorinski turbulence closure and wind friction

Horizontal dispersion coefficient	1 m ² /sec
Mixed k-ε, Smagorinski turbulence model	
Constant bed roughness	0.25
Wind friction coefficient	0.0016
Relative humidity	88%
Clearness coefficient (sky cover)	70%
Standard meridian for time zone	-120 deg.
Beta in Beer's law	0.3
Light extinction coefficient	1.0

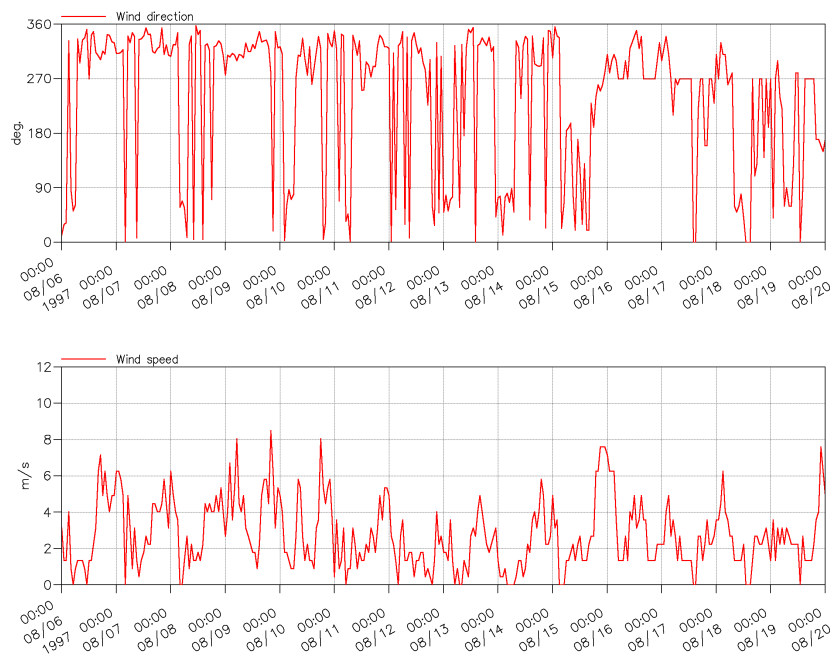


Figure 8-9 Wind direction and speed for August 6-20, 1997

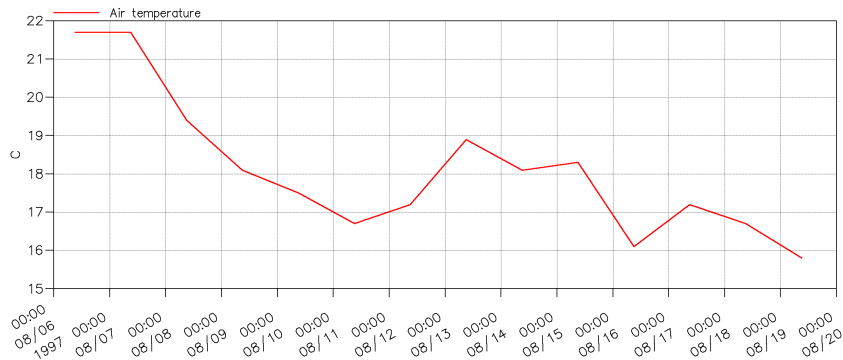


Figure 8-10 Daily Average Air Temperature for August 6-20, 1997

Figure 8-11 shows the location of monitoring stations used to reference model results. Figure 8-12 and Figure 8-13 show simulated lake water surface and vertical water column temperatures respectively at different stations for the selected period August 6-20, 1997. The model predicts a variation in temperature from the bottom on the order of 1.5 to 2 degrees only at the Stations MN, SB and AC. In the shallow areas at Stations HB and BB, there is no vertical variation in temperature. Similarly, the available measurements at Stations MN and SB on August 12 show variations in water temperature in the order of 2 to 3 degrees. At Station EE, however, the measurements reveal a fully mixed system. The vertical mixing process is caused mainly by wind shear, which is very important to the vertical mixing of oxygen. However, there is no data at available for a detailed assessment of the vertical mixing process.

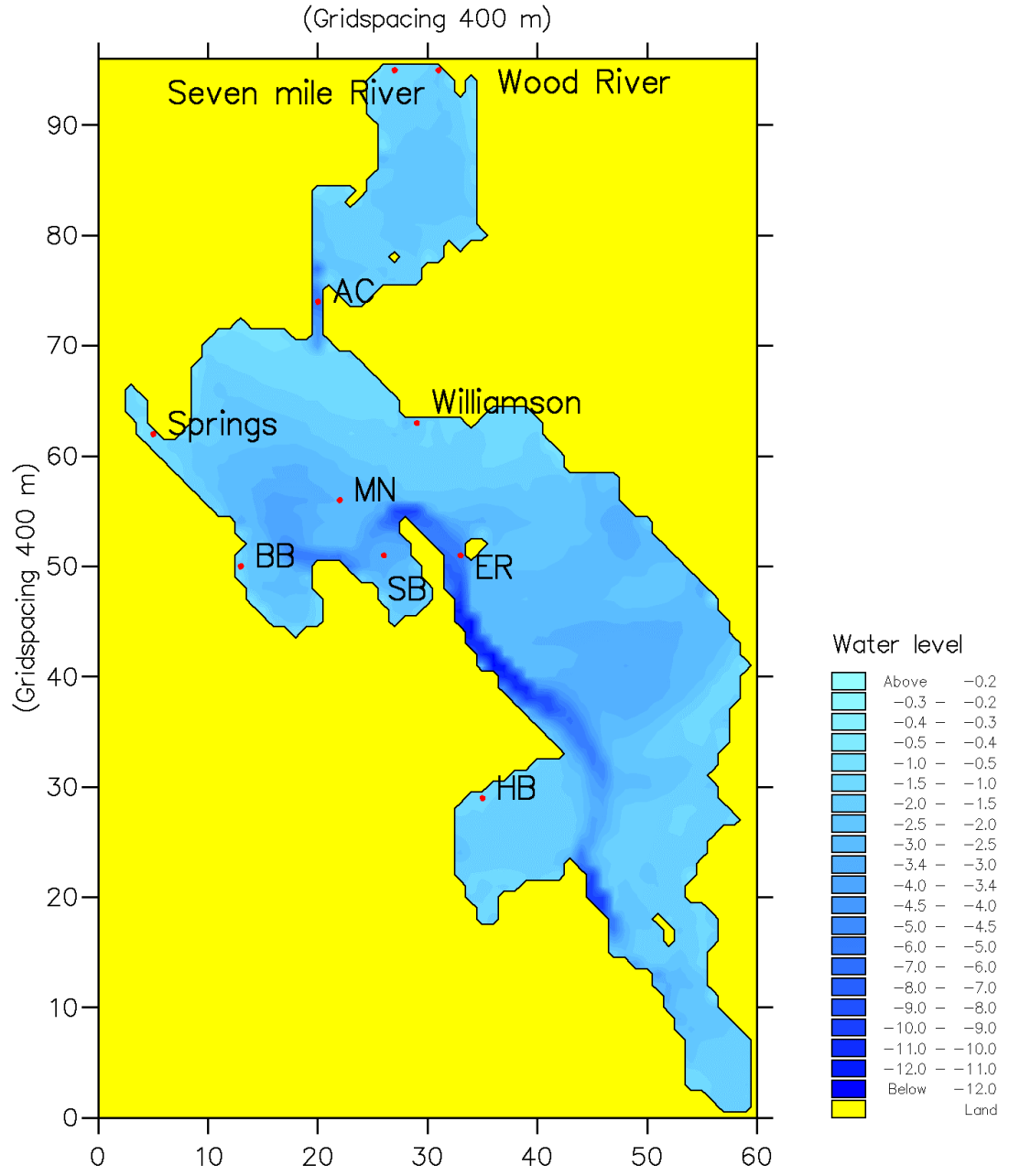


Figure 8-11 Stations on Upper Klamath Lake

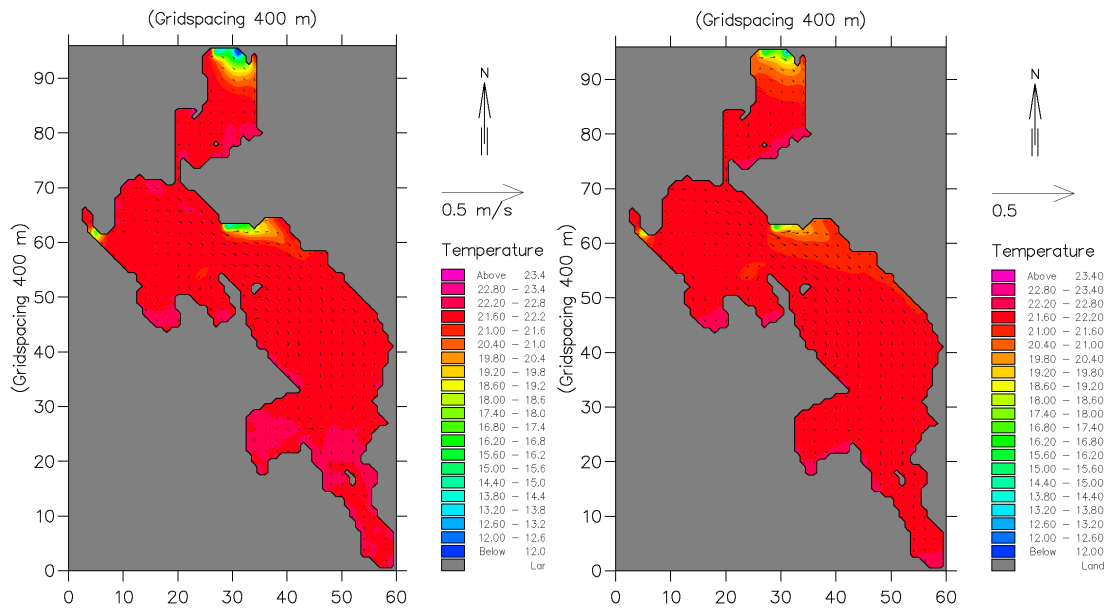


Figure 8-12 Average Spatial Variation in Lake Water Surface Temperature (August 6-20, 1997). (Left figure shows 1997 condition and right figure shows 1997 condition with a decrease in water surface by 1 meter).



Figure 8-13 Vertical Variation in Lake Water Column Temperature (August 6-20, 1997) for Stations BB, HB, MN and SB (from top left to lower right)

8.3.3 Dissolved Oxygen

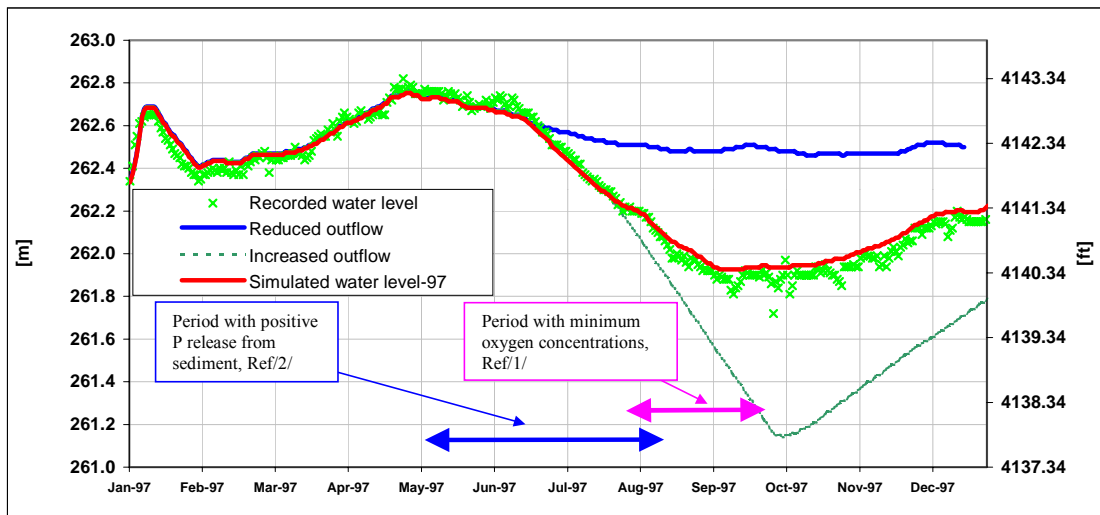


Figure 8-14 Lake Elevation Changes Simulated in the Water Quality and Eutrophication Model

Dissolved oxygen simulations were performed for a one week analysis period, August 10-17. Three scenarios were investigated 1) a reference simulation with an initial water level of 4140.9 feet (262.14m) 2) an increased water level simulation with an initial water level of 4142 feet (262.49 m) 3) a decreased water level simulation with an initial water level of 4140.2 feet (261.94 m).

The 3D scenario modeling of dissolved oxygen demonstrates a combination of the effects of altered water levels (physical change), as well as the change in biological activity (biological change).

Results of MIKE 11 EU simulations are used to estimate rates of algae production, algae respiration, water respiration, and sediment oxygen demand. Rates of sediment oxygen demand (SOD) and water respiration are taken directly from MIKE 11 EU scenario simulations. Algae production and respiration cannot be extracted directly from MIKE 11 EU; however net daily averaged primary production rate ($gC/m^2/day$) is available as model output. Instead of converting the net primary production rate from the MIKE 11 scenario simulations into algae production and algae respiration, the relative change compared to the reference situation is used. During calibration of the MIKE 3 oxygen model, algae production and respiration were estimated from monitoring data in the lake. The monitoring data shows a spatial variation, and hence the lake is divided into 5 representative areas with different levels of biological activity.

The areas comprise of:

- Agency Lake
- Ball Bay
- Upper Klamath Lake (main part)
- Shoalwater Bay
- Wocus Bay

For each area a representative value of algae production and respiration are estimated from monitoring data. These values are used in the reference situation and adjusted for the relative change found in MIKE 11 EU, from simulations of reduced outflow (higher water level) and increased (lower water level) outflow.

Estimated rates in the 3 simulations are shown in Table 8-1, Table 8-2, Table 8-3, and

Table 8-4.

Table 8-1: Maximum primary production at noon [gC/m²/day]

Station	Reference	Reduced flow	Increased flow
Agency Lake	7.0	6.72	7.21
Ball Bay	27.0	25.92	27.81
Klamath lake	20.0	19.2	20.6
Shoalwater Bay	15.0	14.4	15.45
Wocus Bay	30.0	28.8	30.9

Table 8-2: Algae respiration [gO₂/m²/day]

Station	Reference	Reduced flow	Increased flow
Agency Lake	3.50	3.36	3.61
Ball Bay	13.50	12.96	13.91
Klamath lake	10.50	10.08	10.82
Shoalwater Bay	15.00	14.40	15.45
Wocus Bay	10.00	9.60	10.30

Table 8-3: Water respiration [gO₂/m²/day]

Station	Reference	Reduced flow	Increased flow
Agency Lake	1.35	1.36	1.22
Ball Bay	1.56	1.71	1.50
Klamath lake	1.44	1.56	1.33
Shoalwater Bay	1.89	2.01	1.80
Wocus Bay	1.32	1.31	0.94

Table 8-4: Sediment oxygen demand [gO₂/m²/day]

Station	Reference	Reduced flow	Increased flow
Agency Lake	3.89	3.83	3.83
Ball Bay	4.31	3.93	4.34
Klamath lake	4.01	3.70	4.10
Shoalwater Bay	4.10	3.92	4.08
Wocus Bay	4.31	4.11	4.29

Small differences are seen between the simulations. The most significant relative differences are identified for water respiration and sediment oxygen demand, while the most dominant absolute differences are for primary production and algae respiration.

A spin-up period of one week was used to get a steady solution of dissolved oxygen in the lower parts of the lake.

The simulated concentrations of dissolved oxygen at 5 different locations Figure 8-15, Shoalwater Bay, Ball Bay, Wocus Bay, in the middle of Klamath Lake and in Agency lake are shown in Figure 8-16, Figure 8-17, Figure 8-18, Figure 8-19 and Figure 8-20, respectively. The concentration is shown for 3 different depths, surface, middle and bottom layer. The black curve represents the reference situation, the green represents the situation with a higher water level in the lake, and the blue curve represents the situation with lower water level in the lake compared to the reference situation.

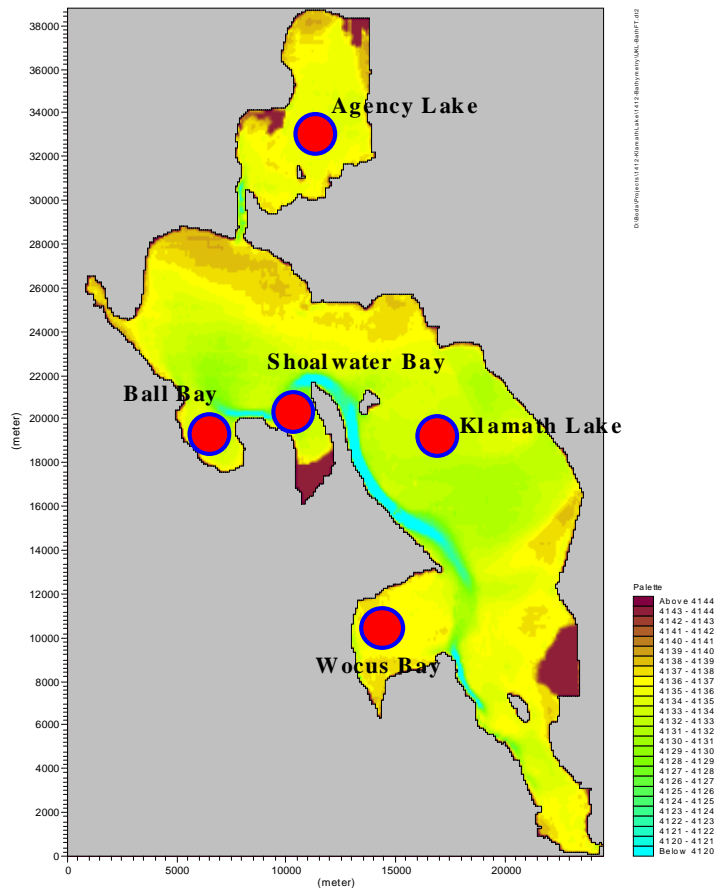


Figure 8-15 Location of Comparison Points

The results for the surface layer show almost similar concentrations of dissolved oxygen in the three simulations. The concentration varies over the course of a day with an average close to the saturation concentration. In the shallow areas, Ball and Wocus Bay, greater diurnal variations than those observed in Klamath Lake may be observed. Simulations suggest that higher phytoplankton biomass, and algae production and respiration may be associated with lower water levels. Such conditions favor greater diurnal variation in oxygen (i.e. higher oxygen concentrations are observed during the day, and lower concentrations are observed during the night). During nighttime hours, oxygen concentrations become critical in Ball and Wocus bays; however such low concentrations are only temporary. During the day, super saturated conditions may be observed at the surface of these same locations.

In the middle of the water column, concentrations of oxygen are both decreased and show less diurnal fluctuation. With a few exceptions, oxygen concentration at middle elevations is greatest for increased water level scenarios, and lowest for decreased water level scenarios. Ball Bay has the most critical oxygen conditions with average oxygen concentrations of around 3 mg/l and minimum levels close to zero mg/l during nighttime hours.

Oxygen concentrations in the deepest part of the lake are low. Minimum concentrations oxygen are less than 2 mg/l. When water levels are increased, oxygen concentrations are somewhat improved in deeper parts of Agency Lake, Klamath Lake and Shoalwater Bay. An increase in oxygen level of up to 0.5 mg/l compared to the reference situation is seen for the whole period. For the remaining areas, (i.e. Ball and Wocus Bays) oxygen conditions are improved by increased water levels; however, this improved is observed mainly during nighttime hours.

In shallow areas (Wocus Bay, North and Northwest parts of the lake) simulations suggest that lower water levels produce higher oxygen concentrations, in contrast to the general trend. This is due to the higher primary production in these areas. The respiration is higher as well, but the net effect gives slightly higher oxygen concentrations. On the other hand, oxygen concentration is lower during nighttime hours where it is most critical.

Differences in oxygen concentration can be up to 1 mg/l but is in generally less than 0.5 mg/l, when comparing the reference with the simulations with higher/lower water level in the lake. The positive effect on the oxygen concentration from increasing the water level is most pronounced in the deeper part of the lake.

Note:

- Color annotation used in the graphs.

REF (Black) Reference data (simulation use data as recorded in 1997)

RED (Green) Reduced outflow

INC (Blue) Increased outflow

- Layer descriptions see Figure 8-21

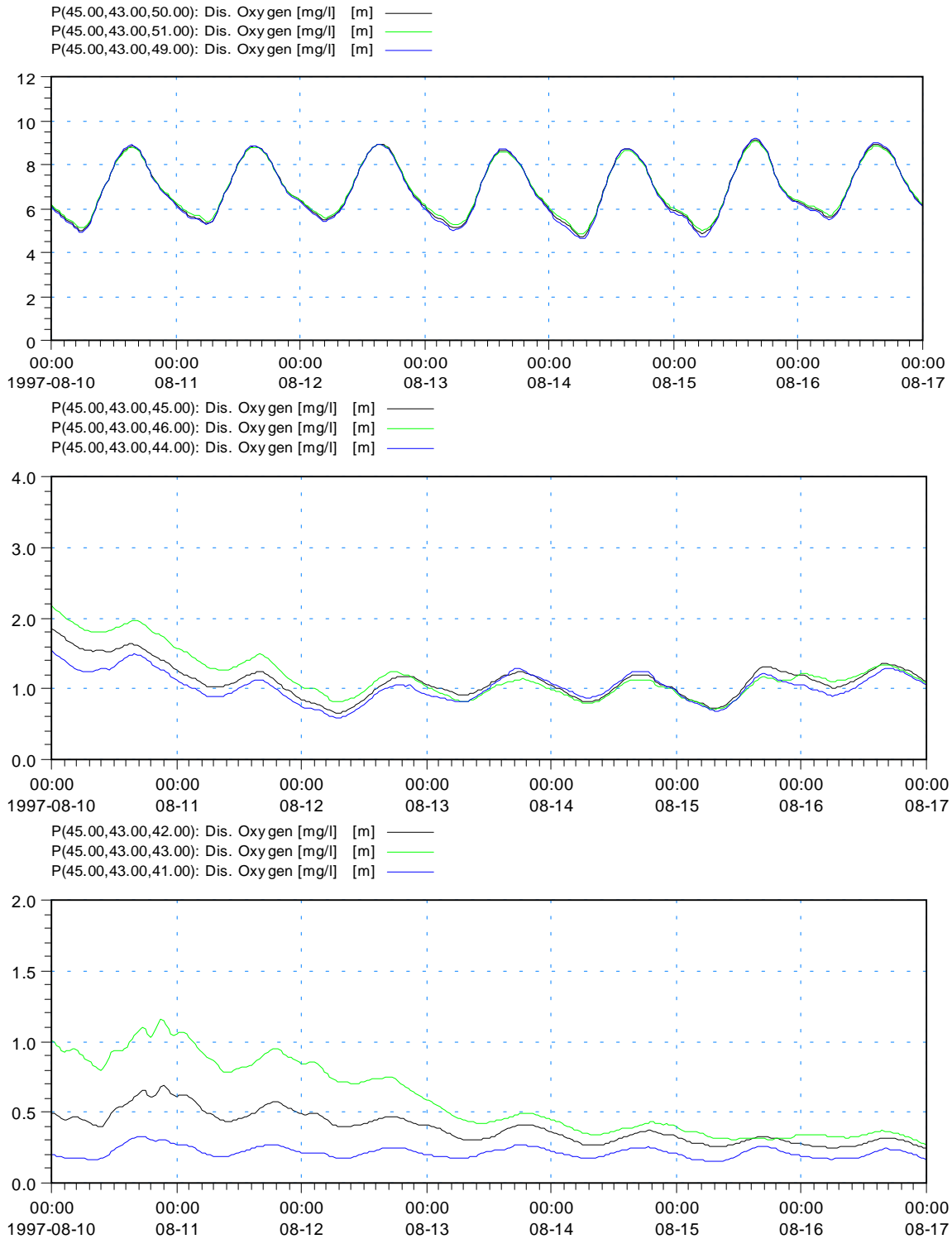


Figure 8-16 Dissolved Oxygen Concentration in Klamath Lake (Upper/Middle/Lower layers)

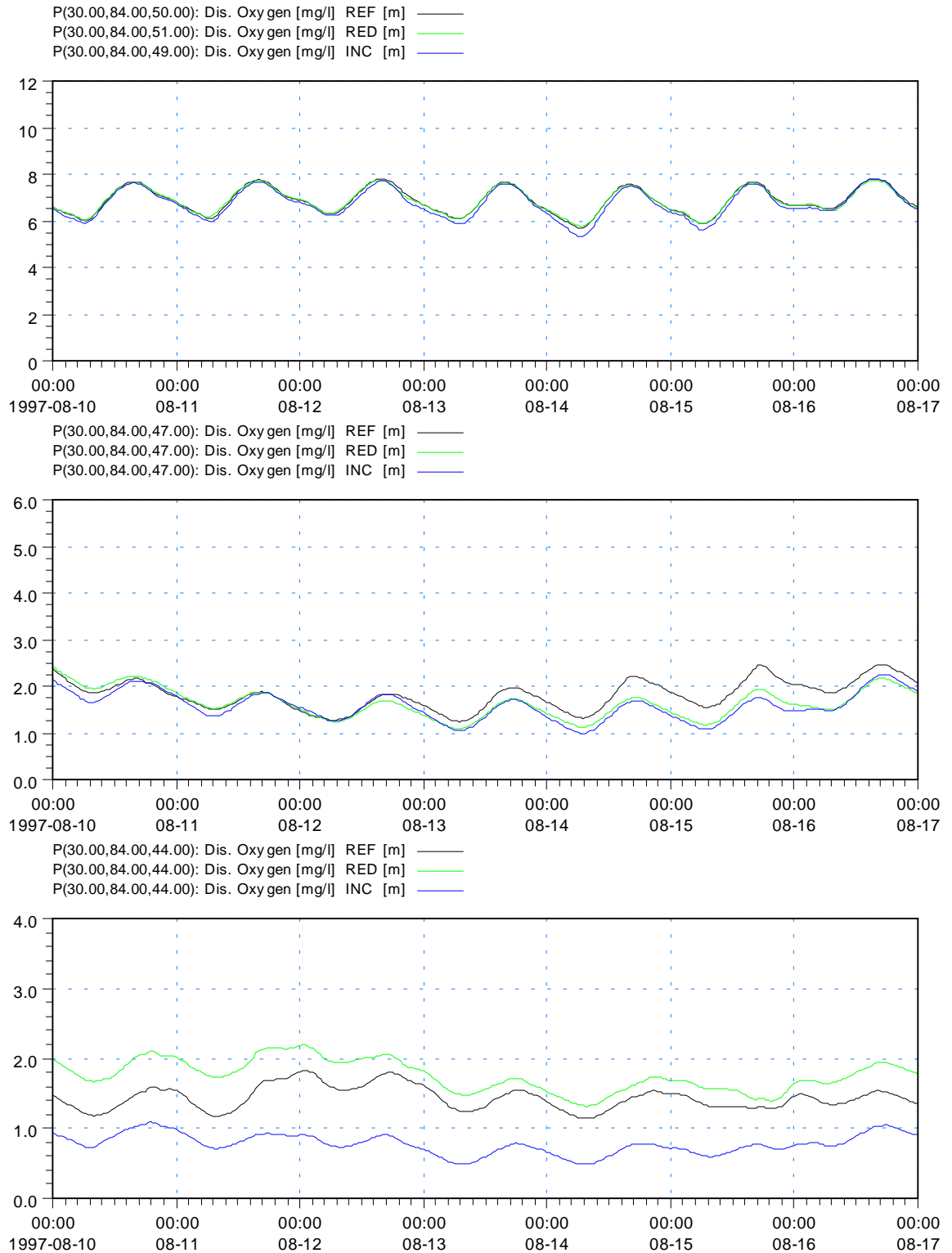


Figure 8-17 Dissolved Oxygen Concentration in Agency Lake (Upper/Middle/Lower layers)

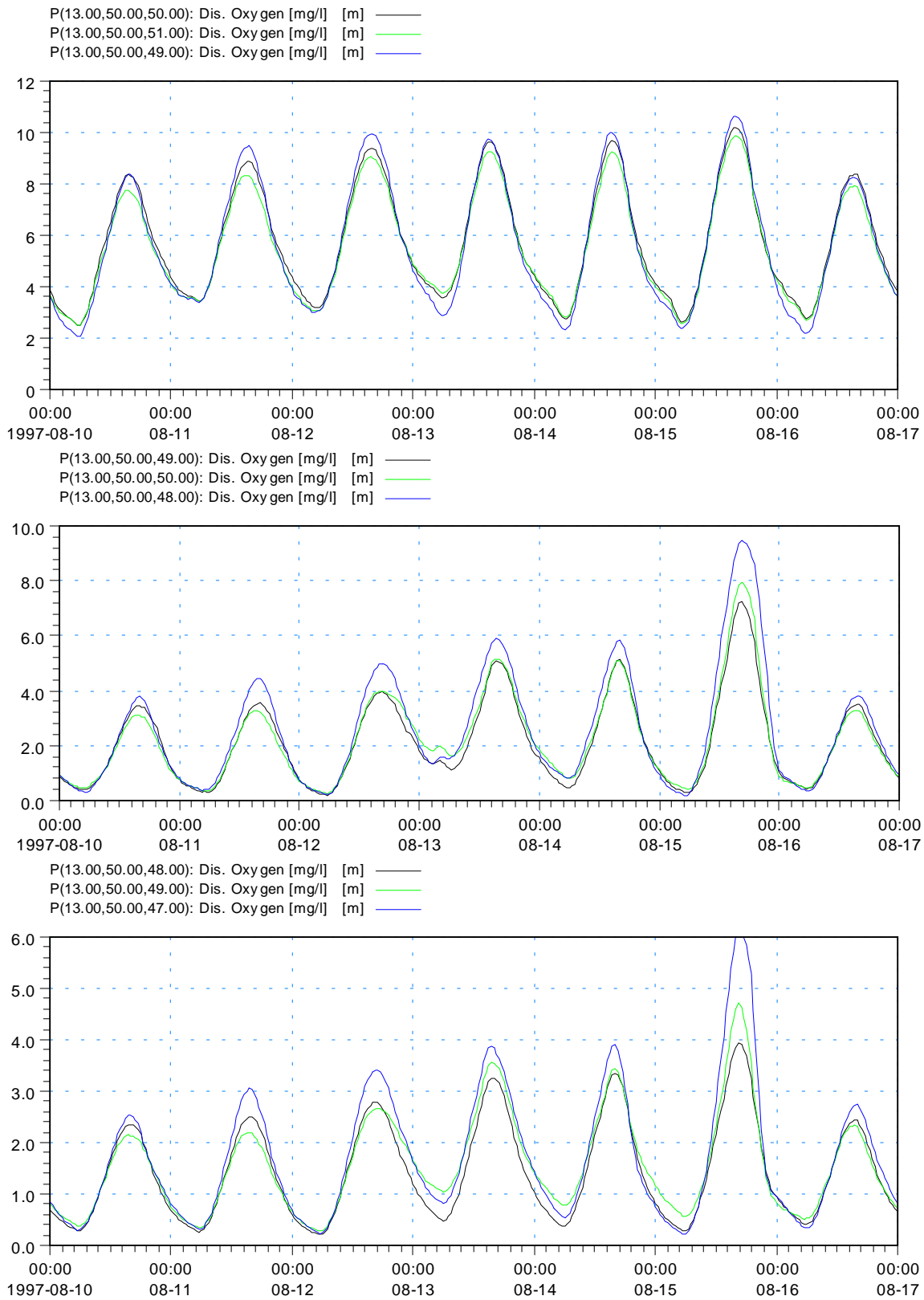


Figure 8-18 Dissolved Oxygen Concentration in Ball Bay (Upper/Middle/Lower layers)

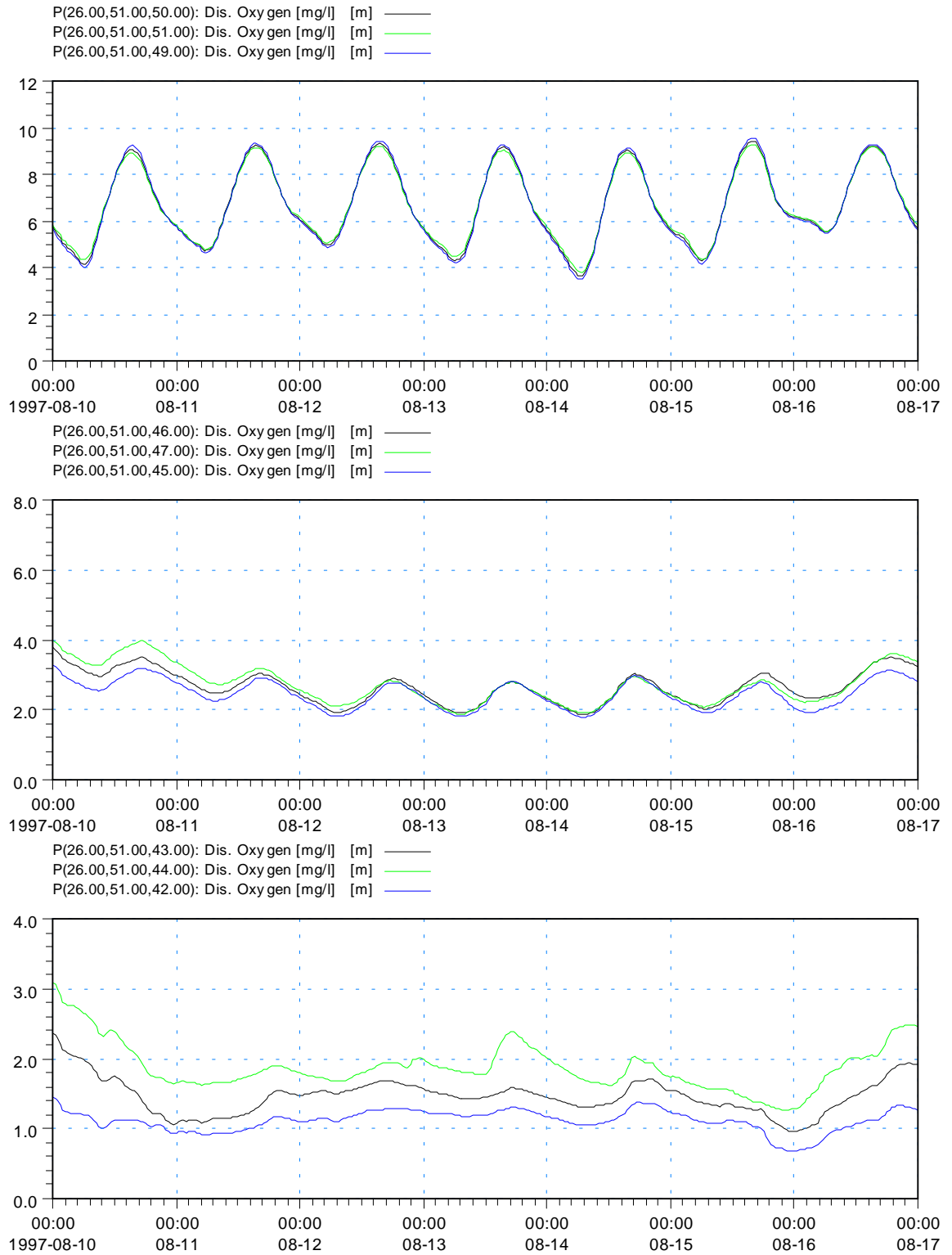


Figure 8-19 Dissolved Oxygen Concentration in Shoalwater Bay (Upper/Middle/Lower layers)

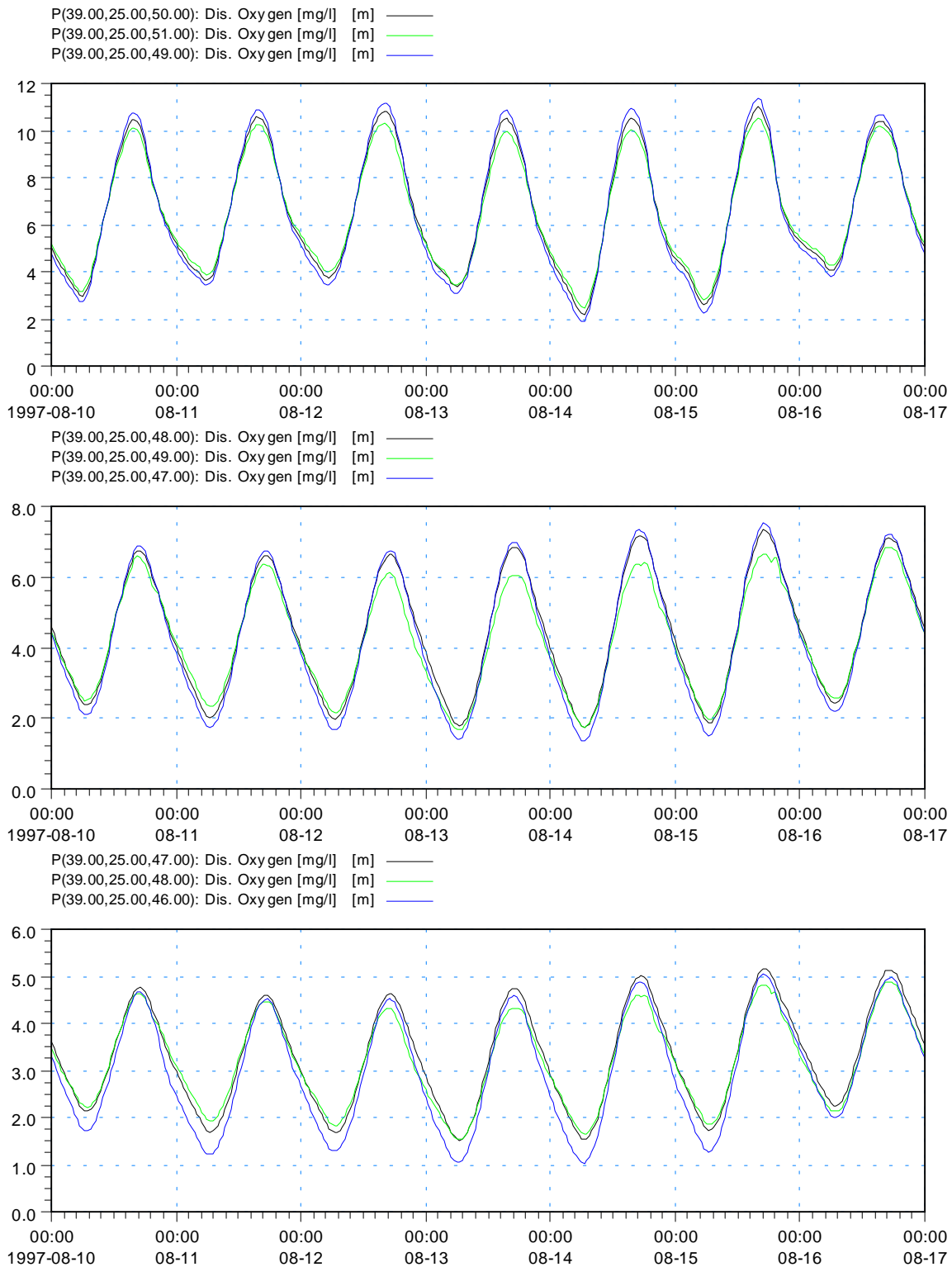


Figure 8-20 Dissolved Oxygen Concentration in Wocus Bay (Upper/Middle/Lower layers)

The model produces values for dissolved oxygen concentration at all locations in the model grid, for each time step simulated.

In order to display these results in a meaningful manner, contour plots were generated. Each of these plots show results for a particular depth. For purposes of analysis, three depths (layers) were selected which were representative of the surface, middle and bottom of the lake.

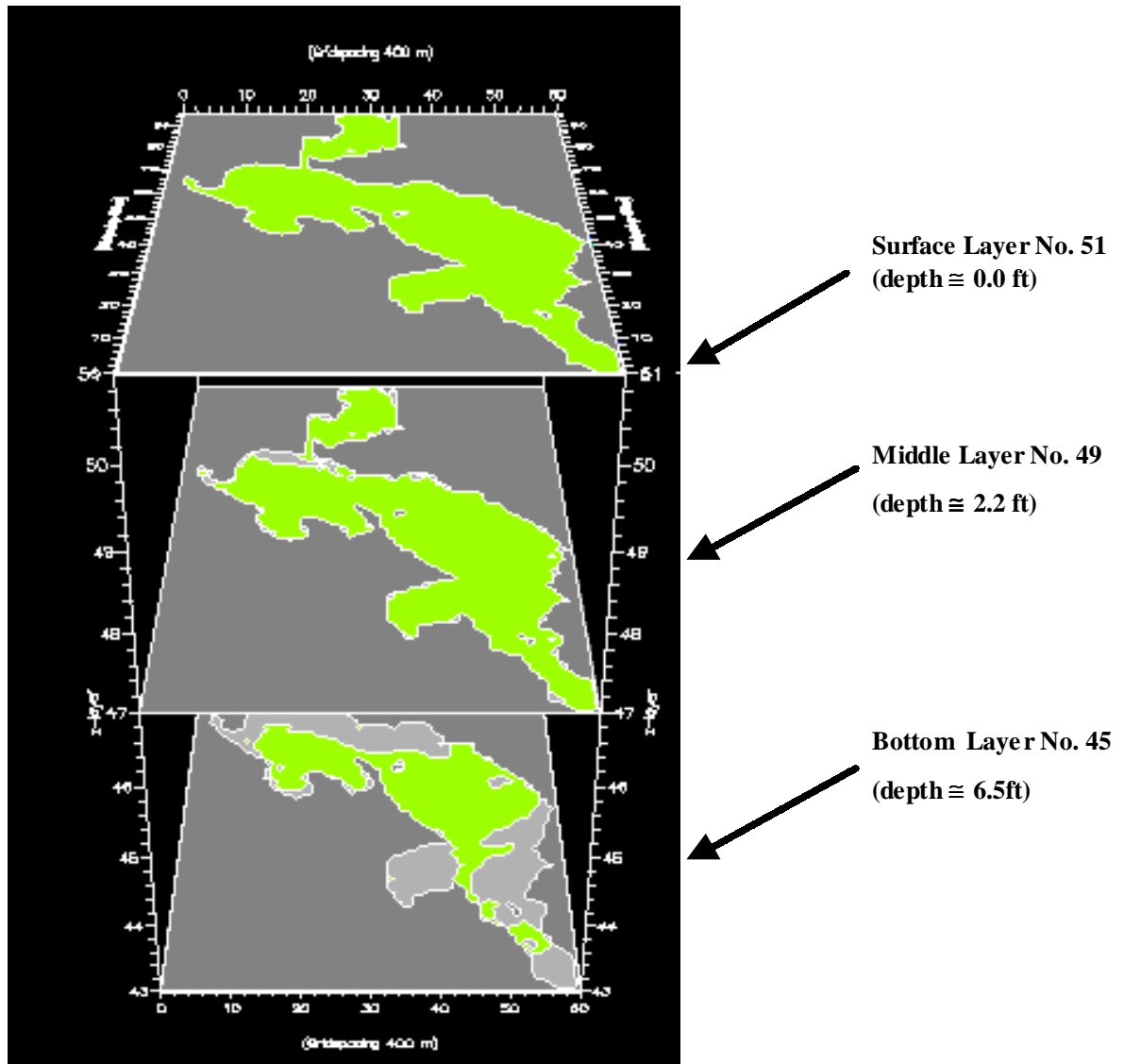


Figure 8-21 Schema of the Layer Presentation - /Layer 51, Layer 49 and Layer 45 are used/.

The results represent Upper Klamath Lake condition during summer (August 10-17, 1997) one week period. (Alternative B base conditions) The figures show minimum oxygen concentration for a particular depth observed during simulation period. Figure 8-22 shows the minimum DO concentration in the surface layer, Figure 8-23 shows minimum DO concentration in the middle layer, and Figure 8-24 shows minimum DO concentration in the bottom layer of UKL.

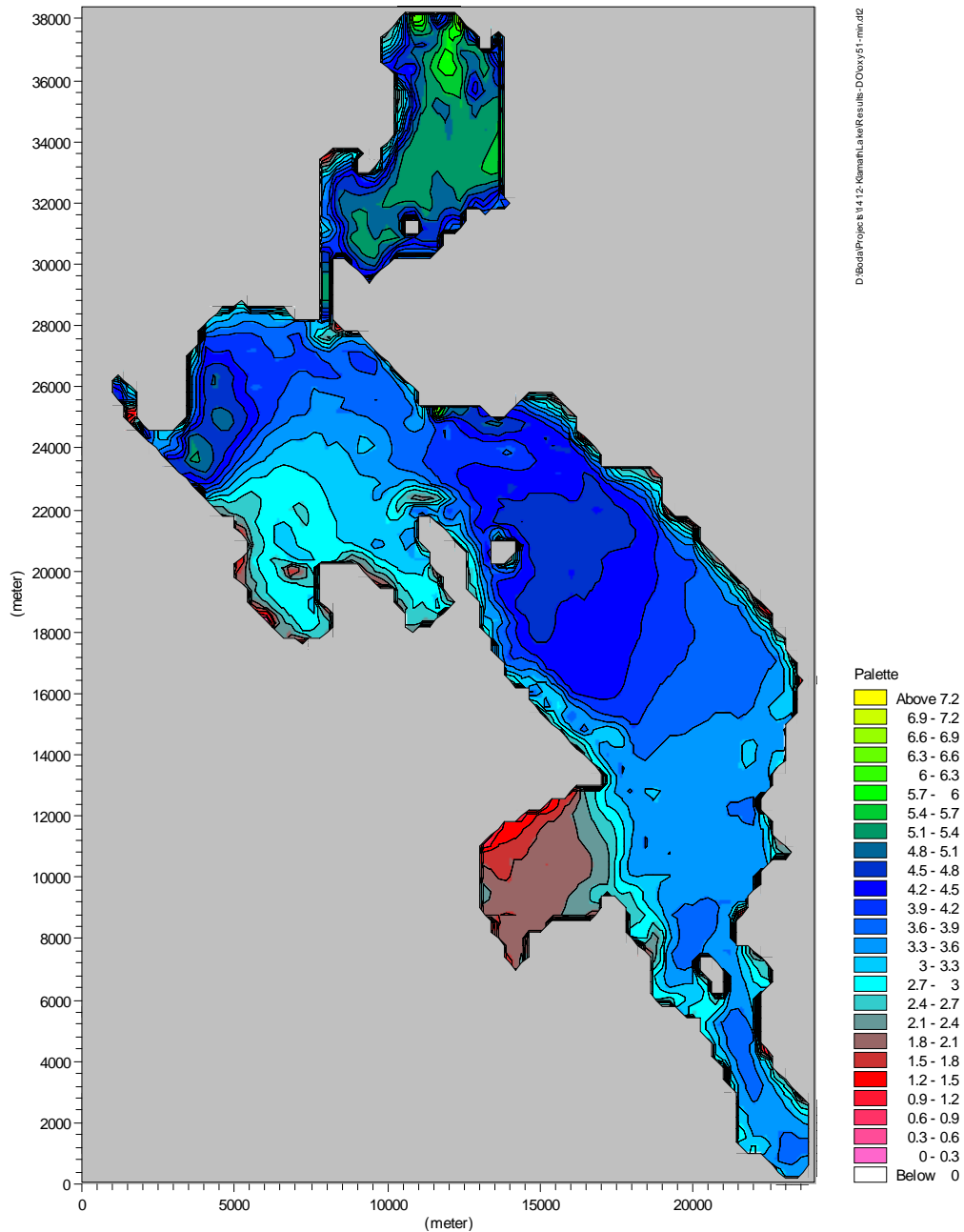


Figure 8-22 Minimum Dissolved Oxygen Concentration for Upper Layer during August 10-17, 1997 simulating period.

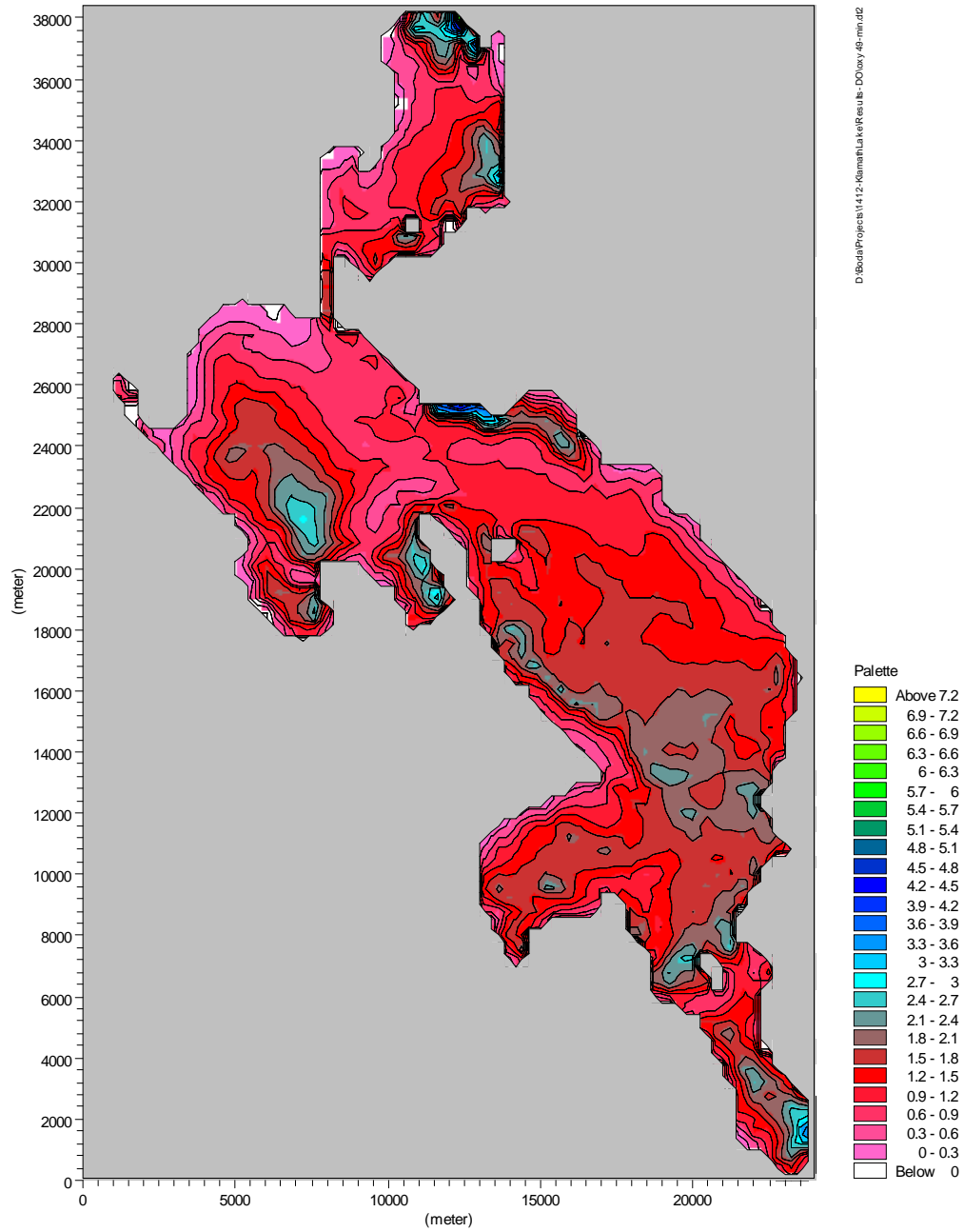


Figure 8-23 Minimum Dissolved Oxygen Concentration for Middle Layer during August 10-17, 1997 simulating period

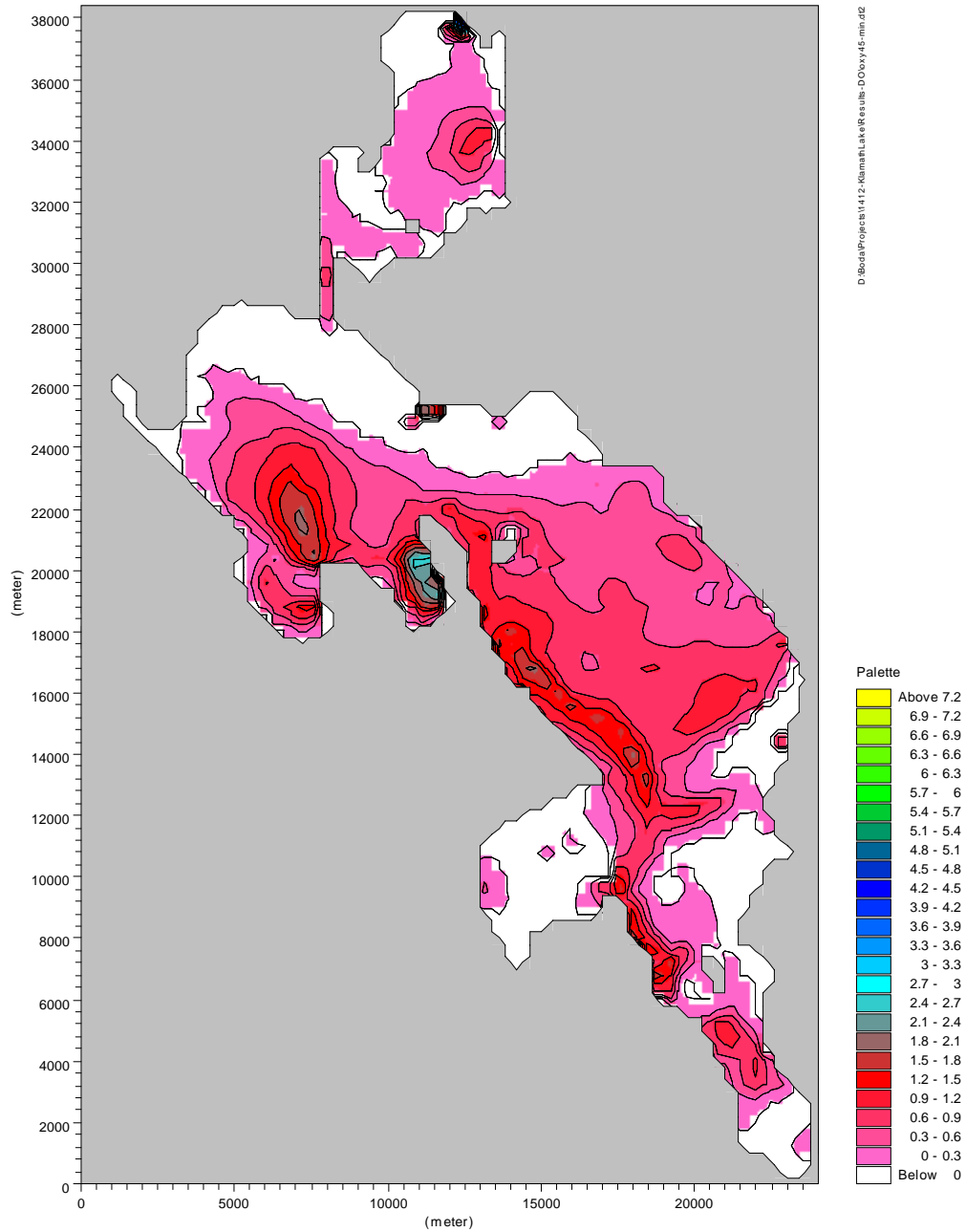


Figure 8-24 Minimum Dissolved Oxygen Concentration for Bottom Layer during August 10-17, 1997 simulating period

The results represent monthly (August 1997) mean Dissolved Oxygen concentration for a particular depth. Figure 8-25 shows the minimum DO concentration in the surface layer, Figure 8-26 shows minimum DO concentration in the middle layer, and Figure 8-27 shows minimum DO concentration in the bottom layer of UKL.

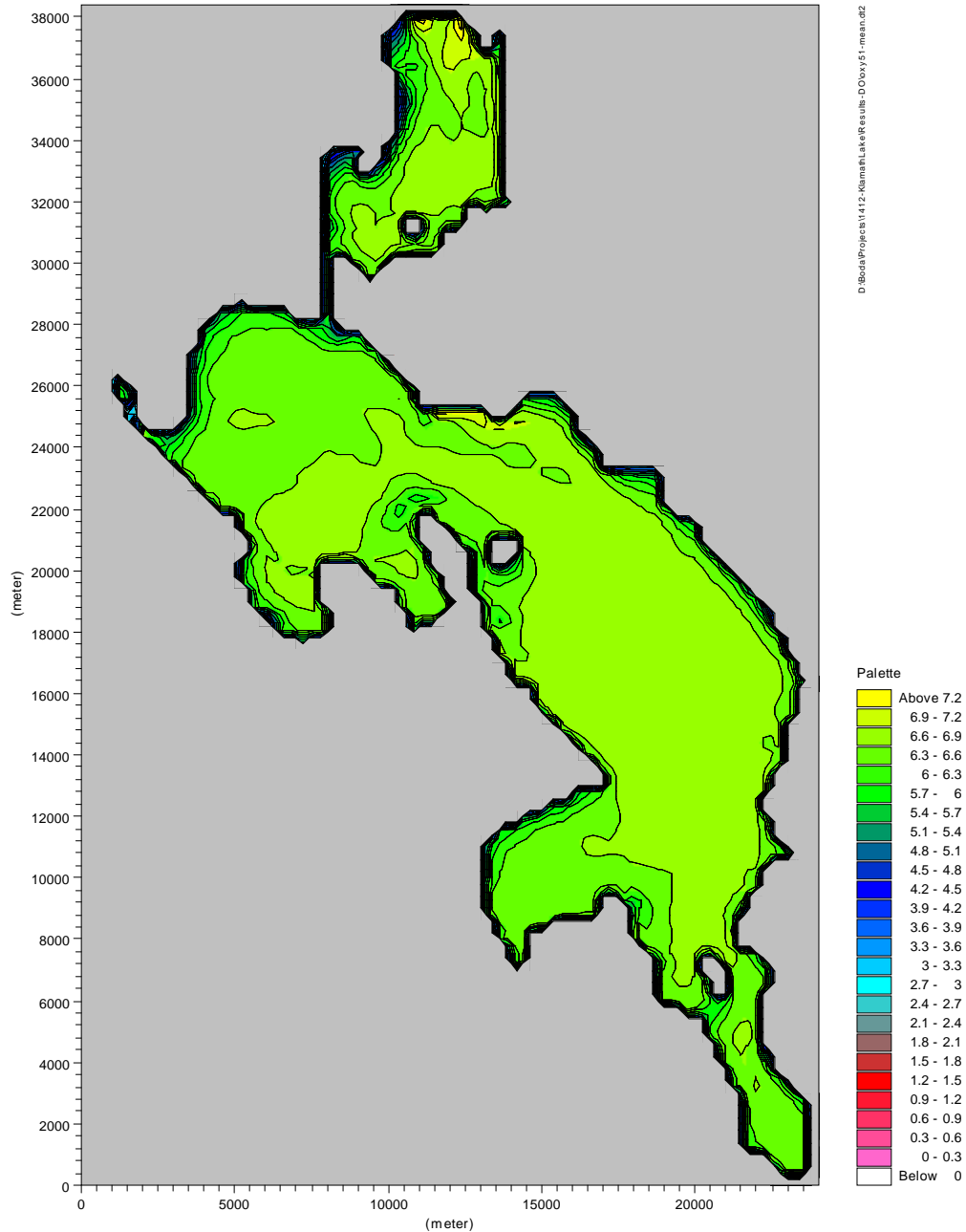


Figure 8-25 Mean Dissolved Oxygen Concentration for Upper Layer during August 10-17, 1997 Simulating Period

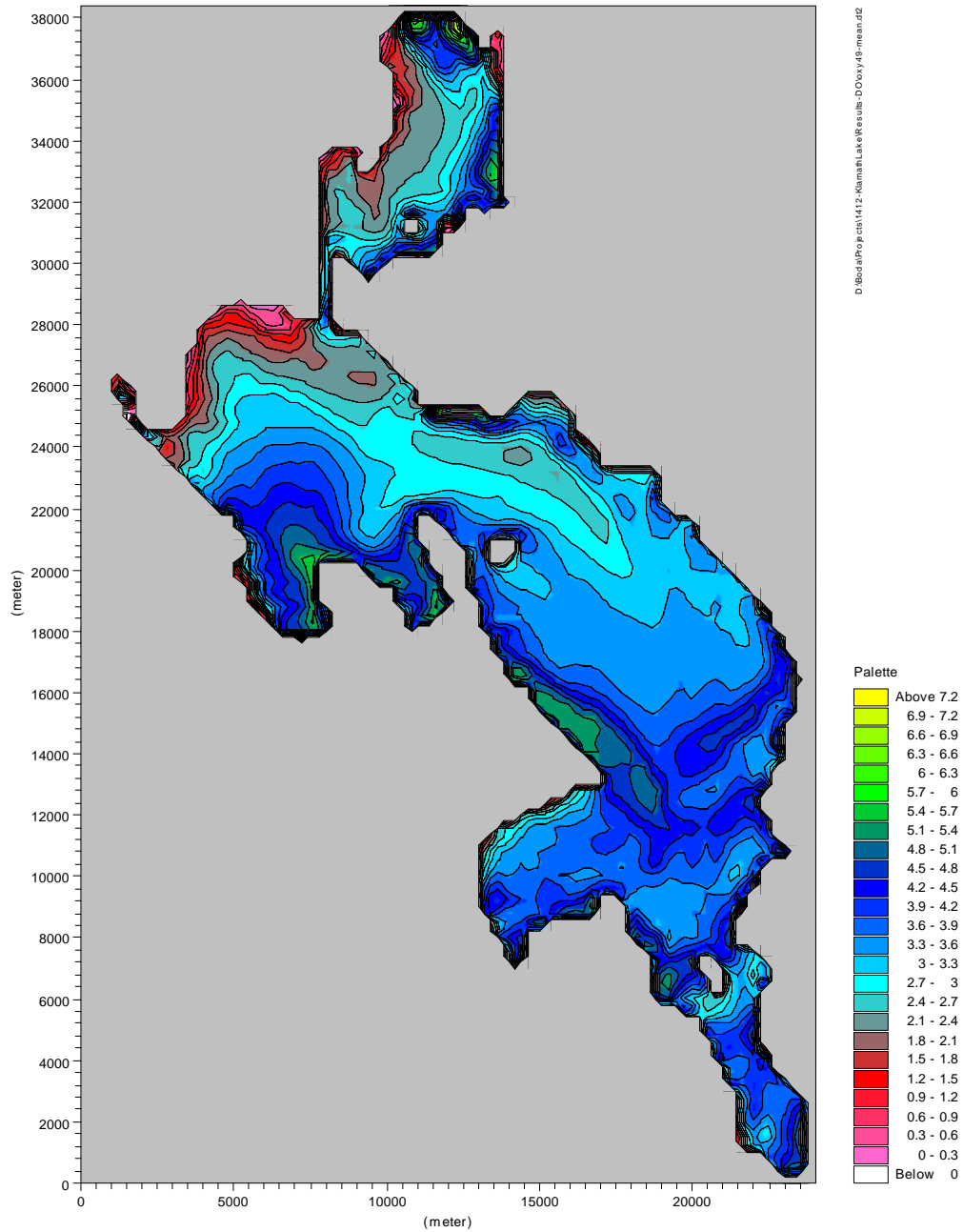


Figure 8-26 Mean Dissolved Oxygen Concentration for Middle Layer during August 10-17, 1997 Simulating Period

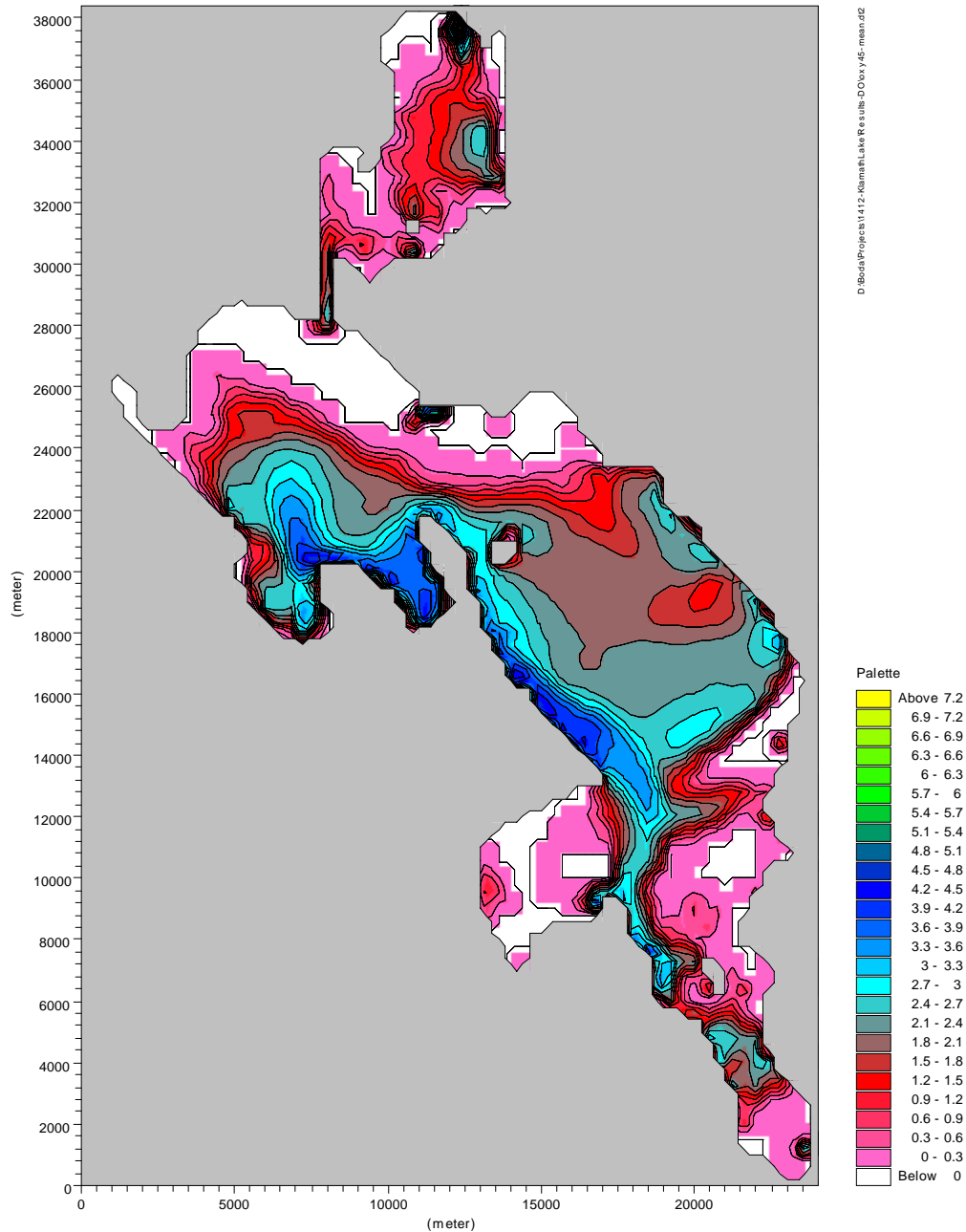


Figure 8-27 Mean Dissolved Oxygen Concentration for Bottom layer During August 10-17, 1997 Simulating Period

It is obvious that concentration of dissolved oxygen depends on the water depth, position and time of the day. Considering 2.0 DO mg/l as a minimum concentration able to sustain reasonable aerobic condition in the water, only middle part of the UKL, areas near Bare Island and Eagle Ridge are close to this limit. In regard of the fish population in the lake it is obvious that environmental stress is high and can produce condition resulting fish kills as was historically observed. The detail assessment of the hydrodynamic, water quality and eutrophication on the biology and lake habitat is not a part of this study.

8.4 MODEL RESULTS OF EUTROPHICATION SIMULATIONS

The MIKE 11 eutrophication model was used to simulate nutrient and phytoplankton concentrations for two scenarios with changed water levels (Figure 8-1) and one scenario with a reduced load. For the scenarios with a changed water level, the year 1997 was chosen as the background year for the simulations.

- Reference simulation (REF): Simulation with water level and nutrient load as recorded in 1997.
- Reduced outflow (RED): Water level does not drop below 4142 feet, Nutrient load as in 1997.
- Increased outflow (INC): Water level is not allowed to drop below 4138 feet, Nutrient load as load as in 1997
- Load simulation: Water level as recorded, P load reduced with 37%.

8.4.1 Regulation of water level

The model results are presented as plots of phytoplankton biomass, TN and TP for Station AC, MN, ER, ML and PM (Figure 8-11) forming a line through Agency and Upper Klamath Lakes (Figure 8-28 and Figure 8-29). Another series of plots has been generated to presenting input data from the EU model to the Water Quality model (Figure 8-31, Figure 8-32, Figure 8-33). These plots present plankton and detritus biomass, net production of oxygen, sediment respiration and respiration in water for Stations AC in Agency Lake and Upper Klamath Lake including Ball Bay, Shoalwater Bay and Wocus Bay.

The changes between the reference simulation and the simulations with increased lake level (reduced outflow) and reduced lake level (increased outflow) has been summarised in Table 7-2 and Table 7-3.

8.4.2 Chlorophyll and phytoplankton biomass

Comparing the reduced outflow and the reference scenarios, with reduced outflow with the reference scenario, the concentration of chlorophyll decreases in Agency Lake and in the northern part of UKL whereas it increases in the southern part of UKL and in the bays. Biomass of phytoplankton in gcm^{-3} decreases for all stations. An increase in water level will reduce the time the phytoplankton will be in the photic zone and thereby reduce the photosynthesis. As a countermeasure for being exposed to less light, phytoplankton can increase the chlorophyll content of the cells. The EU model simulates this by increasing the Chl_a:C ratio. This explains why the chlorophyll concentration increases while the phytoplankton biomass decreases.

The result of reduced outflow (increased water level) is a decrease in net primary production, a decrease in phytoplankton biomass and a variation of chlorophyll concentration close to the reference simulation, but with a over general tendency to higher concentrations. Increasing the

outflow and thereby decreasing the water level provoke increasing chlorophyll concentrations and phytoplankton biomasses on all stations.

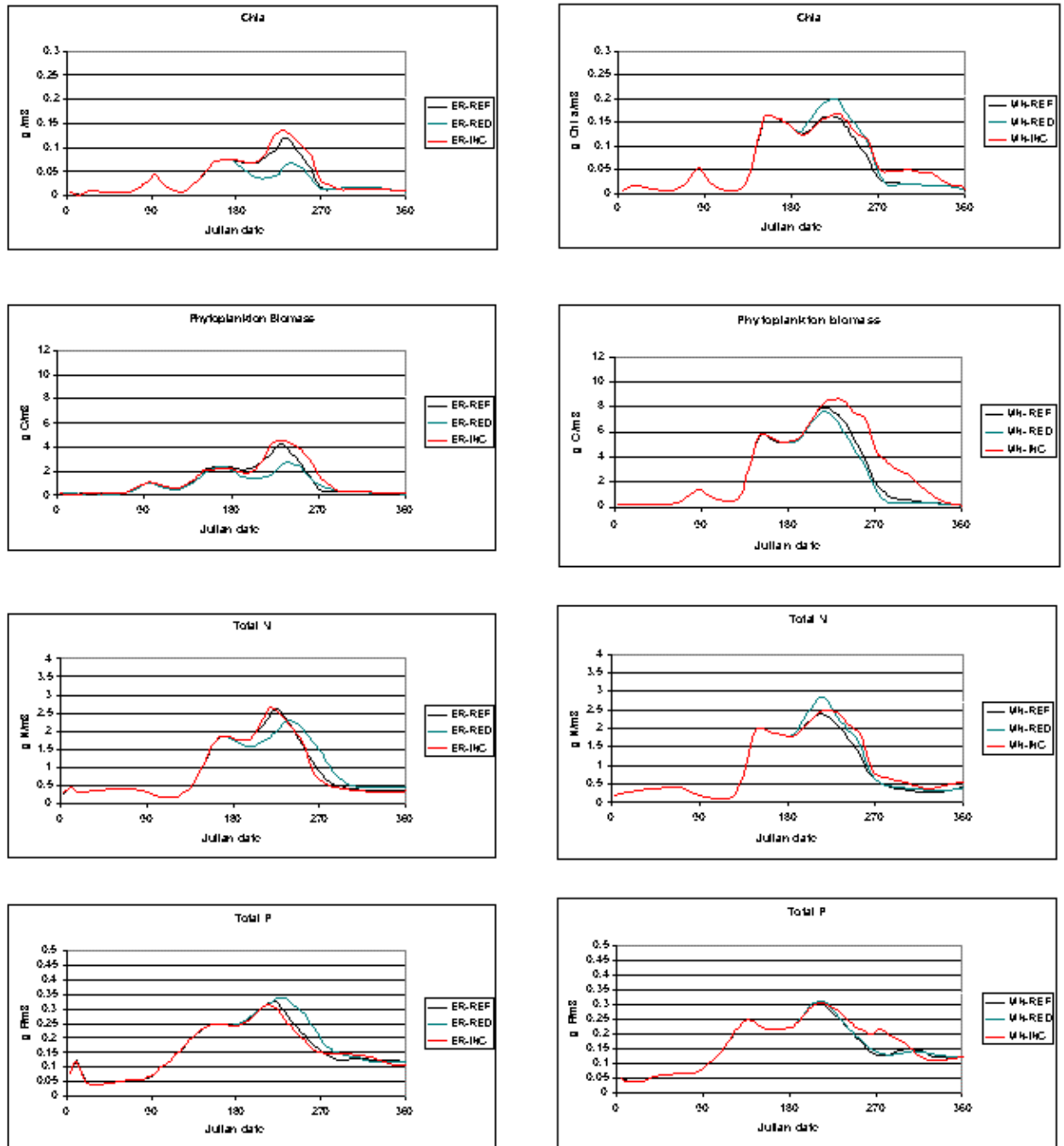


Figure 8-28 Chlorophyll, phytoplankton biomass, TN and TP for the water level scenarios, St. ER and ML in UKL. RED: reduced outflow. INC: increased outflow. REF: reference 1997

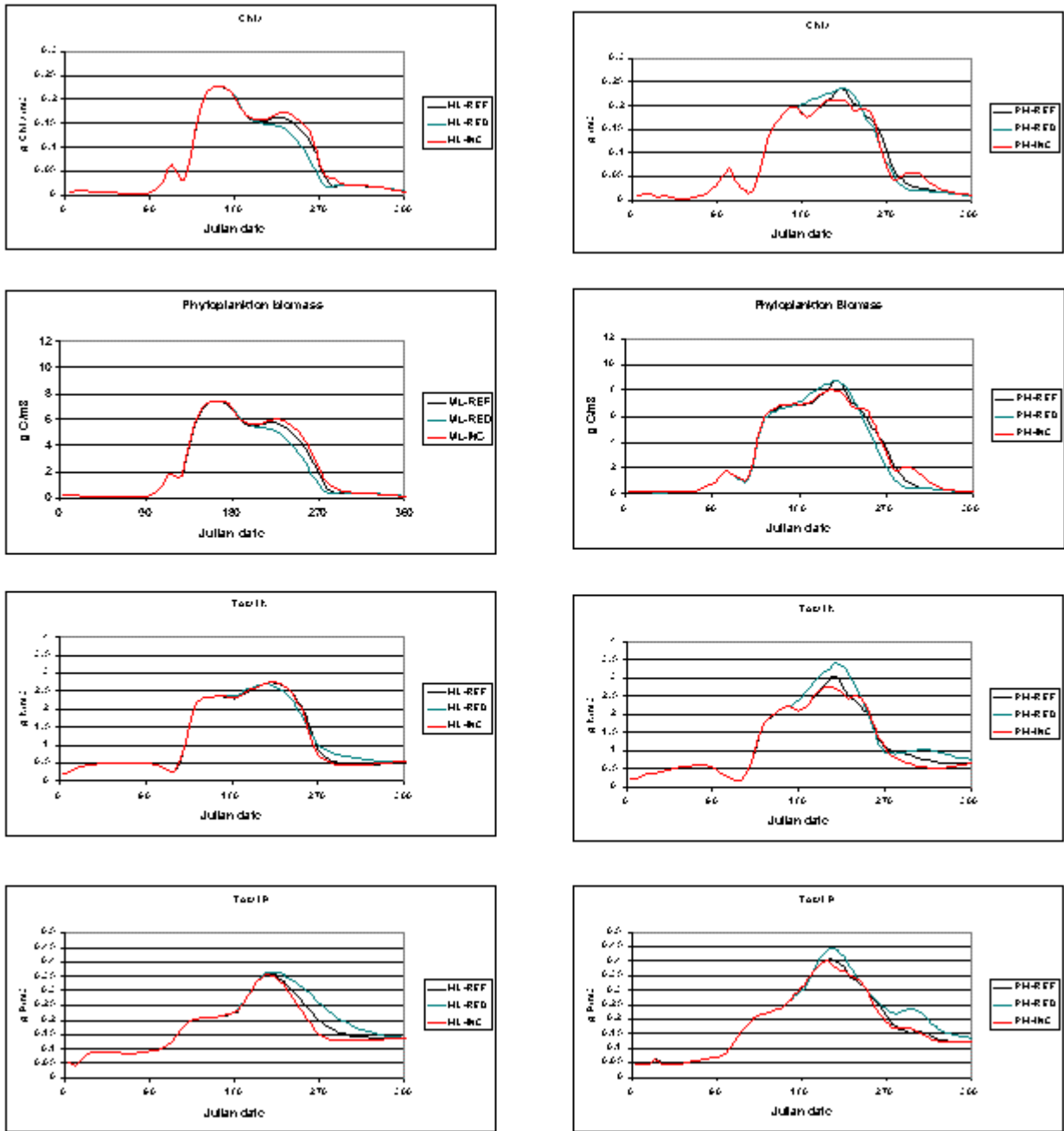


Figure 8-29 Chlorophyll, phytoplankton biomass, TN and TP for the water level scenarios, St. ER and ML in UKL. RED: reduced outflow. INC: increased outflow. REF: reference 1997.

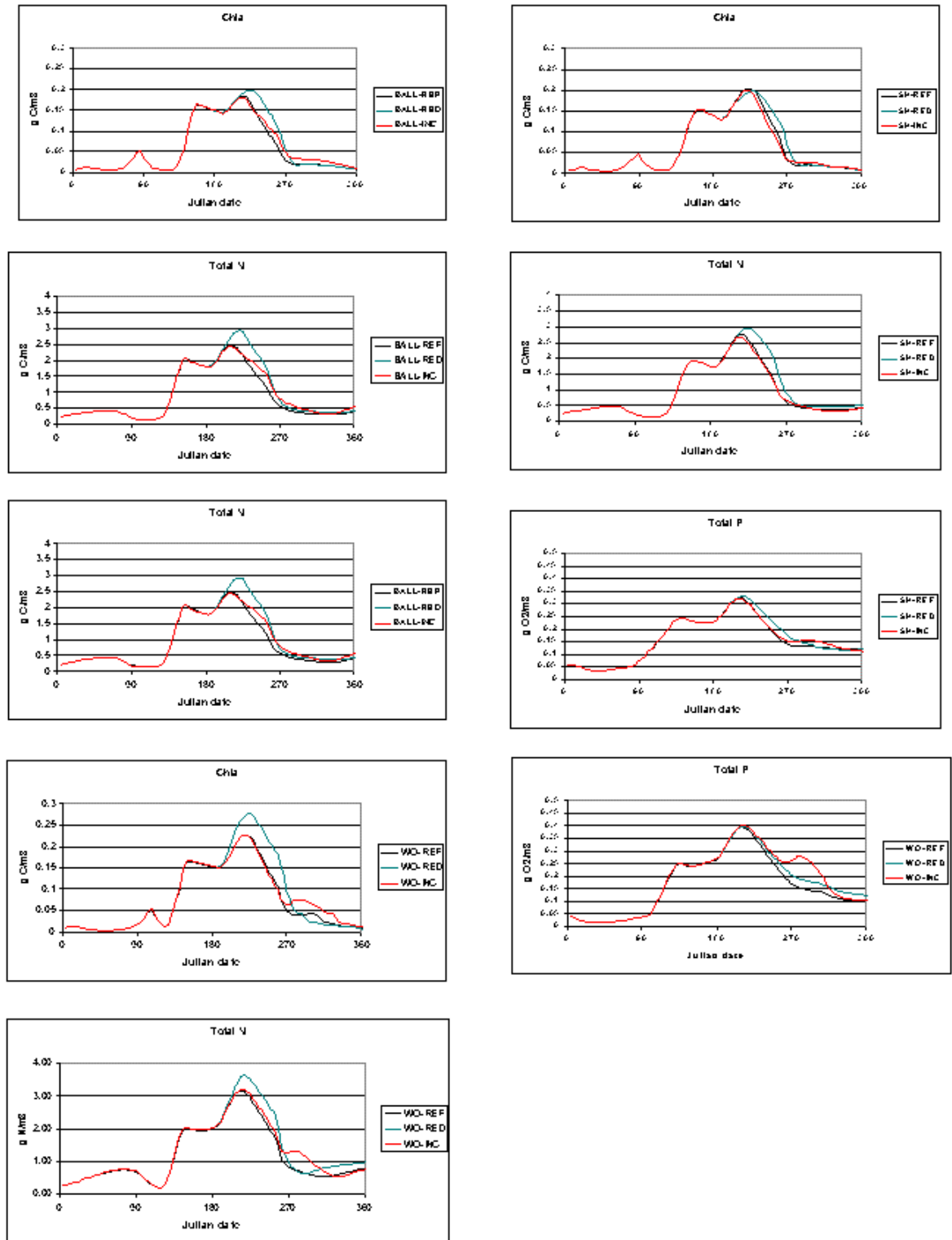


Figure 8-30 Chlorophyll, TN and TP for the Water Level Scenarios, Ball Bay, Shoalwater Bay and Wocus Bay

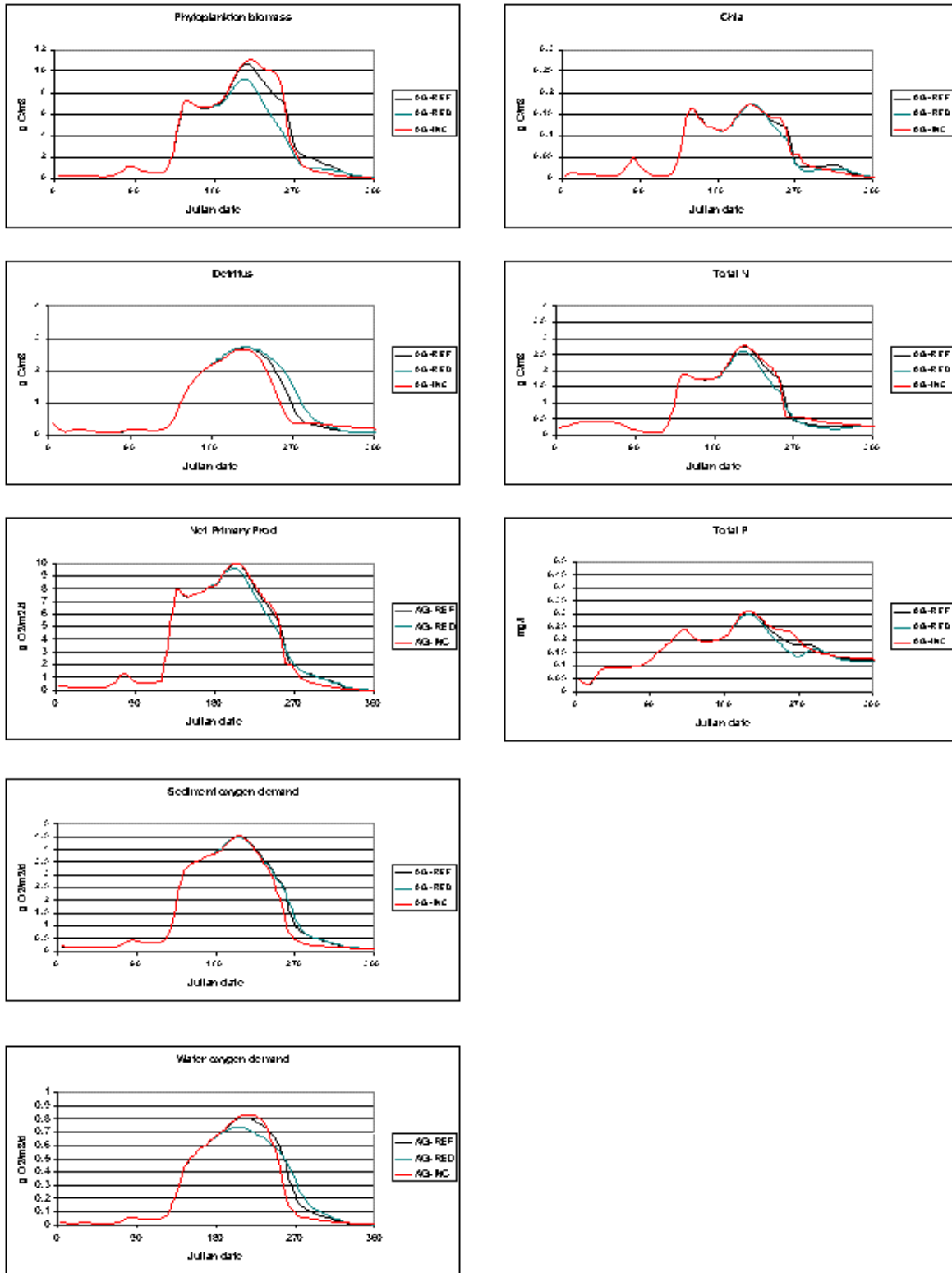


Figure 8-31 Simulated chlorophyll, plankton biomass, DO production and respiration, Agency Lake St. AS

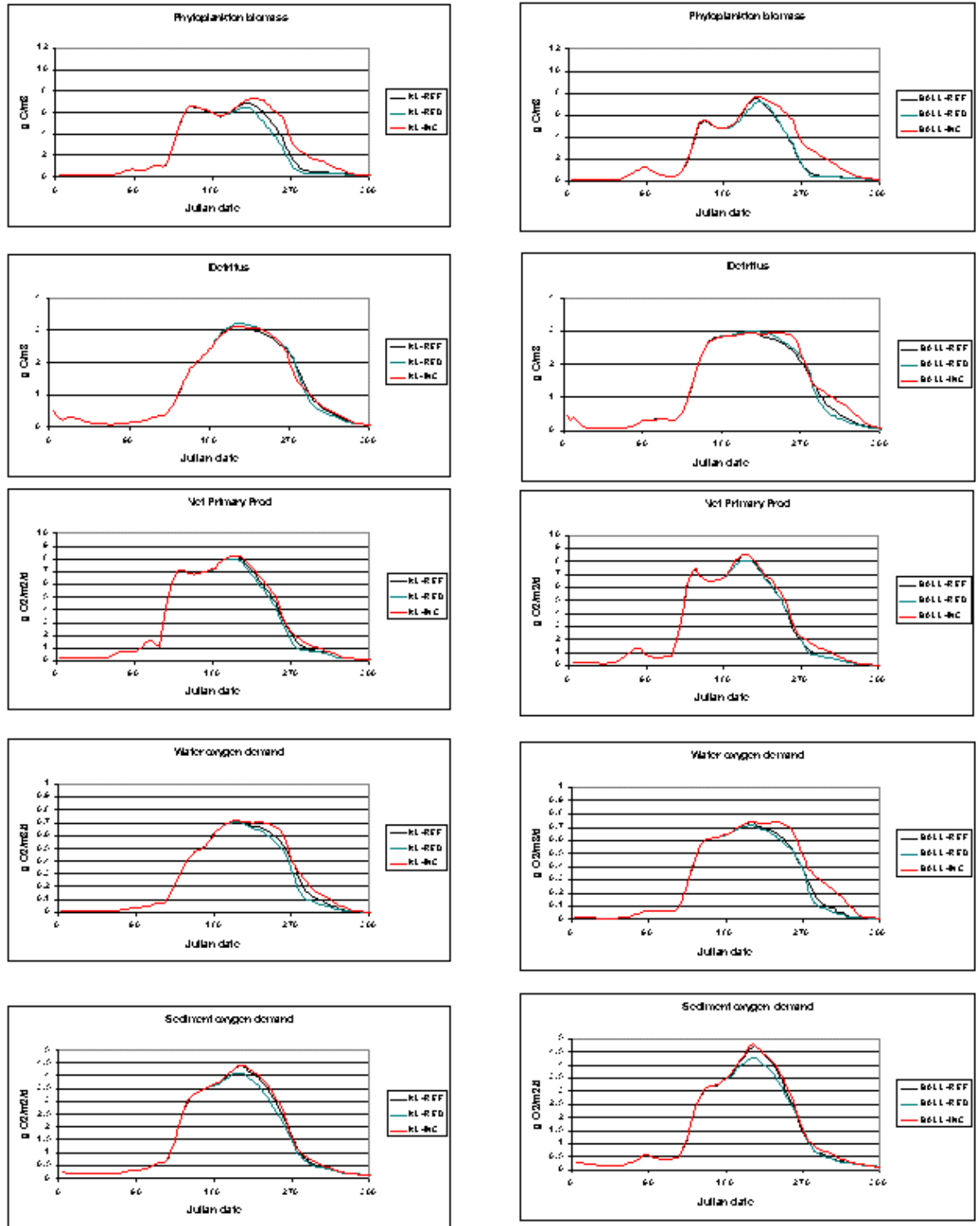


Figure 8-32 Simulated plankton biomass, DO production and respiration, UKL and Ball Bay

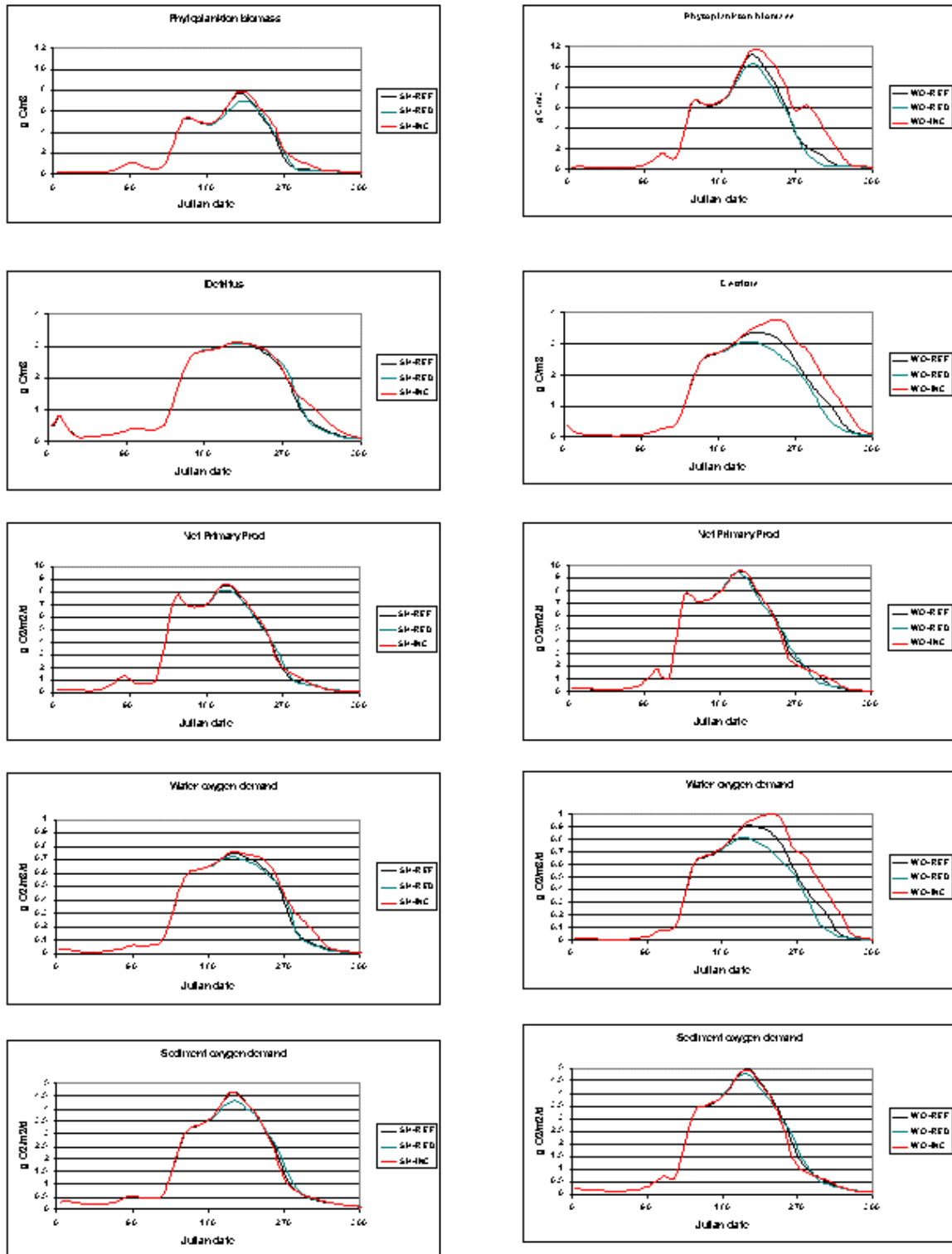


Figure 8-33 Simulated plankton biomass, DO production and respiration, Shoalwater Bay (SH) and Wocus Bay

8.4.3 Total Nitrogen

Reducing the outflow (i.e. increasing lake level) has a mixed impact on the total nitrogen (TN) concentration. In Agency Lake and at the deep station in UKL, (ER)(can't find reference to this station), TN concentration decreases; however, TN is unchanged as a result of increased lake levels at other stations in UKL. In the bays TN concentration increases because of increased lake level.

Inherent in the increased lake level scenario is an increase in lake retention time during the algae grown season. When outflows are reduced, phytoplankton biomass concentration decreases, with a corresponding decrease in total nitrogen concentration. However, as for chlorophyll, the algae can increase the N:C ratio blue green algae to make N fixation.

These two seemingly opposite processes, increased residence time for nitrogen fixation and decreased phytoplankton biomass is the best explanation for decreased TN concentration resulting from increased water levels.

In the scenario with increased outflow (i.e. decreased lake level), the TN concentration increases or is the same for all stations except at the station close to the outlet in UKL (Station PM). Model simulations indicate that the increase in phytoplankton biomass of C is not followed by as large an increase in the energy consuming N-fixation.

8.4.4 Total Phosphorous

At reduced outflow and higher lake levels, total phosphorous (TP) concentration decreases in Agency Lake, remains the same in the northern part of UKL, and increases in the middle to southern part of UKL and in the bays. The internal load in UKL is calculated to be 170% of the external load in water year 1997 ref. (29). As discussed in the previous section, Reducing the outflow and increasing the retention time in the same period as the internal load is at its highest may at some stations give a higher TP concentrations.

At first glance, model results seem to contradict the findings in ref. (26) where the total P concentration in June to August for measurements with chlorophyll concentrations above 0.1 g/m³ were positively correlated with June-August lake volume. However, a review of the data on which this relation is generated shows that if the June-August lake volume was low then the maximum volume in spring is also low, and the two volumes follow each another, Figure 7-1. (23). If the volume in the period from spring until August is lower, then the TP concentration will be higher in June-August, because the high internal load from the sediment will be diluted into a smaller volume. .

In the case of the model scenarios, the lake volumes for the three simulations (REF., RED. and INC.) are the same until the first half of July (day 180-195). Therefore, the simulation shows the response of the TP concentrations if the spring and early summer volume was the same, but

with different volumes in August-September. The hydraulic conditions used for the scenarios are different from the hydraulic conditions behind the data generation the empirical relations between June-August lake volumes and (max.) TP concentrations presented in ref. (23). A comparison between model TP concentrations in June August and concentration estimated by the empirical relation is therefore not possible.

With the same arguments as for TP, the relation presented in ref. (23) between June-August lake volume and maximum Chlorophyll a concentrations cannot directly be compared with presented model response. Though the model response in terms of phytoplankton biomass gives the same trend as the empirical relation for chlorophyll, the spring early summer lake volumes are different in the data set behind the empirical relation and the model simulations.

In the scenario with increased outflow resulting in decreasing water level, the TP concentration increases in Agency Lake and in the northern UKL and has a tendency to decrease or be the same as the reference simulation in the middle and southern UKL. In the bays, an increase in the TP concentration is seen in September-October when the water level is at its lowest.

The decrease in TP concentration can be explained by an export of TP from this lake while decreasing the water level. The TP load to this load is higher per square meter than to UKL, and therefore, TP is exported from Agency Lake into the northern UKL, giving a higher TP concentration at Station MN. The mixed response on the TP concentration in the middle and southern part of the lake is the result of the internal P load minus the export of TP from the lake divided with the lake volume is neutral positive or negative.

8.4.5 Net Primary Production, Sediment Oxygen Demand and Oxygen Consumption in the Water

The EU model calculates the net primary production (NPP), the sediment oxygen demand, and the oxygen consumption in the water through nitrification and decomposition of detritus. Respiration by the algae is not simulated. In eutrophic lakes the total water respiration from algae and bacteria on a yearly average was 1.5 times the NPP, ref. (49). This ratio however varies over the year from 0.6 in early summer to over 2 in August. The respiration from the algae therefore is important for the daily variations in the oxygen concentrations. As a first approximation to evaluate the impact of the changing water levels, the biomass of phytoplankton is used as a parameter. If the biomass increases, the respiration will also increase and vice versa.

The scenario with reduced outflow gives lower phytoplankton biomasses in Agency Lake and UKL except close to the outlet and in Ball Bay where the biomass is the same as the reference. The respiration from algae will therefore also be lower with higher water level.

The NPP decreases in Agency Lake but is the same in UKL and the bays except for Wocus Bay where the NPP decreases. The simulated sediment respiration (SOD) decreases in UKL but

remains unaffected in Agency Lake and Wocus Bay. The water respiration minus algae respiration decreases for all stations with increased water level.

For increased outflow and decreased water level, the biomass of phytoplankton increases whereby the algae respiration will increase. The NPP and the sediment oxygen demand remain close to the reference simulation. The water respiration minus alga respiration increases for all stations in UKL whereas it remains close to the reference simulation in Agency Lake.

8.4.6 Summary

The findings in terms of increase or decrease in concentrations or primary production and respiration are summarized in Table 8-5 and Table 8-6 for lake water levels above and below the reference level, respectively. Each of the simulated concentrations or processes with changed water level has been compared with the reference simulation and been assigned a value “lower” or “higher” if the concentration or process rate was lower or higher than the simulated reference. The tables are constructed so improvements of the water quality are assigned a value “lower” and degradation in water quality is assigned a value “higher”. If there is no change the value is “0” and if the change is small then brackets are used.

At the bottom of the tables the number of values “lower” and “higher” are summed up for biomasses and processes related to DO concentration; i.e., biomass of phytoplankton, detritus, NPP, SOD and water respiration minus algae respiration. Below this score for the DO concentration, a score for the general eutrophic status is summed up using change in chlorophyll and nutrients as indicators. A percent (%) score is calculated and presented in the right column.

For the scenario with reduced outflow the score for improved DO condition (“lower biomass, DO processes”) is 57% against a score of a worse condition is 4%, giving no change in 49%. In contrast, the scenario with increased outflow gives a score of 13% for improvements, 52% for a worse DO condition, and 35% for no changes.

When examining the score for general eutrophication, the scenario with reduced outflow show 67% for increase in nutrient or chlorophyll concentration, 17% for decrease in concentrations and 16% for no change.

The scenario with increased outflow gives a score for increased concentrations of 42%, decrease in concentrations of 25% and a score of no changes of 33%.

Table 8-5 Change In Chlorophyll, TN, TP, And DO Processes In Simulation With Reduced Outflow In The Growth Season Relative To Reference Simulation

Parameter or Process Reduced outflow	Agency-AS	UKL-MN	UKL-ER	UKL-ML	UKL-PM	Ball Bay	Shoalwater Bay	Wocus Bay	% Score
Chlorophyll, g chl/m ³	(lower)	higher	Lower	lower	higher	higher	Higher	higher	
Phyto. Biomass, g C/m ³	lower	lower	lower	lower	0	0	Lower	lower	
Total N, g N/m ³	lower	higher	(lower)	0	higher	higher	Higher	higher	
Total P, g P/m ³	lower	0	higher	higher	higher	higher	Higher	higher	
Detritus, g C/m ³	higher	0				0	0	lower	
NPP, g O ₂ /m ² /d	lower	0				0	Lower	0	
SOD, g O ₂ /m ² /d	0	Lower				0	0	(lower)	
WOD (-algae resp.), g O ₂ /m ³ /d	lower	Lower				lower	Lower	lower	
Score of higher/lower no.									
Higher biomass, DO-processes	1	0				0	0	0	4
Lower biomass DO-processes	3	3				1	3	3	57
Higher Chl. TN, TP	0	2	1	1	3	3	3	3	67
Lower Chl TN, TP	2	0	1	1	0	0	0	0	17

Table 8-6 Change in chlorophyll, TN, TP and DO processes in simulation with increased outflow in the growth season relative to reference simulation

Parameter or Process Increase outflow	Agency-AS	UKL-MN	UKL-ER	UKL-ML	UKL-PM	Ball Bay	Shoalwater Bay	Wocus Bay	% Score
Chlorophyll, g chl/m ³	(higher)	higher	higher	higher	lower	higher	lower	(higher)	
Phyto. Biomass, g C/m ³	higher	higher	higher	higher	(lower)	higher	higher	higher	
Total N, g N/m ³	0	higher	0	0	lower	higher	0	(higher)	
Total P, g P/m ³	lower	higher	(lower)	lower	0	(higher)	0	higher	
Detritus, g C/m ³	lower	0				higher	0	higher	
NPP, g O ₂ /m ² /d	0	(higher)				higher	0	0	
SOD, g O ₂ /m ² /d	lower	0				0	0	0	
WOD (-algae resp.), g O ₂ /m ³ /d	(higher)	higher				higher	higher	higher	
Score of higher/lower no.									
Higher biomass, DO-processes	1	2				4	2	3	52
Lower biomass DO-processes	1	0				0	2	0	13
Higher Chl. TN, TP	0	2	1	1	0	3	1	2	42
Lower Chl TN, TP	2	0	0	1	2	0	1	0	25

Based on the above tables and discussion, it can be concluded that the scenario with reduced outflow and increased water level will improve the DO condition because the oxygen consumption in the water will be lower due to a lower biomass of phytoplankton.

Whereas the DO condition seems to be improved, the concentration of chlorophyll and nutrients tend to increase. For N, the increase is caused by improved conditions for N-fixation by the blue green algae through a higher retention time. For P the increase in concentration is caused by a combination of a high internal loading and increased retention time.

Increasing the outflow in the second half of the summer increases the possibility of getting algae crashes with low DO concentrations. At the same time the concentration of chlorophyll and nutrients tends to increase. Higher biomasses of phytoplankton, and thereby higher oxygen demand in the water, are the explanation of the increased risk of oxygen depletion.

The simulation of the scenarios has been done with the same water level until the start of July. Thus far, the simulations have been done to investigate the impact on the DO condition with increased or reduced water levels until July. However, the present simulations indicate that a reduced water level in spring and early summer will have a negative effect on the DO condition in late summer. While the simulations indicate that an increased water level in spring and early summer will have a positive effect.

8.4.7 EU simulation with reduced load

A reduction of the P load by omitting load from agricultural pumps and load of anthropogenic origin gives a reduction of 37 % in the P load, see table 7-3.

If the load reduction is implemented, the internal pool of exchangeable P in the sediment will decrease over years until a new steady state condition has reached. The time it takes to reach this steady state condition depends mainly on the size of the exchangeable P pool and the morphology and retention time of the lake. The improved water quality can be estimated using empirical relations or dynamic models. Examples of empirical models are the Wollenwider-OCED and the Bathtub model ref. /50/, /51/. Examples on dynamic models the present EU model and the “Glumsoe model”, ref. /52/. Data requirement for using empirical models is normally moderate, whereas data requirements for dynamic models normally are high.

For the EU model to make predictions of the water quality until a new steady state condition is reached information on the pool of exchangeable P in the sediment are important. At present the pool size at the start of the simulation is set to 5.4 g P/m² in the top 30 cm giving an overall pool of 1750 tonnes P. Estimation of the P pools (Organic-P, Fe-P and adsorbed-P) are based on two old investigations. One from 1981 giving rough information on sediment TP and total Fe concentrations, ref. (9), and one from 1977 ref. (47) giving information on Fe-P pool in the upper 10 cm.

There is a need for a proper investigation of the sediment P pools before reliable long-term (decades) predictions can be produced by a dynamic model.

Empirical relations make predictions assuming the lake in question reacts in the same way on a load reduction as the lakes in the database from which the relations are generated. This is an advantage because relative little information on a lake is needed to make a prediction. However if the lake can not be assumed to be “a member” of the lakes of the database, the predictions may be wrong ref. /52/.

In the case of Klamath Lake empirical models for prediction a new steady state water quality is questionable. N fixating blue greens dominates UKL, and a high pH may influence the internal P load and the recruitment of fish. All circumstances making UKL ecosystem different from other lakes. In addition very little is known about the status of the “top down control” by fish on the phytoplankton growth in UKL. For further information about “top down control” see ref. /53/.

Because the sediment P pools virtually is unknown a simulation with reduced P load of 37 % has been restricted to run for one year (1997) with the same initial conditions as for the reference simulation. This simulation will give the immediate improvements in the water quality but the simulation will not give the long-term benefits after a new steady state condition has been reached.

The model results are presented in Figure 8-34 — Figure 8-38 and in Table 8-1 through Table 8-6 the average concentrations and concentration difference in the summer period (April until September) are listed.

The total P concentration difference between reduced and reference load simulations is greatest in Agency Lake (-12%) declining to -7 to -8% as an average from Klamath Lake and the bays. Relative to its size the load reduction is greatest in Agency Lake explaining why the effect is greatest here. In contrast to total N, the decrease in total P concentration is greatest from the beginning of the year and declining until about Julian day 200-240 and then increasing again, see fig 8-22. This seasonal variation is caused by the internal loading from the sediment is set to peak around day 200-230.

The total N decreases between 5 to 11 % reducing the P load with 37 % with the highest decrease in Agency Lake. In contrast, to total P, the decrease in total N is restricted to the summer period, indication that a reduction in the total P result in a reduced N fixation by the phytoplankton.

The chlorophyll concentration from April until September decreases most in Agency Lake (18%) and least in Klamath Lake (6 %) with the bays in between (11% to 14%). The biomass of phytoplankton follows this pattern except for Wocus bay, where the decrease is smallest.

The processes determining the oxygen condition (primary production, sediment oxygen demand and DO consumption in the water) is close to be the same for the reference simulation and the simulation with reduced load.

No improvements in the DO conditions therefore should be expected the first years after a P load reduction.

This can be explained by the system been light limited rather than being nutrient limited. The reduction in the P load does not led to a sufficient reduction in the total P concentration to hamper phytoplankton growth. After one year the internal load is still high, however the internal P load will decrease over some years depending on the size and composition of pools of exchangeable P in the sediment. At a point the total P concentration can reach a level where also the production of plankton and respiration in the sediment and the water is decreased resulting in improved DO conditions.

As discussed earlier it is not possible to specify the time before neither a new equilibrium is reached nor is it possible to quantify the final water quality.

Over the year 1992-1998 the annual export from UKL was 22 tonnes of P lower than the annual load. By decreasing the load this will change to a net export of P for some years. The estimated pool of exchangeable P is set to 1750 tonnes in the model but it may be bigger or smaller. Assuming the new steady state pool of sediment P is 37 % of the present, it is clear that it will take no less than a decade before a new equilibrium is reached. The largest changes in the sediment pool and the water quality will happen just after a reduction of the load has been implemented giving a shorter response time for visible improvements in the water quality than the time for reaching a new steady state condition.

Agency

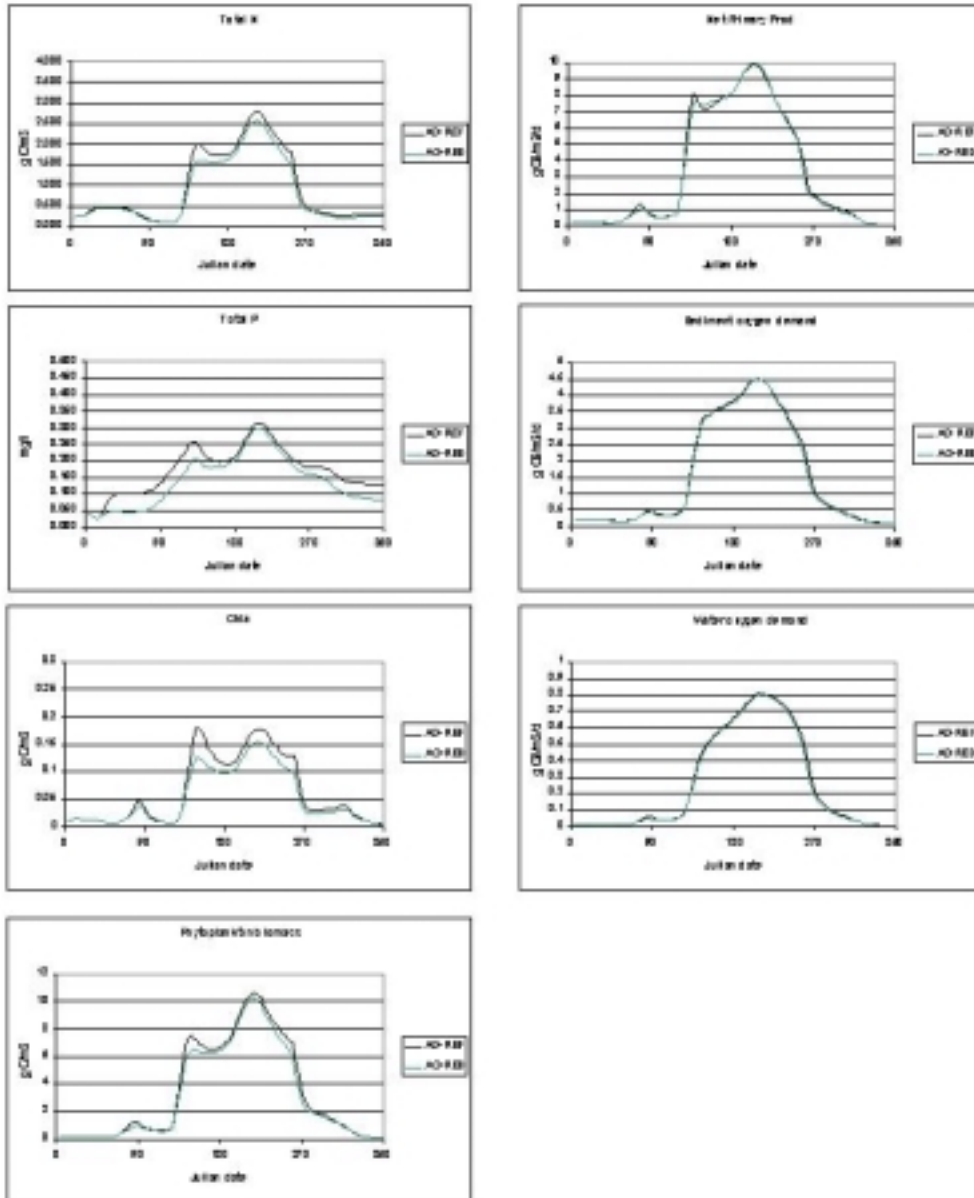


Figure 8-34 Simulated water quality in Agency Lake (St. AS) with reduced P load (RED) and present load (REF): TN, TP, Chlorophyll, Phytoplankton biomass, Net primary production, Sediment DO consumption and Do consumption in the water.

Klamath Lake

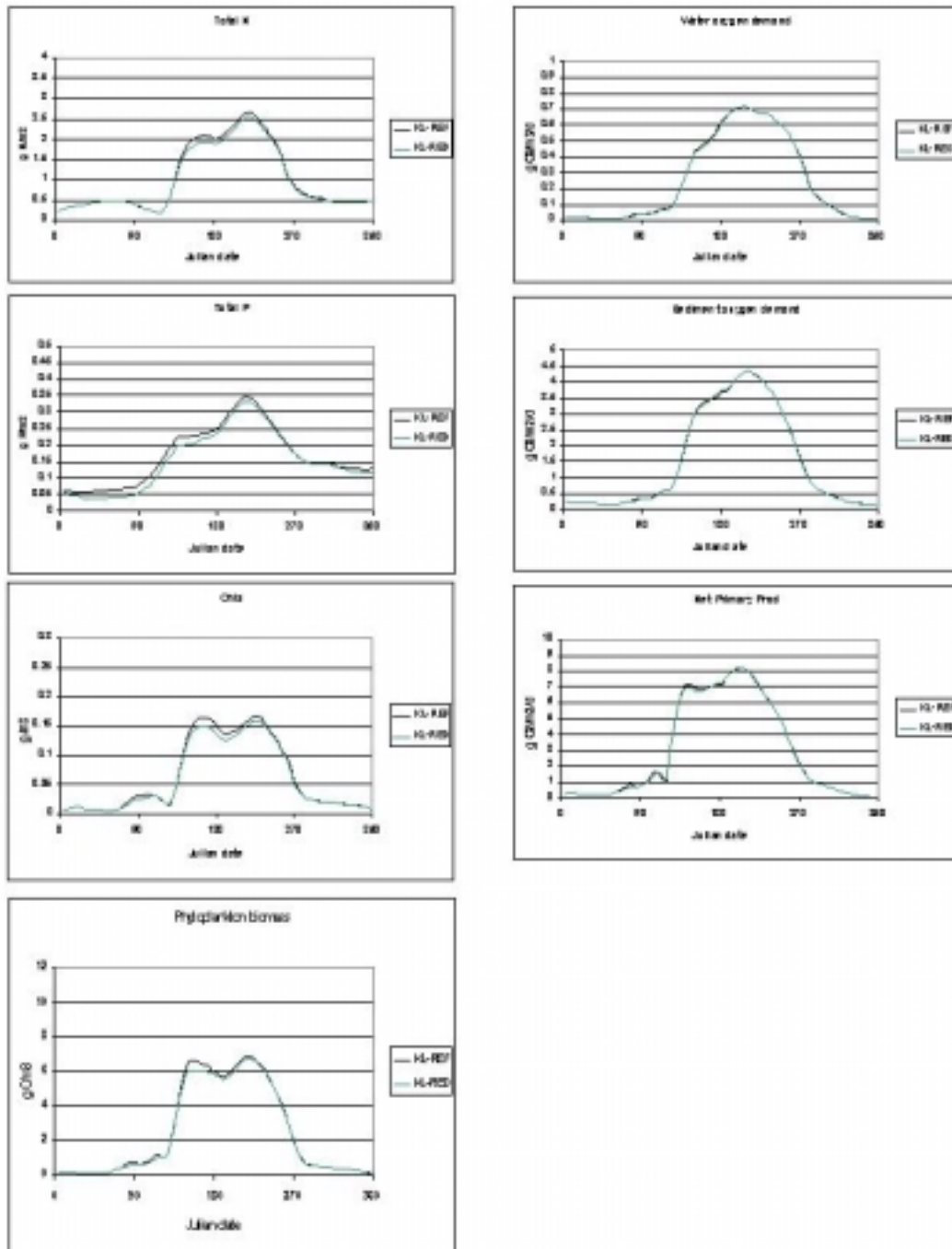


Figure 8-35 Simulated water quality in Klamath Lake (avg. of St. MN, ER, ML & PM) with reduced P load (RED) and present load (REF): TN, TP, Chlorophyll, Phytoplankton biomass, Net primary production, Sediment DO consumption and Do consumption in the water.

Ball Bay

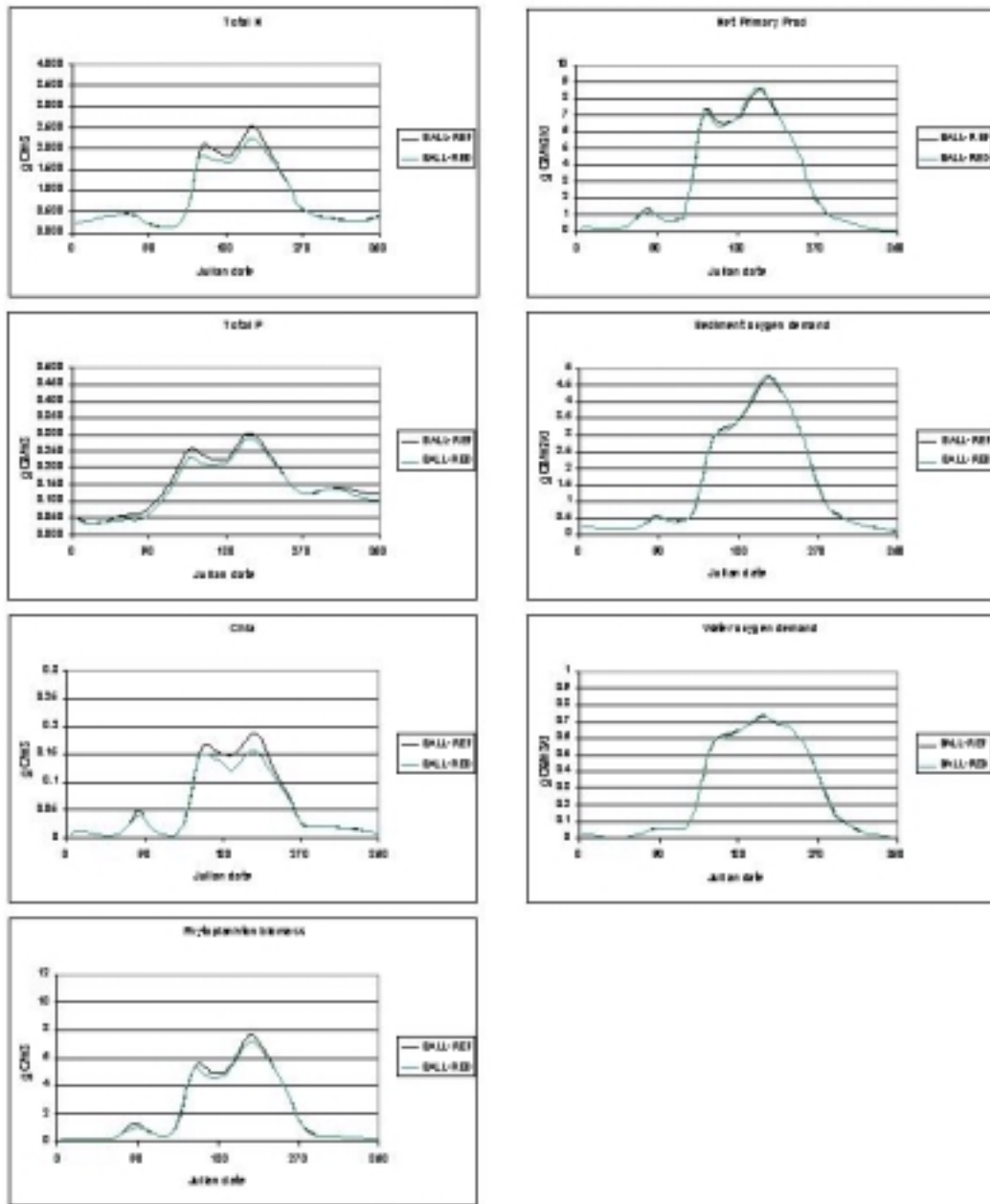


Figure 8-36 Simulated water quality in Ball Bay with reduced P load (RED) and present load (REF): TN, TP, Chlorophyll, Phytoplankton biomass, Net primary production, Sediment DO consumption and Do consumption in the water.

Shoal water bay

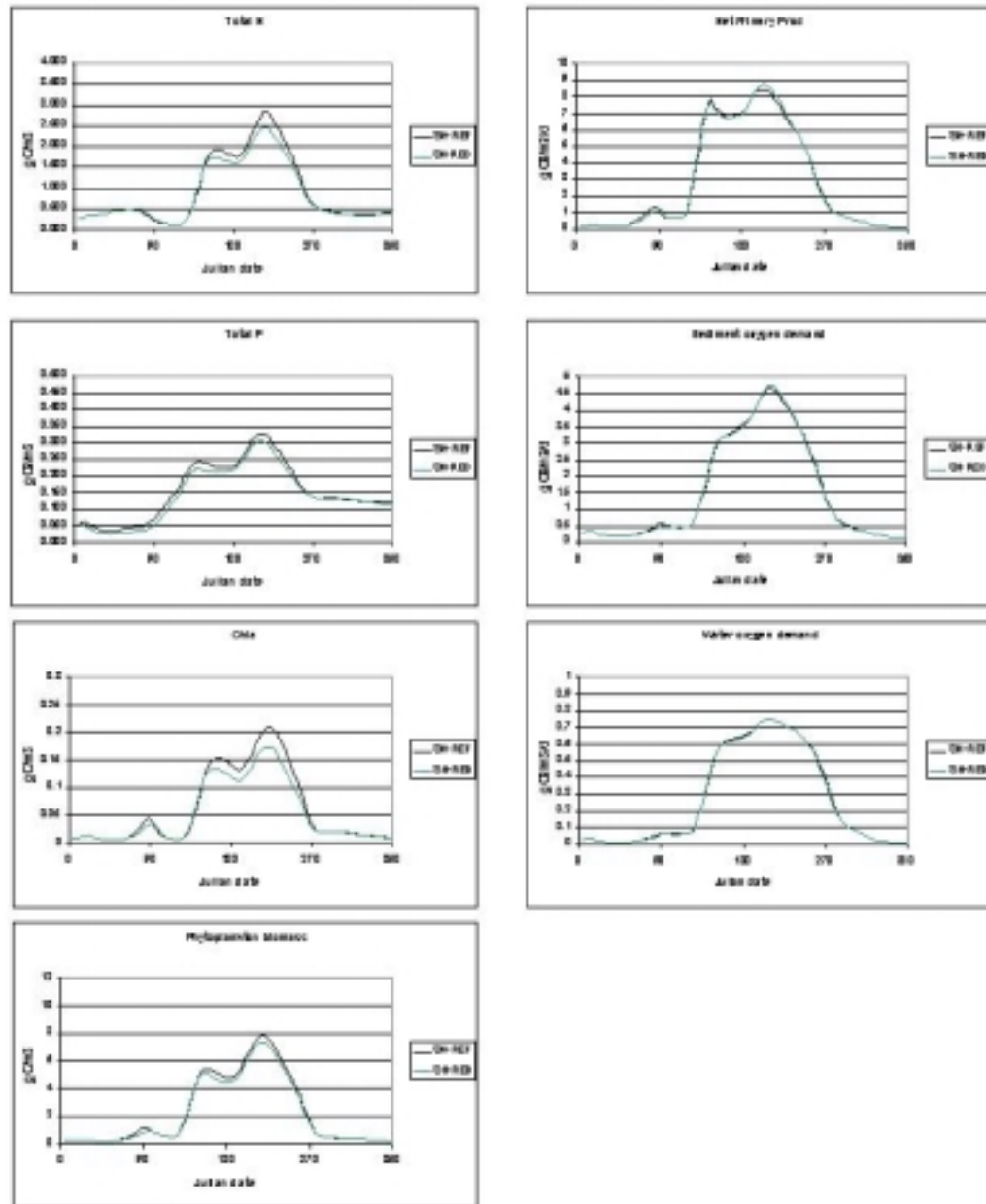


Figure 8-37 Simulated water quality in Shoalwater Bay with reduced P load (RED) and present load (REF): TN, TP, Chlorophyll, Phytoplankton biomass, Net primary production, Sediment DO consumption and Do consumption in the water.

Wachus bay

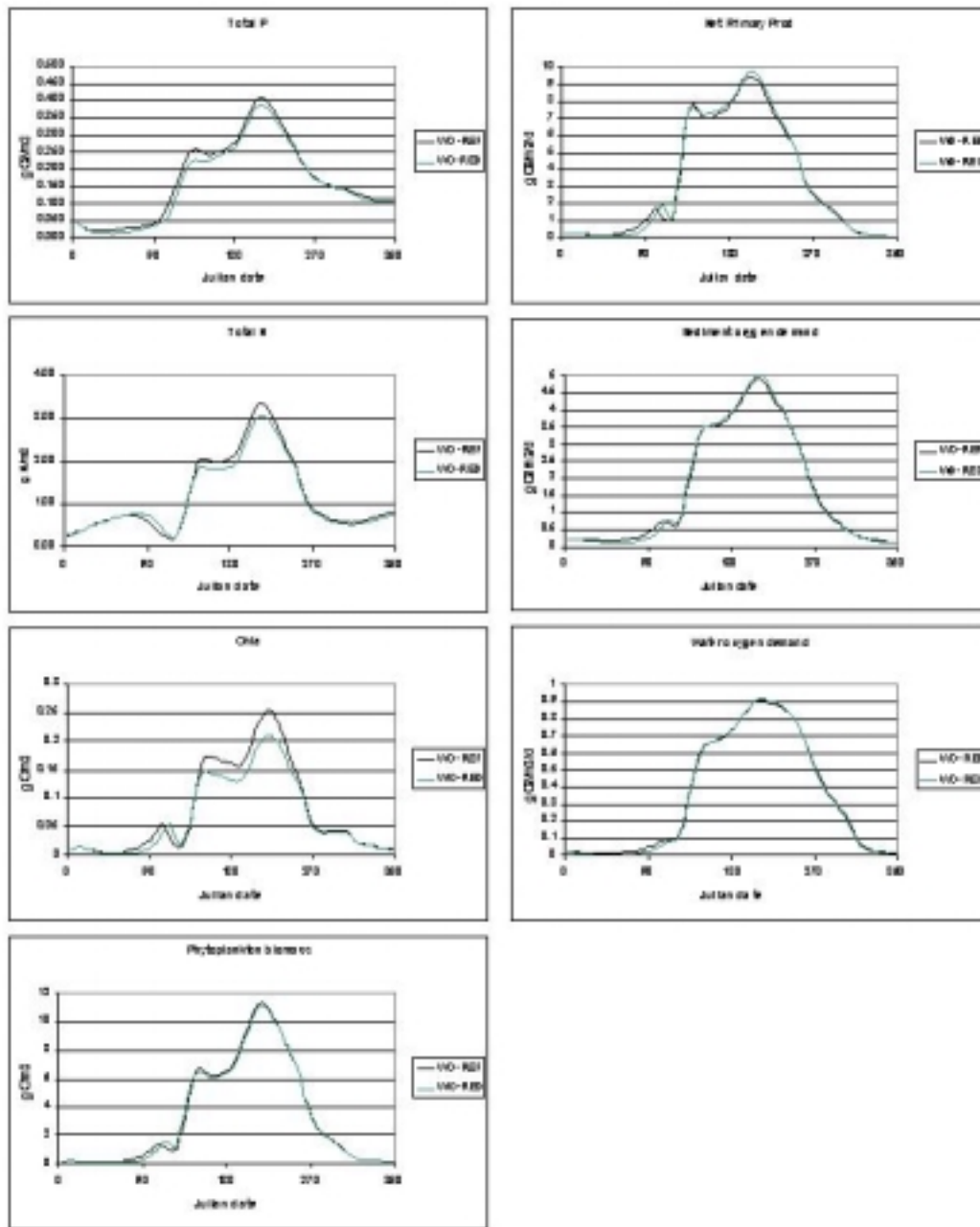


Figure 8-38 Simulated water quality in Wachus Bay with reduced P load (RED) and present load (REF): TN, TP, Chlorophyll, Phytoplankton biomass, Net primary production, Sediment DO consumption and Do consumption in the water.

Table 8-7 Mean concentrations from April to September in reference simulation. AG (Agency), KL (Klamath Lake), Ball (Ball Bay), SH (Shoalwater Bay), WO (Wocus Bay).

Parameter	AG-REF	KL-REF	BALL-REF	SH-REF	WO-REF
Chlorophyll g/m ³	0.106	0.110	0.102	0.109	0.136
Plankton biomass, g C/m ³	6.0	4.5	4.0	4.2	6.1
TN, g/m ³	1.520	1.589	1.364	1.442	1.783
TP, g/m ³	0.227	0.235	0.213	0.221	0.256

Table 8-8 Mean concentrations from April to September in simulation with 37% P reduction. AG (Agency), KL (Klamath Lake), Ball (Ball Bay), SH (Shoalwater Bay), WO (Wocus Bay).

Parameter	AG-RED	KL-RED	BALL-RED	SH-RED	WO-RED
Chlorophyll g/m ³	0.087	0.104	0.090	0.094	0.117
Plankton biomass, g C/m ³	5.60	4.35	3.87	3.94	5.99
TN, g/m ³	1.355	1.515	1.259	1.307	1.692
TP, g/m ³	0.199	0.218	0.198	0.204	0.238

Table 8-9 Difference in concentrations from April to September between simulation with 37% P reduction and reference simulation. AG (Agency), KL (Klamath Lake), Ball (Ball Bay), SH (Shoalwater Bay), WO (Wocus Bay).

Parameter	AG-dif	KL-dif	BALL-dif	SH-dif	WO-dif
Chlorophyll g/m ³	-0.019	-0.006	-0.011	-0.015	-0.018
Plankton biomass, g C/m ³	-0.41	-0.15	-0.17	-0.22	-0.07
TN, g/m ³	-0.165	-0.075	-0.105	-0.135	-0.091
TP, g/m ³	-0.027	-0.016	-0.015	-0.017	-0.018

Table 8-10 Difference in % from April to September between simulation with 37% P reduction and reference simulation. AG (Agency), KL (Klamath Lake), Ball (Ball Bay), SH (Shoalwater Bay), WO (Wocus Bay).

Parameter	AG-dif	KL-dif	BALL-dif	SH-dif	WO-dif
Chlorophyll %	-18	-6	-11	-14	-13
Plankton biomass, %	-7	-3	-4	-5	-1
TN, %	-11	-5	-8	-9	-5
TP, %	-12	-7	-7	-8	-7

8.5 WAVE MODELING – SEDIMENT TRANSPORT

8.5.1 Wave Modeling

The main purpose of the wave modeling was to simulate the wave-induced contribution to the bottom bed shear stress. The waves in Upper Klamath Lake are wind generated, and due to the direction of prevailing summer winds, the wave-generated currents are sufficient to evoke re-suspension of bottom sediments. (32)

An example of a wind time series from the Klamath Falls Airport is shown in Figure 8-39 and Figure 8-40. The most dominant wind direction is northwest which is in-line with the lake orientation. This is even more pronounced during the summer period where typical wind speeds are in the order of 10 miles /hour (4.5 m/s) in Figure 8-40.

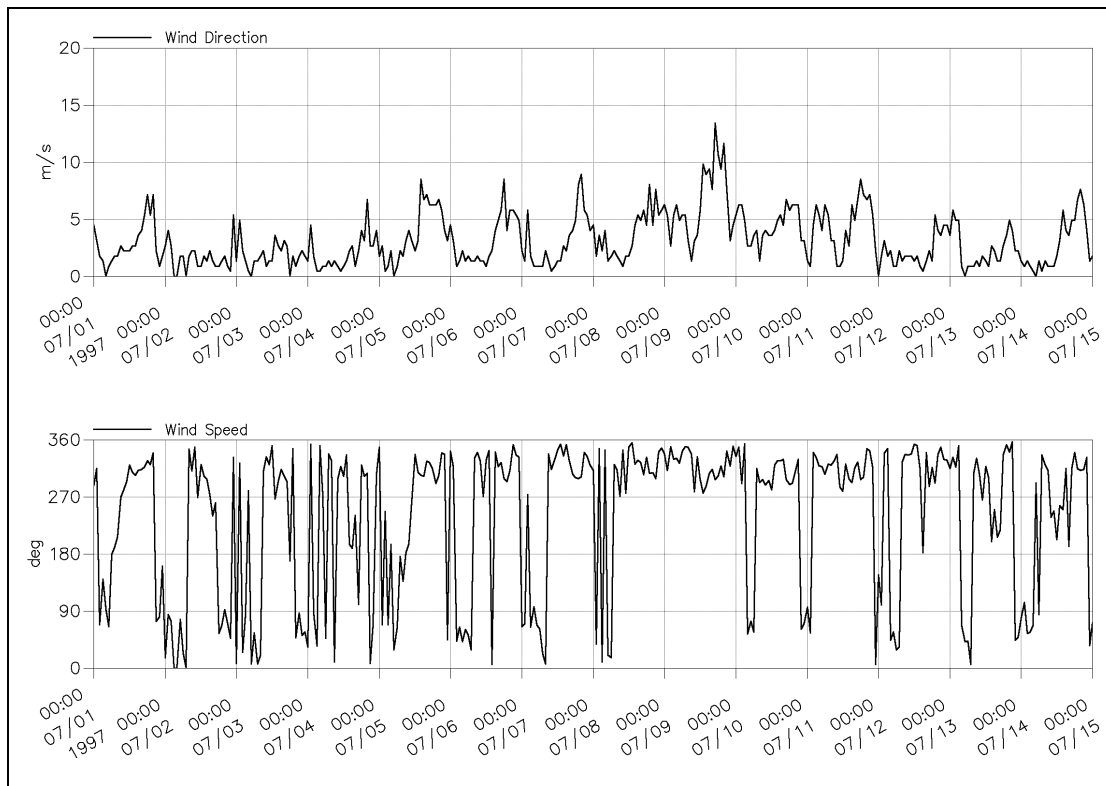


Figure 8-39 Wind Time Series from The Klamath Falls Airport

Based on the above data, a “wind rose” comprising the statistical distribution of wind-speeds and directions has been constructed. Figure 8-40 shows two wind roses for the summer period (5/1/1997 - 10/1/1997) and entire period 1995-2000.

As can be seen in Figure 8-40 for summer 1997, the wind speed exceeds 10 miles/hour (4.5 m/s) from the northwest (270 through 360 degrees) in approximately 25% of the time. In approximately 10% of the time the wind speed exceeded 13.5 miles/ hour (6 m/s).

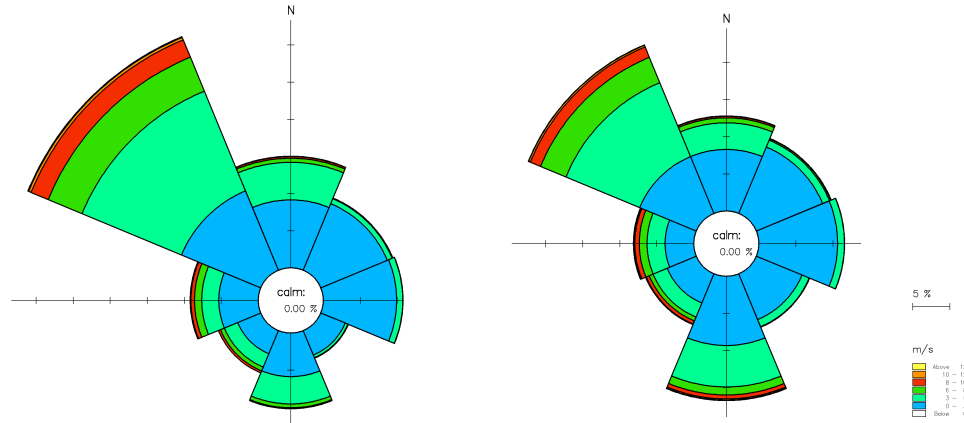


Figure 8-40 Wind Roses for The Summer Period (5/1/1997 - 10/1/1997) (Right) and Entire Period 1995-2000 (Left)

The Near-Shore-Wave (NSW) module in MIKE 21 was used to establish the wave fields expressed in significant wave heights and periods for different combinations of wind speed from northwest and combinations of water levels in the lake (lake levels of 4138, 4141 and 4142 feet and wind speed of 10 and 13.5 miles /hour). The wave model utilizes the lake bathymetry file as established in the hydrodynamic model. Since the main objective of the succeeding sediment modeling is to provide a relationship between wind speed and lake level with respect to re-suspension, only stationary wave fields have been considered. This implies that the corresponding stationary wave field can be represented in its spectral form. Dissipation of wave energy due to bottom friction and wave breaking has been ignored. Likewise, the effect of combined wave-current interaction on the boundary layer has been ignored.

An example of the calculated wave heights and wave periods for a lake level of 4141 feet and a wind speed of 10 miles/hour is shown in Figure 8-40. As expected, the waves are highest near the eastern shore of the lakes where the wind fetch is largest. The maximum significant wave height and corresponding periods are in the order of 0.2 m (0.6 feet) and 2 sec respectively. These findings agree well with reference (32). No attempt has been made with respect to further calibration or verification of this model at this time

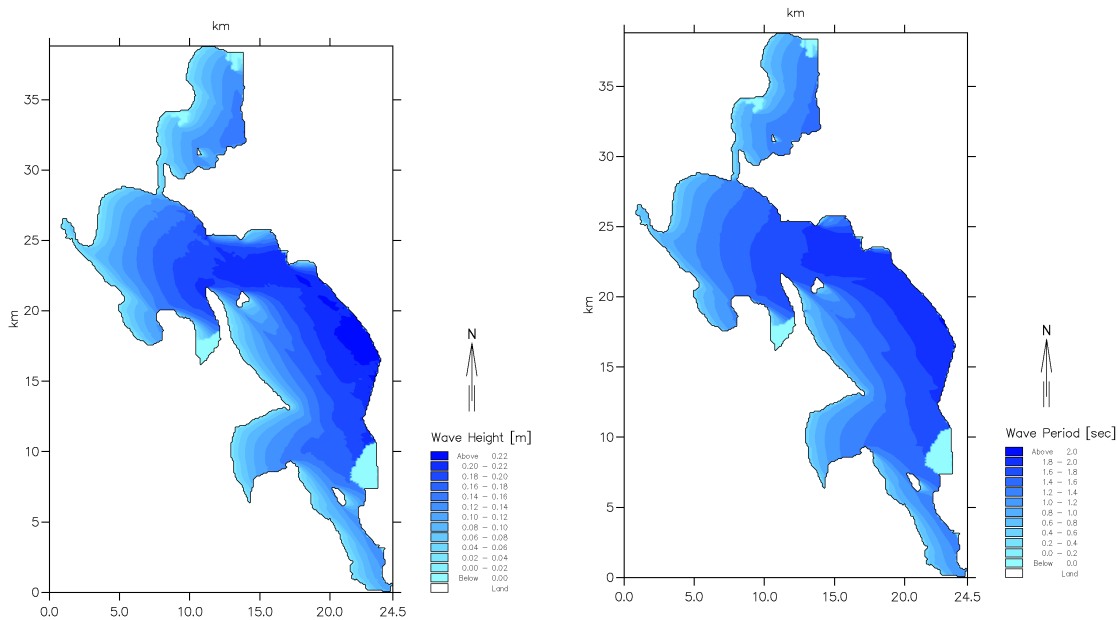


Figure 8-41 Simulated significant wave height and wave period. Lake level 4141 feet, wind speed 10 miles/hour from northwest

The main parameters of the Near-Shore-Wave module in MIKE 21 include the following:

- Surface elevation: The mean surface elevation of the area must be specified. In the present example, a mean surface elevation of 262.28 meters and 262.42 meters has been applied.
- Bottom friction. The wind energy is converted into wave energy. Some energy may be lost due to bottom friction. The default is to exclude this effect, which in most cases is negligible. It is not included here.
- Wave breaking. Also this is a way to dissipate energy. Wave breaking is not included here as the effect is limited.
- The wind speed and wind direction needs to be specified in all cases. This is the driving force.
- Wave-current interaction that is excluded from the present application, as the effect is not important.
- Boundary conditions comprise only land.

In the example above, a wind speed of 4.6 m/s was assumed from the northwest (300 degrees.). As expected, the waves are highest along the eastern shore of the lakes where the wind fetch is largest. The maximum significant wave height and corresponding periods are in the order of 0.2 m (0.6 feet) and 2 sec respectively.

8.5.2 Sediment Modeling

As mentioned, the wind generates both waves and currents. The currents are not sufficiently strong by themselves to generate resuspension of sediment. For this, wave generated shear stress at the bottom is required. Thus, waves will “stir up” the sediment, where as the current will transport the re-suspended sediment around in the lake, until the waves are sufficiently small to allow deposition of the sediment again.

The MIKE 21 Multi-Layer mud model was employed as it allows definition of waves as driving forces. The sediment model was constructed on top of the hydrodynamic model, i.e. the two models run in parallel. Critical sediment parameters are as follows.

Boundary conditions

In the hydrodynamic model, boundary conditions are included as source and sink terms. It is assumed that the concentrations of sediment of these sources are nil meaning that only re-suspended sediment is considered.

Initial conditions

It is assumed that the concentration of sediment in suspension is nil at the beginning of the simulation period. Also an initial condition for the sediment on the bed is required. As a first estimate, it is assumed that the thickness of the top layer of sediment exposed to re-suspension is 10 mm. In principle, it is possible with the multi-layer model also to define under-lying bed layers with different erosion characteristics (denser layers). However, due to lack of data there is no justification to extent the model to more layers.

Bed roughness

The Nikuradse bed roughness (for mud flats corresponding to effective grain size) needs to be defined in order to convert simulated flow velocities to a bed shear stress. A Nikuradse bed roughness of 1 mm has been applied.

Waves

A wave database is specified. With this database, it is possible to interpolate among simulated wave fields to obtain wave data as a function of wind speed, wind direction and water level. However, only one set of data is applied as a simulation is carried out with a constant wind speed, wind direction and water level. More data sets would be required if a time-varying wind field was applied for the simulation. The wave data set contains four items: Wave height, wave period, wave direction, and wave direction spreading.

Erosion characteristics

The erodibility of the top layer of sediment is as follows:

Critical Shear Stress	$\tau_{\text{critical, erosion}} = 0.05 \text{ N/m}^2$ and
Erosion rate	$E = 0.01 \cdot (\tau / \tau_{\text{critical, erosion}} - 1)$
Dry density	$\rho = 150 \text{ kg/m}^3$

Deposition characteristics

The deposition of suspended sediment is determined by the following parameters:

Settling velocity	$w_s = 0.0004 \text{ m/s}$ for $C < 340 \text{ g/m}^3$ $w_s = 1.34 \cdot 10^{-7} \cdot C^{1.37} \text{ m/s}$ for $C > 340 \text{ g/m}^3$
Critical Shear Stress	$\tau_{\text{critical, deposition}} = 0.02 \text{ N/m}^2$

A number of sensitivity simulations are required (and more measurements of suspended sediment concentration, composition, fall velocity test etc.) in order to optimize the choice of model parameters. However the critical shear stress for erosion will be in the order of 0.02 to 0.1 N/m². A shear stress of 0.05 N/m² has been assumed in previous study and for the sake of comparison the same value has been applied initially. With the present set of parameters, the simulations have been carried out for the two depths 261.28 and 262.42 m. The results are shown in terms of bed shear stress for the two depths. The distribution follows the wave height distribution (maximum waves generates maximum shear stress in the order of 0.7 N/m² (7 dyn/cm²) which was also estimated as maximum bed shear stress in the previous study. Increasing the water level to 262.42 m result in an almost 10 times lower mean shear stress. Indeed, the critical shear stress of 0.05 is only exceeded very locally. Thus, the increase of water level may have a significant impact on the re-suspension of sediment.

It is noted that re-suspension only takes place in local areas where the highest waves occur. Again, it should be emphasized that the sediment model calibration parameters need further refinement.

Although no data are available with respect to sediment characteristics, the critical shear stress for erosion will typically be in the order of 0.02 to 0.1 N/m² for fine lake bottom sediments (clays, silt). A shear stress of 0.05 N/m² (0.5 dynes/cm²) has been assumed in previous study and for the sake of comparison the same value has been applied initially. With the present set of parameters, the simulations have been carried out for different depths corresponding to lake levels of 4138, 4141 and 4142 feet respectively and for wind speeds corresponding to 10 and 13.5 miles /hour respectively.

The results are shown in terms of bed shear stress for the different depths in Figure 8-42 through Figure 8-44 for a wind speed of 10 miles / hour. From a statistical point of view, 10 miles/hour is exceeded 25% of the time from the direction northwest (270 through 360 degrees).

As can be seen, the distribution follows the wave height distribution and can be noted, that re-suspension only takes place in local areas, where the highest waves occur.

Maximum waves generate maximum shear stress in the order of 0.7 N/m² (7 dyn/cm²) for a lake level of 4138 feet which is in agreement with previous estimates (Ref (32)) Increasing the water level to 4142 feet result in an almost 10 times lower mean shear stress. Indeed, the critical shear stress of 0.05 is only exceeded very locally for this wind speed and direction. Thus, the increase of water level from 4138 to 4142 feet will have a significant impact on the re-suspension of sediment. In Figure 8-1, the period where phosphorous is available for re-suspension and release, provided the pH value is sufficiently high, is typically in the period from May through August. In this period the change in water level from the proposed alternative operations is only in the order of 1 foot (from 4141 to 4142 feet) thus the effect with respect to reducing the phosphorous load from sediment re-suspension is only relevant in this period. Figure 8-45 and Figure 8-46 show the lake areas where the critical shear stress is exceeded for the two water levels of 4141 and 4142 feet and for a wind speed of 10 miles /hour. As can be seen the impact of increasing the water level 1 foot is only minor. Figure 8-47 and Figure 8-48 show similar plots for an increased wind speed corresponding to 13.5 miles/hour (exceeded in more than 10% of the time from the direction northwest).

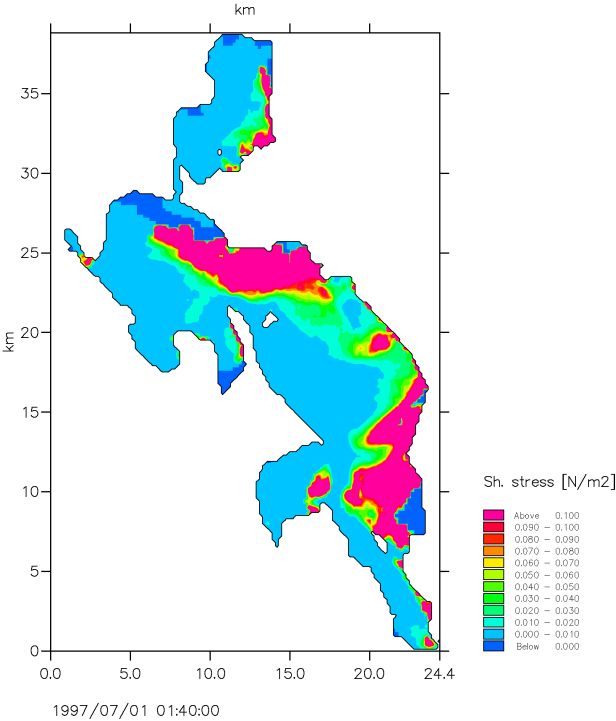


Figure 8-42 Simulated bottom shear stress. Lake level of 4138 feet, Wind speed of 10 miles/hour from northwest

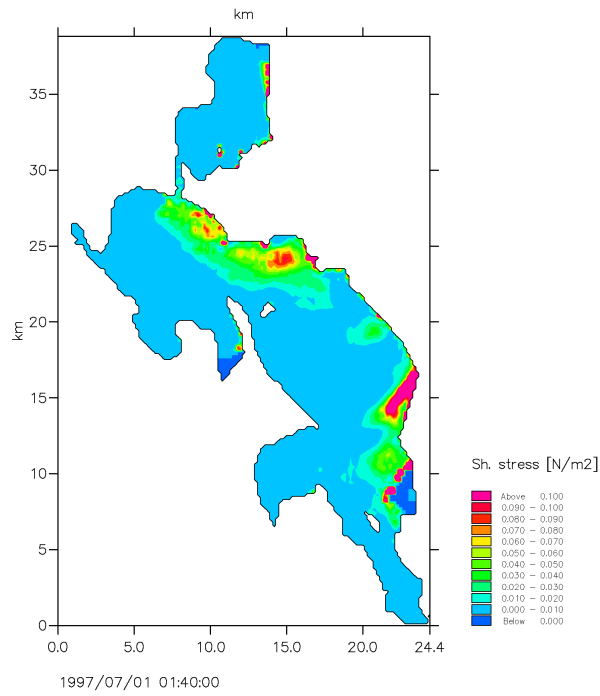


Figure 8-43 Simulated bottom shear stress. Lake level of 4141 feet, Wind speed of 10 miles/hour from northwest

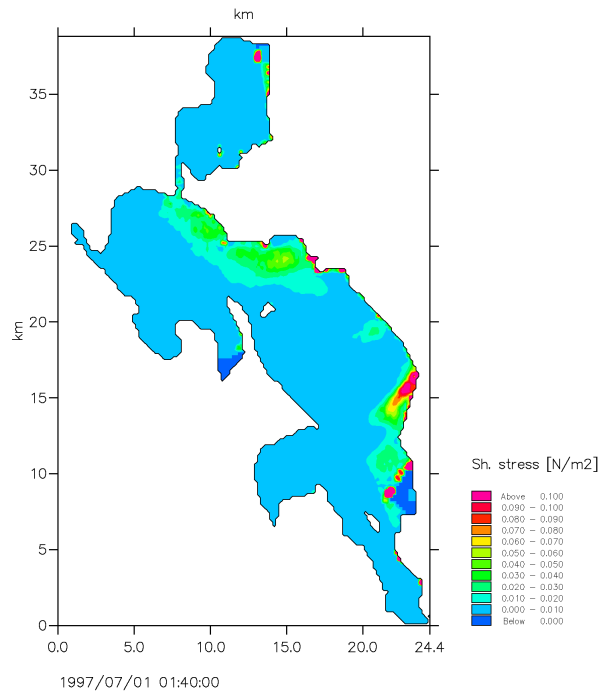


Figure 8-44 Simulated bottom shear stress. Lake level of 4142 feet, Wind speed of 10 miles/hour from northwest

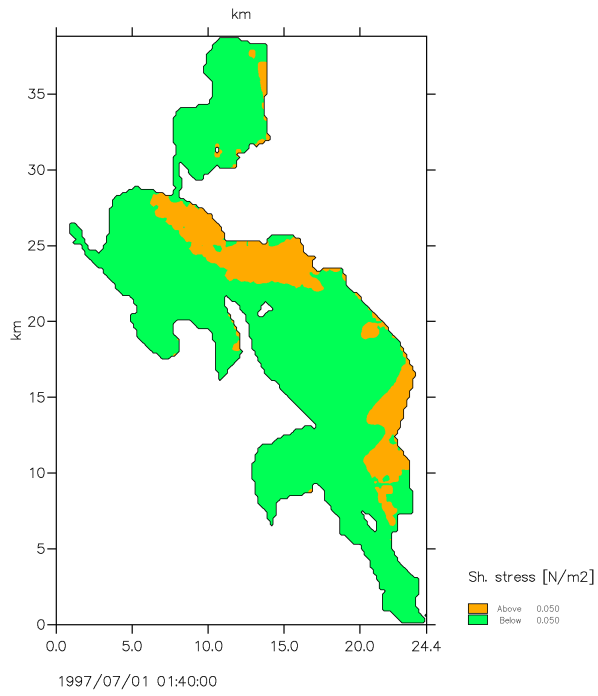


Figure 8-45 Simulated bottom shear stress. Critical shear stress of 0.05 m²/sec., Lake level of 4141 feet, Wind speed of 10 miles/hour from northwest

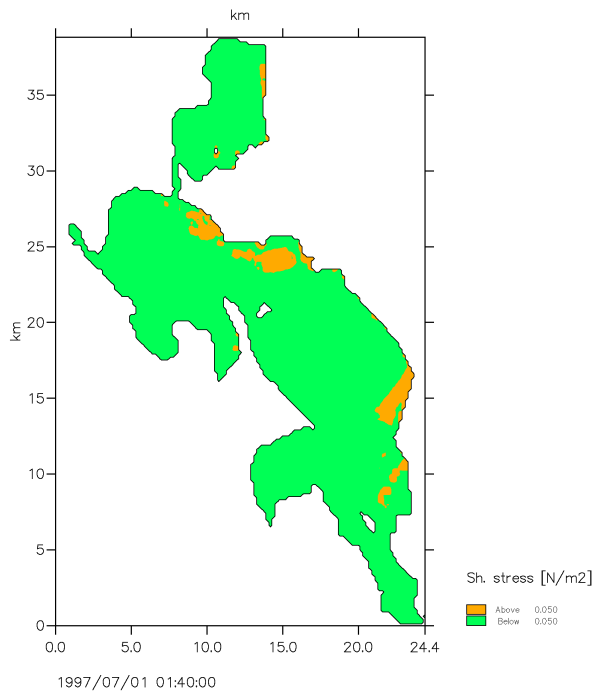


Figure 8-46 Simulated bottom shear stress. Critical shear stress of 0.05 m²/sec. Lake level of 4141 feet, Wind speed of 13.5 miles/hour from northwest

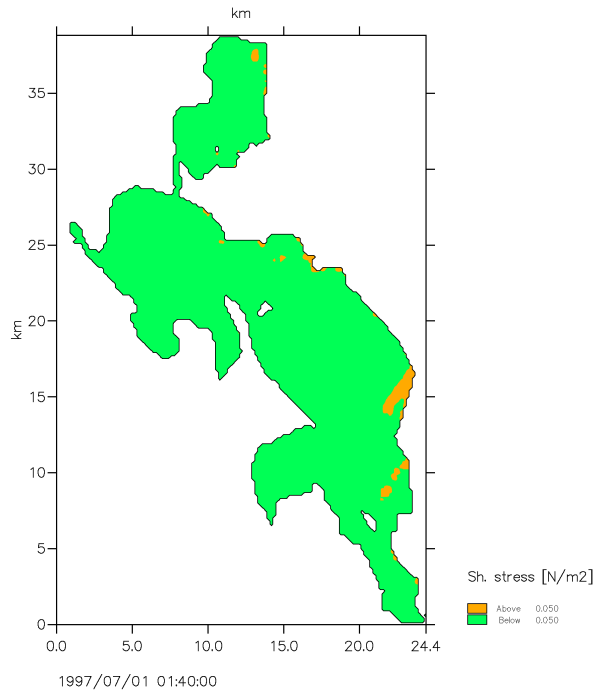


Figure 8-47 Simulated bottom shear stress. Critical shear stress of 0.05 m²/sec. Lake level of 4142 feet, Wind speed of 10 miles/hour from northwest

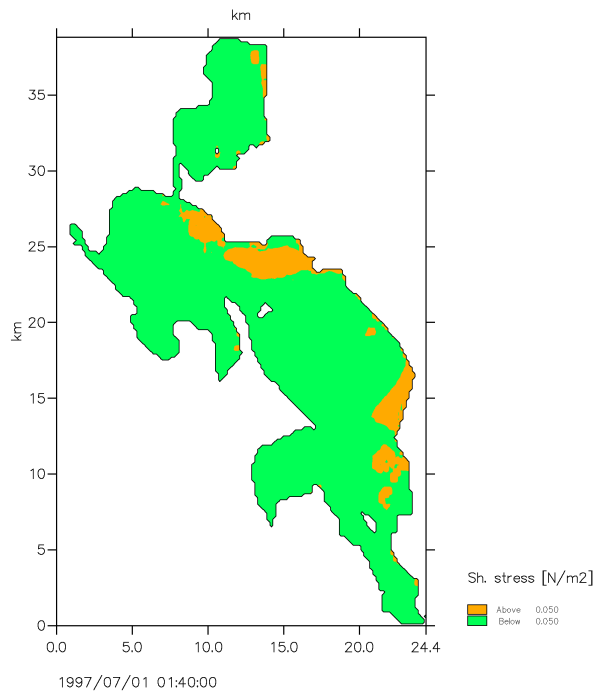


Figure 8-48 Simulated bottom shear stress. Critical shear stress of 0.05 m²/sec. Lake level of 4142 feet, Wind speed of 13.5 miles/hour from northwest

9. RECOMMENDATIONS

The following recommendations relate to ways in which the modeling may be refined as additional data becomes available and as additional lake management questions arise:

1. The wave modeling is reasonably accurate in comparison to the sediment modeling. Thus, no further calibration of the wave modeling is envisaged.
2. For the sediment modeling, the bed roughness as well as the critical shear stresses for erosion are critical parameters for getting sediment into suspension.
3. As the amount of data (re-suspension rates, critical shear stresses for erosion, concentration of suspended sediment etc.) is limited or not available, the scope of modeling work has to be selected accordingly. It is not realistic to simulate the exact concentration of re-suspended sediment will not be realistic to achieve. Instead, emphasis must be given to relative considerations among different modeling scenarios.
4. Investigate the effect of various wind speed and wind direction during critical summer time.
5. Investigate the effect various surface elevations in the lake, which influence both wave heights as well as bed shear stresses generated by waves.
6. The rectangular grid network for the 2-D models may be refined to include a nested grid having a finer (smaller) grid spacing located where lake management issues are more of concern. For example, grid spacing along selected portions of the lakeshore may be reduced to investigate nearshore processes and water quality conditions as they relate to the fishery.
7. The use of the lake modeling may be expanded to include new boundary conditions that describe “what if” scenarios involving restoration of the watersheds tributary to the lake system and associated reduction of external water quality problems.
8. Lake modeling may be expanded to include simulation of the effect of the lakeshore marshes on phosphorous loading to the lake system.

The following recommendations relate to investigations that may increase the understanding of water quality issues in the UKL system:

1. External sources of phosphorous to the lake system should be investigated and attempts should be made to apportion the sources among the various land uses so that management responses can be better directed.

2. Sediment / concentration resuspension - critical shear stress

It is strongly recommended that the monitoring program be expanded to include measurement of the spatial distribution of bed sediment composition, depth of mud layers and phosphorous content.

3. Lake circulation

Surface and subsurface velocity measurement is not currently available for UKL. To support further efforts and better understanding of lake circulation and dynamics, detailed velocity data are needed. For example, an Acoustic Doppler Current Profiler (ADCP) and/or Acoustic Doppler Velocimeter (ADV) could be used to accurately measure velocity profiles. Results data could confirm the wind-driven influence on currents, which were predicted in the MIKE-21 hydrodynamic model.

10. REFERENCES

- (1) Andersen J. M. 1975. Influence of pH on release of phosphorus from lake sediments. *Arch. Hydrobiol.* 76, 4 PP 411-419. 1975.
- (2) Andersen, V.J.M, 1974. Nitrogen and phosphorus budgets and the role of sediments in six shallow Danish lakes. *Arch. Hydrobiol.* 74(4):528-550.
- (3) Barbiero, R.P. and E.B. Welch, 1992. Contribution of benthic blue-green algal recruitment to lake populations and phosphorus translocation. *Freshwater Biology* 27:249-260.
- (4) Barbiero, R.P. and J. Kann, 1994. The importance of benthic recruitment to the population development of *Aphanizomenon flos-aquae* and internal loading in a shallow lake. *J. Plankton Research* 16(11):1581-1588.
- (5) Bortleson, G.C. and M.O. Fretwell, 1993. A Review of Possible Causes of Nutrient Enrichment and Decline of Endangered Sucker Populations in Upper Klamath Lake, Oregon. USGS Water-Resources Investigations Report 93-4087.
- (6) Boyle, J.C., 1964. Regulation of Upper Klamath Lake. Report.
- (7) Brownell, D.L. and M.R. Rinallo, 1995. A Selected Bibliography of Water Related Research in the Upper Klamath Basin, Oregon. USGS Open-File Report 95-285 prepared in cooperation with the Bureau of Reclamation.
- (8) Chapra, S.C., 1997. *Surface Water-Quality Modeling*. McGraw Hill Series in Water Resources and Environmental Engineering.
- (9) COE (US Army Corps of Engineers, San Francisco District), 1982. Potential Eutrophication Control Measures for Upper Klamath Lake, Oregon: Data Evaluation and Experimental Design. Klamath River Basin Water Resources Development Project Contract No. DACW07-81-C-0045. October.
- (10) DHI (Danish Hydraulic Institute), 1995. MIKE 11. A Microcomputer Based Modelling System for Rivers and Channels. User and Scientific Manual.
- (11) DHI MIKE 11 version 3.2 General Reference Manual 1st^t edition 1997
- (12) DHI (Danish Hydraulic Institute), 1995. MIKE 3. A 3D Modelling System for Rivers, Lakes, Estuaries, Coasts and Oceans. User and Scientific Manual.

- (13) DHI (Danish Hydraulic Institute), 1999. MIKE 21. A Modelling System for Estuaries, Coastal Waters and Seas. User and Scientific Manual.
- (14) Fredsoe, J., R. Diegaard, 1992. Mechanics of Coastal Sediment Transport, Advanced Series on Ocean Engineering – Volume 3. ISBN 9810208405 World Scientific Publishing.
- (15) Gahler, A.R., 1969. Field Studies on Sediment-Water Algal Nutrient Interchange Processes and Water Quality of Upper Klamath and Agency Lakes, July 1967-March 1969. WP-66. US Dept. of the Interior, Federal Water Pollution Control Admin., NW Region, Pacific NW Water Lab., October.
- (16) Gahler, A.R., 1969. Field Studies on Sediment Water Algal Nutrient Interchange Processes and Water Quality of Upper Klamath and Agency Lakes, July 1967-March 1969. Working Paper No. 66. U.S. Department of the Interior, Federal Water Pollution Control Administration, Northwest Region. October.
- (17) Gahler, A.R., and W.D. Sanville, 1971. Lake Sediment – Characterization of Lake Sediments and Evaluation of Sediment Water Nutrient Mechanism in the Upper Klamath Lake System. Pacific Northwest Water Laboratory, Water Quality Office, U.S. Environmental Protection Agency, Oregon, April.
- (18) GMA (Graham Matthews & Associates), 1999. Sediment Transport Measurements – WY1999. Report prepared for the Nature Conservancy of Oregon. October.
- (19) Harrison, M.J., 1970. Bacteria-Phosphate Interactions in Upper Klamath Lake Sediments. MS Thesis.
- (20) Harrison, M.J., R.E. Pacha and R.Y. Morita, 1972. Solubilization of Inorganic Phosphates by bacteria Isolated from Upper Klamath Lake Sediment. *Limnology and Oceanography* 17(1):50-57.
- (21) Hazel, C.R., 1969. Limnology of Upper Klamath Lake, Oregon, with Emphasis on Benthos. Doctorate Thesis, Oregon State University
- (22) Jacobsen O.S. 1978. Sorption, adsorption and chemisorption of phosphate by Danish lake sediments. *Vatten*, 4, 78
- (23) Jassby, A.D. and C.R. Goldman, 1995. Klamath Lake Preliminary Assessment of Surface Elevation and Water Quality. Prepared for the Natural Resources Dept., The Klamath Tribes, Chiloquin, OR. February.

- (24) Jensen H.S., Andersen F. Ø. 1992. Importance of temperature, nitrate and pH for phosphate release from aerobic sediments of four shallow, eutrophic lakes. *Limnol. Oeanogr.* 37(3), 1992, PP 577-589.
- (25) Jensen H. S., Kristensen P., Jeppesen E., Skytte A. 1992. Iron:phosphorus ratio in surface sediment as an indicator of phosphate release from aerobic sediments in shallow lakes. *Hydrobiologia* 235/236 PP 731-743 1992
- (26) J. *Kann-Klamath Tribes National Resources*– Effect of Lake Level Management on Water Quality and Native Fish Species in Upper Klamath Lake , Oregon Draft Report-February 1995
- (27) Kann, J. Effect of Lake Level Management on Water Quality and Native Fish Species in Upper Klamath Lake, Oregon. Draft Report – February 1995.
- (28) Kann, J. and V.H. Smith, 1999. Estimating the probability of exceeding elevated pH values critical to fish populations in a hypereutrophic lake. *Can. J. Fish Aquat. Sci.* 56:2262-2270.
- (29) Kann, J. and W.W. Walker, Jr., 1999. Nutrient and Hydrologic Loading to Upper Klamath Lake, Oregon, 1991-1998. Prepared for Klamath Tribes Natural Resource Department and U.S. Bureau of Reclamation
- (30) Kann, J., 1998. Ecology and Water Quality Dynamics of a Shallow Hypereutrophic Lake Dominated by Cyanobacteria. Doctorate Thesis, Chapel Hill, NC.
- (31) Kristensen, P., M. Søndergaard and E. Jeppesen, 1992. Resuspension in a shallow eutrophic lake. *Hydrobiologia* 228:101-109.
- (32) Laenen, A. and A.P. LeTourneau, 1996. Upper Klamath Basin Nutrient-Loading Study – Estimate of Wind-Induced Resuspension of Bed Sediment During Periods of Low Lake Elevation. USGS Open-File Report 95-414.
- (33) Lund-Hansen, L.C., M. Peterson and W. Nurjaya, 1999. Vertical Sediment Fluxes and Wave-Induced Sediment Resuspension in a Shallow-water Coastal Lagoon. *Estuaries* 22(1):39-46, March.
- (34) Martin, B.A. and M.K. Saiki, 1998. Notes – Effects of Ambient Water Quality n the Endangered Lost River Sucker in Upper Klamath Lake, Oregon. In: Transactions of the American Fisheries Society 128(5):953-961, 1999.

- (35) Martin, E.A. and C.A. Rice, 1981. ^{210}Pb Geochronology and Trace Metal Concentrations of Sediments from Upper Klamath Lake and Lake Euwana, Oregon. *Northwest Science* 55(4):269-280.
- (36) Nōges, P. and A. Järvet, date unknown, Water level control over light conditions in shallow lakes. Report Series in Geophysics No. 32.
- (37) OECD 1982. Eutrophication of Water. Monitoring, Assessment and Control. Organization for Economic Cooperation and Development, Paris. 154pp.
- (38) Oregon State Sanitary Authority, 1964. Final Report on the Quality of Klamath Basin Waters in Oregon, July, 1959, to December, 1963.
- (39) Risley, C.J. and A. Laenen, 1999. Upper Klamath Lake Basin Nutrient Loading Study – Assessment of Historic Flows in the Williamson and Sprague Rivers. U.S. Geological Survey Water Resources Investigation Report 98-4198 prepared in cooperation with Bureau of Reclamation.
- (40) Snyder, D.T. and J.L. Morace, 1997. Nitrogen and Phosphorus Loading from Drained Wetlands Adjacent to Upper Klamath and Agency Lakes, Oregon. US Geological Survey Water-Resources Investigations Report 97-4059 prepared in cooperation with the Bureau of Reclamation.
- (41) Søndergaard, M., 1986. Seasonal Variations in the Loosely Sorbed Phosphorus Fraction of the Sediment of a Shallow and Hypereutrophic Lake. *Environ. Geol. Water Sci.* 11(1):115-121.
- (42) US Department of the Interior, Bureau of Reclamation, Mid-Pacific Region, 1999. Scoping Report – Long-term Operations Plan for the Klamath Project.
- (43) USGS, 1999. Oregon District Active Projects -- Measurement of Sediment Oxygen Demand (SOD) in Upper Klamath and Agency Lakes, Oregon (OR 189). http://or.water.usgs.gov/projs_dir/or189/or189.html.
- (44) USGS Water Investigation report 96-4079 Relation between Selected Water Quality Variables and Lake Level in Upper Klamath and Agency Lakes, Oregon
- (45) Water quality data base. 2000. Reclamation internal data base in MS Access.
- (46) Walker Jr., W.W., 1995. A Nutrient-Balance Model for Agency Lake, Oregon. Prepared for the U.S. Dept. of Interior, Bureau of Reclamation, Denver, CO. April.

- (47) Wildung, R.E., R.L. Schmidt and R.C. Routson, 1977. The Phosphorus Status of Eutrophic Lake Sediments as Related to Changes in Limnological Conditions – Phosphorus Mineral Components. *J. Environ. Qual.* 6(1):100-104.
- (48) Wood, T.M., G.J. Fuhrer and J.L. Morace, 1996. Relation between Selected Water-Quality Variable and Lake Level in Upper Klamath and Agency Lakes, Oregon. US Geological Survey Water-Resources Investigations Report 96-4079 prepared in cooperation with the Bureau of Reclamation.
- (49) Andersen J. M. 1978. Plankton primary production and respiration in eutrophic Frederiksborg Slotssø, Denmark. *Verh. Internat. Verein. Limnol.* 29, PP 702-708, 1978
- (50) Vollenwider R. A., Kerekes J 1980. The loading concept as basis for controlling eutrophication philosophy and preliminary results of the OECD program on eutrophication. *Progress in Water Technology* 12 PP5-38, 1980
- (51) Walker W.W. 1987 Empirical methods for predicting eutrophication in impoundment; Report 4 phase III Application Manual. Technical Report E-81-9, prepared for Office of Chief, U:S: Army Corps of Engineers, Waterways Experiment Station, Vicksburg, Mississippi.
- (52) Reynolds C.S. 1992 Eutrophication and the management of planktonic algae: what Vollenwieder couldn't tell us. In *Eutrophication, Research and application to water supply*, D.W. Sutcliffe & J.G. Jones (ed.) ISBN 0-900386-52-5
- (53) Jeppesen E. 1998 The Ecology of Shallow Lakes- Trophic Interactions in the Pelagial. Doctor's dissertation (DSc). ISBN: 87-7772-414-3 National Environmental Research Institute, P.O. box. 314, Vejlsovej 25, DK-8600 Silkeborg, Denmark.

Hydraulics In General

- Chow, T V (1959) *Open-Channel Hydraulics*, McGraw-Hill, New York.
- Lamb, H (1945) *Hydrodynamics*, Dover, New York.
- Milne-Thomson, L M (1950) *Theoretical Hydrodynamics*, Macmillan, New York.
- Phillips, O M (1966) *The Dynamics of the Upper Ocean*, Cambridge University Press.
- Rouse, H (1946) *Elementary Mechanics of Fluids*, John Wiley and Sons, New York.
- Rouse, H (editor) (1959) *Advanced Mechanics of Fluids*, Wiley, New York.
- Schlichting, H (1960) *Boundary Layer Theory*, McGraw-Hill, New York.
- Streeter, V L (1961) *Handbook of Fluid Dynamics*, McGraw-Hill, London.
- Svendsen, I A and Jonsson, I G (1976) *Hydrodynamics of Coastal Regions*, Technical University of Denmark.
- U.S. Army Coastal Engineering Research Center (1984) *Shore Protection Manual*.

Computational Hydraulics In General

- Abbott, M B (1979) *Computational Hydraulics, Elements of the Theory of Free Surface Flows*, Pitman, London.
- Abbott, M B and Basco, D R (1989) *Computational Fluid Dynamics, an Introduction for Engineers*, Longman, London, and Wiley, New York.
- Abbott, M B and Cunge, J A (1982) *Engineering Applications of Computational Hydraulics*, Pitman, London.
- Abbott, M B, McCowan, A D and Warren, I R (1981) *Numerical Modelling of Free-Surface Flows that are Two-Dimensional in Plan. Transport Models for Inland and Coastal Waters*, edited by Fischer, H.B., Academic Press, New York.
- Abbott, M B and Larsen, J (1985) *Modelling Circulations in Depth-integrated Flows. Journal of Hydraulic Research*, 23, pp 309-326 and 397-420.
- Aupoix, B (1984) *Eddy Viscosity Subgrid Scale Models for Homogeneous Turbulence. In Macroscopic Modelling of Turbulent Flow, Lecture Notes in Physics, Proc. Sophie-Antipolis, France.*
- Falconer, R A and Mardapitta-Hadjipandeli (1987) *Bathymetric and Shear Stress Effects on an Island's Wake: A computational Study. Coastal Engineering*, 11, pp 57-86.
- Horiuti, K (1987) *Comparison of Conservative and Rotational Forms in Large Eddy Simulation of Turbulent Channel Flow. Journal of Computational Physics*, 71, pp 343-370.

Leonard, A (1974) Energy Cascades in Large-Eddy Simulations of Turbulent Fluid Flows. *Advances in Geophysics*, 18, pp 237-247.

Lilly, D K (1966) On the Application of the Eddy Viscosity Concept in the Inertial Subrange of Turbulence. NCAR Manuscript No. 123, National Center for Atmospheric Research, Boulder, Colorado.

Madsen, P A, Rugbjerg, M and Warren, I R (1988) Subgrid Modelling in Depth Integrated Flows. *Coastal Engineering Conference*, 1, pp 505-511, Malaga, Spain.

Smagorinsky, J (1963) General Circulation Experiment with the Primitive Equations. *Monthly Weather Review*, 91, No. 3, pp 99-164.

Wang, J D (1990) Numerical Modelling of Bay Circulation. *The Sea, Ocean Engineering Science*, 9, Part B, Chapter 32, pp 1033-1067.

Wind Conditions In General

Duun-Christensen, J T (1975) The Representation of the Surface Pressure Field in a Two-Dimensional Hydrodynamic Numerical Model for the North Sea, the Skagerak and the Kattegat. *Deutsche Hydrographische Zeitschrift*, 28, pp 97-116.

NOAA, National Weather Service (1972) Revised Standard Project Hurricane Criteria for the Atlantic and Gulf Coasts of the United States, Hurricane Research Memorandum HUR 7-120.

Smith, S D and Banke, E G (1975) Variation of the Sea Drag Coefficient with Wind Speed. *Quart. J. R. Met. Soc.*, 101, pp 665-673, 1975.

US Weather Bureau (1968) Meteorological Characteristics of the Probable Maximum Hurricane, Atlantic and Gulf Coasts of the United States, Hurricane Research Interim Report, HUR 7-97 and HUR 7-97A.

Near Shore Wave In General

Battjes, J A and Janssen, J P F M (1978) Energy Loss and Set-Up Due to Breaking of Random Waves. *Proc. 16th Coastal Eng. Conf. Hamburg*, pp 569-587.

CERC (1984) Shore Protection Manual. U.S. Army Coastal Eng. Res. Center, Corps Engineers, Vol 1.

Holthuijsen, L H, Booij, N and Herbers, T H C (1989) A Prediction Model for Stationary, Short-crested Waves in Shallow Water with Ambient Currents. *Coastal Engineering* 13, pp 23-54.

Svendsen, I A, Jonsson, I G (1980) Hydrodynamics of Coastal Regions. Den Private Ingeniørfond, Lyngby.

11. LIST OF PREPARERS

This report was prepared by the following staff:

Philip Williams & Associates:

Kevin Coulton, P.E., Project Manager
John Gardiner, Ph.D., C.Eng., Principal-in-Charge
Bo Juza, Ph.D., Senior Associate
Michael Barad, P.E., Associate
Cindy Lowney, Ph.D. Associate

DHI Institute for Water and Environment:

Mads Madsen
Erik Kock Rasmussen